REACTOR CORE MATERIALS

A Quarterly Technical Progress Review

Prepared for U. S. ATOMIC ENERGY COMMISSION by BATTELLE MEMORIAL INSTITUTE

4 - SEP 21
Copy 1959

August 1959

● VOLUME 2

● NUMBER 3

TECHNICAL PROGRESS REVIEWS

To meet the needs of industry for concise summaries of current atomic developments, the AEC is publishing this series, Technical Progress Reviews. Issued quarterly, each of the reviews digests and evaluates the latest findings in a specific area of nuclear technology and science.

The three journals currently published in this series are:

Power Reactor Technology, Walter H. Zinn and associates, General Nuclear Engineering Corporation

Reactor Fuel Processing, Stephen Lawroski and associates, Chemical Engineering Division, Argonne National Laboratory

Reactor Core Materials (covering solid material developments), R. W. Dayton, E. M. Simons, and associates, Battelle Memorial Institute

Each journal may be purchased ($2.00 per year for subscription and individual issues $0.55) from the Superintendent of Documents, U. S. Government Printing Office, Washington 25, D. C. See back cover for remittance instructions and foreign postage requirements.

●

Availability of Reports Cited in This Review

Unclassified AEC reports are available for inspection at AEC depository libraries and are sold by the Office of Technical Services, Department of Commerce, Washington 25, D. C.

Unclassified reports issued by other Government agencies or private organizations should be requested from the originator.

Unclassified British and Canadian reports may be inspected at AEC depository libraries. British reports are sold by the British Information Service, 45 Rockefeller Plaza, New York, N. Y.; Canadian reports (AECL series) are sold by the Scientific Document Distribution Office, Atomic Energy of Canada, Ltd., Chalk River, Ontario, Canada.

Classified U. S. and foreign reports identified in this journal as Secret or Confidential may be purchased by properly cleared Access Permit Holders from the Technical Information Service Extension, U. S. Atomic Energy Commission, P. O. Box 1001, Oak Ridge, Tenn. Such reports may be inspected at classified AEC depository libraries.

REACTOR CORE MATERIALS

a review of recent developments in
solid materials for reactor cores

prepared by
BATTELLE MEMORIAL INSTITUTE

AUGUST 1959 · VOLUME 2 NUMBER 3

foreword

This is one of a series of Technical Progress Reviews prepared at the request of the Division of Information Services of the U. S. Atomic Energy Commission. *Reactor Core Materials* is written quarterly by staff members of Battelle Memorial Institute, who comb the current literature and report significant accomplishments in the form of critical correlated reviews.

These Reviews are intended as a convenient, condensed reference for those who wish to skim through the extensive research and development activities in the nuclear-materials field. Persons wishing to delve deeper into particular areas will find the bibliographies most helpful.

Those considering a particular, uncommon material for some special reactor application are frequently faced with such questions as: Is it available commercially? How much does it cost? What kinds and amounts of impurities does it contain? Where can I get technical information about it? These questions are answered in two AEC-sponsored compilations: one by Wilhelm and McCarley of Ames Laboratory, entitled "List of High-purity Metals Available From American Producers" (Report ISC-1029), and the other, "Sources of High-purity Elements," by Snyder et al., of University of California Radiation Laboratory (Report UCRL-5368).

R. W. DAYTON
E. M. SIMONS
Battelle Memorial Institute

contents

ii		Foreword
1	I	FUEL AND FERTILE MATERIALS
1		Unalloyed Uranium
2		Alpha-Uranium Alloys
3		Gamma-phase Alloys
6		Epsilon-phase Alloys
6		Dilute Uranium Alloys
9		Plutonium and Its Alloys
9		Thorium and Its Alloys
11		Dispersion Fuel Materials
14		Refractory Fuel and Fertile Materials
16		Diffusion Studies
17		Mechanism of Corrosion of Fuel Alloys
18		Basic Studies of Radiation Effects in Fuel Materials
22	II	MODERATOR MATERIALS
22		Graphite
22		Beryllium Metal and Alloys
23		Beryllium Compounds
23		Solid Hydrides
25	III	NUCLEAR POISONS
25		Metals and Alloys for Control Rods and Burnable Poisons
25		Control and Burnable-poison Dispersions
28	IV	CLADDING AND STRUCTURAL MATERIALS
28		Corrosion
32		Radiation Effects in Nonfuel Materials
33		Selected Metallurgical Aspects of Cladding and Structural Materials
36		Selected Mechanical Properties of Cladding and Structural Materials
45		Recent Literature Surveys
48	V	SPECIAL FABRICATION TECHNIQUES
48		Melting, Casting, Heat-treatment, and Hot Working
49		Cladding
53		Welding and Brazing
53		Nondestructive Testing

Issued quarterly by the U. S. Atomic Energy Commission. Use of funds for printing this publication approved by the Director of the Bureau of the Budget on Nov. 1, 1957.

REACTOR CORE MATERIALS

FUEL AND FERTILE MATERIALS

Unalloyed Uranium

Experimental work at Du Pont[1] has shown that a uranium grain size of approximately 0.10 mm may be produced in beta-transformed uranium by quenching from a beta-phase temperature and subsequently annealing in the alpha phase above 600°C. In contrast, grain sizes of 0.35 mm and greater are produced in metal that is air-cooled after beta transformation. A significant portion of the grain refinement is brought about by recrystallization of the beta-quenched structure during the high alpha anneal.

Preliminary in-pile tests indicate that uranium plate that is heat-treated by the quench and anneal process undergoes no surface roughening, such as occurs in air-cooled plate, and is dimensionally stable. Similarly, heat-treated rods also show improved surfaces but are dimensionally less stable than the plate. There is no significant difference between the dimensional stability of alpha-phase uranium extrusions and standard rolled uranium after irradiation, according to Hanford.[2] The influence of fabrication and heat-treatment on the structure and properties of uranium metal is reported by Russian investigators in a 1958 Geneva Conference paper.[3]

Leach[4] reports on a study of the phenomenon known as breakaway corrosion in uranium-water systems. This phenomenon is characterized by a sudden increase in the rate of corrosion after an initial period of a relatively low corrosion rate and is believed to be associated with a change in the protective uranium oxide film. In this study the oxide film is considered as the dielectric of an electrolytic condenser which separates the underlying metal, acting as one electrode, from the corrosive liquid, acting as the other. Experimental techniques were devised allowing measurements to be expressed as the capacitance and resistance of an analog circuit consisting of a condenser and resistance in parallel.

It is known that the presence of hydrogen in gamma-phase uranium alloys will increase the corrosion rate about 20 times. To study this effect, capacitance and resistance measurements of the oxide films on the surfaces of specimens which were hydrogen-free and hydrogen-charged were obtained. The capacitance measurements were within ±10 per cent of one another. The electrical resistance of the oxide on the hydrogen-free specimens was greater than 10^6 ohm/cm^2 but was of the order of 3×10^5 ohm/cm^2 on the hydrogen-charged samples. This indicated that a marked increase in conductivity of the oxide is associated with the presence of hydrogen in the metal. No data on the hydrogen content of the oxide layer are available; however, it is expected that an increase in the hydrogen content of the metal would cause an increase of hydrogen content in the oxide layer.

Measurements[5] of the self-diffusion of uranium in the gamma phase have been performed recently. The self-diffusion coefficients were obtained by two different methods. U^{233} was deposited on natural uranium and heat-treated at a given temperature in the gamma region. Counting of alpha radiation derived from machined layers of the diffusion specimen permitted the determination of the diffusion coefficients presented below.

Temp., °C	Self-diffusion coefficient (D), 10^{-8} cm^2/sec
800	0.48
900	1.17
1000	2.8
1050	4.5

This method yielded an activation energy of 26,600 cal/gram-atom. For comparison, diffusion coefficients obtained by an autoradiographic technique are tabulated below. The activation energy obtained by this method is 21,000 cal/gram-atom.

Temp., °C	Self-diffusion coefficient (D), 10^{-8} cm^2/sec
800	0.9
900	2.0
1000	4.0

Results on postirradiation annealing of uranium subjected to 0.17 per cent burn-up are reported by the British.[6] It was found that alpha-phase (610°C) annealing produced an initial density decrease of 0.1 per cent, with no further significant change over the first 140 hr. Beta-phase (710°C) annealing produced cracking in the specimens, which was responsible for about a 1 per cent density decrease. No systematic decrease in density with time of annealing was established by the results, and most of the density decrease apparently occurred as a result of heating and cooling through the alpha-to-beta phase change. Annealing at 880°C caused a sudden 2 per cent density decrease, presumably as a result of homogeneous nucleation of the fission-product gases, with subsequent plastic yield. During annealing over a period of 30 to 40 hr, further swelling occurs at the rate of 0.1 per cent per hour from creep or further migration of gas molecules into pores. Between 50 and 60 hr, rapid swelling at a rate of 2 per cent per hour occurs, leveling off at a total swelling of 30 per cent for periods of annealing longer than 60 hr. (M. S. Farkas)

Alpha-Uranium Alloys

Transformations in uranium alloys with high solute solubility in the gamma phase are reported by the British.[7] The high-temperature gamma phase in uranium alloys with approximately 10 at.% titanium, niobium, zirconium, or molybdenum can be rendered metastable under critical cooling conditions. The alloyed gamma phase may transform by a shear mechanism to form a characteristic banded structure or by a nucleation and growth process to form equiaxed grains. Although these decomposition structures differ metallographically, they have similar X-ray patterns. The structure is designated distorted α', since the patterns correspond to alpha uranium contracted in the b-direction of the orthorhombic cell. The formation of these metastable structures is apparently dependent upon composition, cooling rate, and the effect of the solute element on the incubation period and decomposition rate of the metastable gamma phase.

A similar study,[8] on uranium−5, −10, and −20 at.% titanium, showed that the metastable gamma phase in this system decomposes to one of three metastable phases. For example, a shear transformation to α'_s occurred when the 10 at.% titanium alloy was quenched in mercury. Similar treatment of the 15 at.% titanium alloy produced a phase, γ^o, exhibiting some degree of anisotropy. At slower cooling rates, e.g., about 1 in. from the quenched tip of a mercury end-quenched specimen, transformation to distorted α', α'_n occurs by nucleation and growth. A metastable gamma phase may be retained when the 20 at.% titanium alloy is mercury quenched. Marked hardness variations, ranging from 150 to 650 VPN, were developed along the end-quenched rods apparently because of dispersion hardening associated with U_2Ti preprecipitation from the supersaturated metastable phase.

Sylvania-Corning[9] has attempted to improve the strength at elevated temperatures of a uranium−1.5 wt.% molybdenum alloy. Uranium carbide was added by powder metallurgical methods with the aim of forming a continuous network of UC and thus improving hot strength. Compositions containing up to 10 wt.% UC were evaluated by hot-hardness tests at temperatures from 550 to 700°C. The additions did not improve the strength of the base alloy over the temperatures tested. Metallographic examination showed that the UC was present as discrete particles and not as a continuous network.

Results obtained by Argonne[10] on the corrosion of uranium−3 wt.% titanium in 260°C water are presented in Table I-1. A gamma-quenched sample, aged at 400°C for 1 hr, was broken into small pieces after 1.9 days in 260°C water. The early corrosion failure of the uranium-titanium alloys by cracking was believed to be due to hydrogen damage. Therefore ternary additions were investigated in which the third element was introduced to remove hydrogen and possibly increase the stability of the gamma phase. Exploratory work indicated that the optimum composition for high uranium alloys

Table I-1 CORROSION OF URANIUM–3 WT.% TITANIUM IN 260°C WATER (GAMMA QUENCHED)*

Exposure time, days		Corrosion rate, mg/(cm²)(day)
Incremental	Total	
1.9	1.9	22
5.8	7.7	9
6.8	14.5	Sample broken into small pieces

*Data taken from reference 10.

is uranium–3 wt.% titanium–1.5 wt.% niobium, and further study was confined to this alloy. In the 1000°C water-quenched condition, this alloy corroded in 260°C water at a rate of 1 mg/(cm²)(day) for 50 days. During the next 25 days, the rate decreased to about 0.5 mg/(cm²)(day); however, fine cracks may have developed during the last 14 days. In the 750°C quenched condition, the alloy also exhibited considerable corrosion resistance, Table I-2, although the lifetime was shorter. Aging for 2 hr at 400°C after a 1000°C quench produced very little change in the initial corrosion resistance.

Table I-2 CORROSION OF URANIUM–3 WT.% TITANIUM–1.5 WT.% NIOBIUM IN 260°C WATER (QUENCHED FROM 750°C)*

Exposure time, days		Corrosion rate, mg/(cm²)(day)
Incremental	Total	
2.6	2.6	14.9
4.7	7.3	13.2
7.8	15.1	9.4
6.8	21.9	5.5
8.6	30.5	12.2
9.9	40.4	41.0

*Data taken from reference 10.

The corrosion resistance of uranium–3 wt.% titanium–1.5 wt.% niobium is superior to that of uranium–5 wt.% zirconium–1.5 wt.% niobium in the quenched condition; however, the 3 wt.% titanium alloy is not so resistant to thermal effects. Initial studies of uranium–3 wt.% titanium–0.5, –1, and –2 wt.% zirconium showed that, at the end of 3 days of exposure in 260°C water, the corrosion rates were independent of zirconium content and equal to about 4.5 mg/(cm²)(day). Corrosion tests on uranium–5 wt.% zirconium–1.5 wt. % niobium fuel elements in the unirradiated and irradiated conditions showed that, after 0.06 at.% burn-up, the corrosion resistance in 270°C water was improved by radiation. However, only one irradiated fuel element was tested.

In a 1958 Geneva Conference paper,[11] the uranium-zirconium, uranium-titanium, and uranium-zirconium-titanium phase diagrams are reported. (M. S. Farkas)

Gamma-phase Alloys

Uranium-Niobium

Samples of transformed uranium–10 wt.% niobium and uranium–10 wt.% niobium–4 and –6 wt.% zirconium have been irradiated at –30 to –40°C by Bettis.[12] Electrical-resistivity measurements show that the alloys revert to the gamma phase and that zirconium slows down the retransformation. X-ray diffraction evidence[13] for gamma-phase reversion has also been obtained.

Studies have been made[10,13] of the kinetics of gamma-phase decomposition in uranium alloys containing about 10 wt.% niobium with additions of zirconium. Transformation-temperature-time (TTT) curves have been worked out[10] for these alloys with 0 to 6 wt.% zirconium. In this range the alloys have a C-curve with a double nose. The upper nose is associated with the formation of lamellar $\alpha + \gamma_2$ structures and occurs at approximately 550°C, except for the ternary alloy containing 6 wt.% zirconium. For this alloy the nose decreases to 500°C. The nose for the lower transformation occurs near 360°C, and data are insufficient to establish the influence of zirconium on this temperature. The nature of this transformation is uncertain, but it proceeds submicroscopically and is accompanied by density and hardness increases; the X-ray diffraction pattern resembles that of alpha uranium, but with quite diffuse reflections. The transformation product is unstable since it dissolves on heating to higher temperature in the $\alpha + \gamma_2$ region. Increasing the niobium content reduces the rate of transformation at the lower nose, but zirconium has little effect up to 4 wt.%. Both elements reduce the rate of transformation at the upper nose. Alloys containing 8 wt.% niobium and 2 to 20 wt.% zirconium were found[13] to transform more rapidly at 450 than at 550°C; alloys containing 10 wt.% niobium transform more slowly at 450 than at 550°C. A more rapid shift of the upper C-curve nose to lower temperatures with increasing zirconium is indicated for the 8 wt.% niobium alloy. Specimen

history has a marked influence[10] on transformation rate at 550°C. The rate decreases with increasing grain size and with increasing homogeneity.

The effect of uniaxial stress on transformation of the uranium–10 wt.% niobium–4 wt.% zirconium alloy is being studied. Hardness data did not reveal any significant effect of differences in stress level on specimens transformed under the same conditions. However, metallographic evidence of directional precipitation of transformation products was observed under some conditions. Stress also increased the kinetics of transformation of the alloy.

Results of an investigation[13] of age hardening in the uranium-niobium system indicate that two hardening mechanisms are operative, although their nature is unknown.

The effect of stressing uranium–10 wt.% niobium and uranium–10 wt.% niobium–4 wt.% zirconium alloys to 20,000 psi on corrosion resistance in 680°F water was investigated.[13] There was no effect on the binary alloy even at 20,000 psi, but there was an effect on the ternary alloy.

In studies of the effect of cold reduction up to 10 per cent on the corrosion resistance of intentionally defected Zircaloy-2-clad plates of uranium alloyed with 10.6 wt.% niobium–4 wt.% zirconium in 680°F water, there was some indication of decreased corrosion resistance as a result of cold reductions on production-processed plates, but corrosion properties of the diffusion zone were not harmed.[13] Tests show that specimens with thin diffusion zones are superior to those with thicker zones when tested with 40-mil defects in 680°F water, although tests to determine the maximum allowable diffusion-zone thickness are inconclusive as yet.[13]

Corrosion tests of clad uranium–10 wt.% niobium–4 wt.% zirconium platelets with 40-mil defects have been discontinued after 315 days in 680°F water. Metallography revealed that fuel, cladding, and diffusion zones were intact.

Experiments aimed at obtaining a better understanding of the corrosion behavior of uranium-niobium and uranium-niobium-zirconium alloys are under way. These include attempts to relate mechanical properties with corrosion resistance, measurements of solution potential of these alloys, and studies of intergranular corrosion attack and the role of hydrogen in corrosion.

Studies of the effect of impurities on corrosion resistance indicate that oxygen, sulfur, and beryllium individually and iron, beryllium, and tantalum combined reduce the corrosion resistance of bare uranium–10 wt.% niobium–4 wt.% zirconium in 680°F water. Tin has a beneficial effect on corrosion resistance;[13] the role of iron and carbon is uncertain. In Zircaloy-2-clad specimens[13] with controlled carbon, oxygen, sulfur, iron, beryllium, and tin contents, only sulfur leads to rapid failure. Test periods longer than the present 62 days are required to establish the effects of the other impurities.

Tests have been run[10] to compare the behavior of uranium–10 wt.% niobium–0 to 8.8 wt.% zirconium in 360°C water with that in 360°C oxygen at 60 cm Hg pressure. The results indicate that, although behavior is similar, corrosion and oxidation rates are not identical. They further indicate that hydrogen is not necessary for corrosion failure.

The kinetics of oxidation of uranium–10 wt.% niobium–4 wt.% zirconium in oxygen at 12 and 60 cm Hg pressure at 680°F and in water at 680°F are also under study. Rate of weight loss in oxygen at 60 cm Hg was roughly five times that in oxygen at 12 cm Hg.

The results of irradiation of a series of uranium-niobium-zirconium alloy specimens[13] are presented in Tables I-3 through I-5. All specimen trains are being reinserted to continue the irradiation to higher burn-ups. Two of the specimens listed in Table I-3, which were irradiated in the $\alpha + \gamma_2$ condition, exhibited gross swelling and are being removed. Specimen B2, which was blistered after irradiation, and Specimen D3, which was cracked during reassembly (Table I-4), are also being removed from their particular specimen train. Other specimens are being substituted for those removed from test. Additional tests are in the reactor, and new tests are planned.

Uranium-Molybdenum

Atomic Power Development Associates, Inc., briefly summarizes[14] constitution, transformation kinetics, and properties of the uranium–10 wt.% molybdenum fuel alloys. Factors affecting the irradiation performance of the alloy are discussed, and irradiation test results are briefly presented.

A British paper[15] describes the metallographic appearance of gamma-phase uranium-molyb-

Table I-3 SUMMARY OF DATA OBTAINED ON LOW BURN-UP SPECIMENS

Specimen	Composition (balance uranium), wt.%	Burn-up, at.%	Vol. increase, %	Temp., °F	
				Design	Operating
S1	10.6 Nb–4 Zr	0.31	Negligible	705	659 (σ = 19)
S2	10.6 Nb–2 Zr	0.49	Negligible	787	
S3	10.6 Nb–4 Zr	0.49	Negligible	787	771 (σ = 104)
S4	10.6 Nb–6 Zr	0.49	Negligible	787	777 (σ = 14.5)
S5	10.6 Nb–4 Zr*	0.49	27.3	787	798 (σ = 8.3)
S6	10.6 Nb	0.24	Negligible	685	689 (σ = 190)
S7	10.6 Nb*	0.24	23.8	688	692 (σ = 18)

*Irradiated in $\alpha + \gamma_2$ condition; remaining samples irradiated in γ condition.

Table I-4 SUMMARY OF DATA OBTAINED ON INTERMEDIATE BURN-UP SPECIMENS

Specimen	Composition (balance uranium), wt.%	Burn-up, at.%	Max. thickness increase, %*	Av. temp., °F	Position
S1D	10.6 Nb–4 Zr	0.3	2.3	720	Top
D1	10.6 Nb–5 Zr	0.9	8.0	715	Top
C3	10.6 Nb–4 Zr	0.8	4.5	713	Top
C4	10.6 Nb–4 Zr	0.8	5.7	713	Top
C5	10.6 Nb–4 Zr	0.3	4.5†	715	Top
D3	10.6 Nb–5 Zr	0.8	5.7	715	Top
B2	10.6 Nb–2 Zr	0.3	2.3‡	697	Bottom

*Fuel, micrometer readings.
†Localized at one end.
‡Not counting blister.

Table I-5 SUMMARY OF DATA ON HIGH BURN-UP SPECIMENS*

Specimen	Composition (balance uranium), wt.%	Observed temp., °F	Estimated burn-up, %†	Volume increase, %	
				Total	Per at.% burn-up
P1	10.6 Nb–2 Zr	641	1.00	3.6	3.6
P2	10.6 Nb–6 Zr	660	1.12	3.3	3.0
P3C	10.6 Nb–4 Zr	675	1.30	4.0	3.1
H4	10.6 Nb	672	1.32	5.5	4.2
H5	10.6 Nb	665	1.29	6.3	4.9
LU2B	10.6 Nb–4 Zr	675	1.27	5.7	4.5‡
				4.8	3.8
LH2A	10.6 Nb–4 Zr	653	1.19	4.3	3.6‡
				4.0	3.4

*Data taken from reference 13.
†As of Feb. 23, 1959.
‡Two sets of fillers in each of these specimens. One set in each specimen is in a lower flux region.

Table I-6 KINETIC DATA FOR AS-CAST AND HOMOGENIZED ALLOYS

Nominal composition (balance uranium), wt.%						Time at 550°C, hr	Estimated per cent transformation
Nb	Zr	Mo	Ti	V	Cr		
12	4	4	0	1.5	0	840	5–30
8	4	4	0	1.5	0.75	840	80
12	2	4	0	0	0	840	50–60
12	4	0	1.5	1.5	0	840	<5*
12	4	0	1.5	0	0.75	840	5

*X-ray examination showed two cubic phases present after 24 hr.

denum alloys after heating in water at 300°C and in hydrogen gas at 850°C. Hydride platelets were found to form under both conditions. The crystallographic habit of these platelets in the body-centered cubic structure is given.

The Russians have presented a review[16] of the properties of uranium-molybdenum alloys and their application as fuel elements in heterogeneous nuclear reactors.

Complex Alloys

Fabrication, phase, transformation kinetics, and corrosion studies of gamma-phase uranium alloys containing niobium, zirconium, molybdenum, titanium, vanadium, and chromium are in progress at Bettis.[13] In transformation kinetics studies, of 25 compositions tested 5 were not completely transformed after 840 hr at 550°C. Compositions and estimated percentages of transformation based on metallographic examination are given in Table I-6.

The results of a survey of the effects of ternary and quaternary alloying on stability and properties of uranium-zirconium, uranium-niobium, and uranium-molybdenum base gamma-phase alloys conducted at Battelle are summarized.[10] These results were presented in a previous issue of this Review.

(A. A. Bauer)

Epsilon-phase Alloys

Uranium-Silicon

Argonne[10] found that a bare uranium–3.8 wt.% silicon sample irradiated to a burn-up of 0.085 at.% had a corrosion rate of approximately 0.1 mg/(cm^2)(day) in 260°C water for 31.4 days. The sample was cracked after 62.8 days, with cracking continuing for a total of 75.7 days. There was no hydrogen pressure build-up.

A Zircaloy-2-clad sample with bare ends, irradiated to 0.069 at.% burn-up, showed no change after 46.4 days in 260°C water.

(A. A. Bauer)

Dilute Uranium Alloys

Aluminum-Uranium Alloys

The Nuclear Energy Section of Field Intelligence Agency, Technical (FIAT) in Italy[17] has investigated the effect of burnable poisons on certain properties of the aluminum–16 wt.% uranium alloy. Alloys containing ternary additions of 0.15 wt.% boron and 2 wt.% lithium, as well as alloys with additions of both 0.05 wt.% boron–2 wt.% lithium and 0.05 wt.% boron–0.1 wt.% lithium, were studied. The boron additions formed an intermetallic compound which was tentatively identified as a complex boride. These additions did not change the properties of the binary alloys. The high lithium alloys (2 wt.%) have tensile properties and elastic moduli higher than the binary alloys or those ternary alloys containing boron. The 2 wt.% lithium addition reduced the density by about 7.5 per cent. However, the 0.1 wt.% lithium addition did not affect the properties of the alloys. No corrosion data were reported.

The silicon-modified wrought alloy, aluminum–48 wt.% uranium, developed by Oak Ridge[18] apparently does not have the tensile strength of the wrought binary alloy. Tensile tests were performed on specimens rolled at 600°C with a 75 per cent reduction. The binary alloy had ultimate tensile strengths of 25,900 and 2,460 psi at room temperature and 500°C, respectively. The binary modified with 3 wt.% silicon had ultimate tensile strengths of 15,800 and 1,790 psi at room temperature and 500°C, respectively. Modified alloy extruded at 600°C had an ultimate tensile strength of only 12,770 psi at room temperature. Data from the one 3 wt.% tin alloy tested indicate that its properties were similar to those of the silicon alloy. The theory is advanced that decreased amounts of compound caused by the suppression of UAl_4 produced a weaker structure, resulting in the reduction in strength. Although the authors did not mention it, there is the possibility that the silicon additions might embrittle the compound particles and thus contribute to weakening of the structure. Although the ternary tin alloy was reportedly fabricated at 600°C, some doubt is raised since the addition of tin lowers the eutectic temperature to about 590°C.

The 3 wt.% silicon addition improves hot-rolling characteristics. To prevent serious edge cracking, it is necessary to restrain the binary alloy with aluminum sheet, but the ternary can be rolled without this. Two full-size MTR fuel elements were prepared from the alloy with a uranium enrichment of 20 per cent. These were irradiated to burn-ups of 25 and 62 per cent of the U^{235} atoms, with no apparent effect on either

element. Additional irradiation tests are in progress.

Since it is known that emulsions of colloidal silica adversely affect pulsed column operation, a brief chemical reprocessing study of this alloy is in progress. High acid conditions were only slightly effective in reducing emulsification of the silica. The corrosion of the alloy in 60 and 90°C water seems to be characterized by very little general surface attack, although some blisters do form.

Current studies by Battelle of the effect of additions on the various properties of the aluminum–35 wt.% uranium alloys corroborate other reported data which show that UAl_4 is suppressed by 3 wt.% additions of silicon and of tin. Also, a similar addition of zirconium is an excellent suppressor. The Battelle data[19] reveal that, in the cast condition, the ternary additions improve the tensile strength of the binary alloy (35 wt.% uranium). The alloy containing tin and zirconium exhibited definite increases in elongation and per cent reduction in area. The fractured surfaces of the tensile test bars indicated that both tin and zirconium were exceptionally good grain refiners. The results of extrusion tests showed that the alloys containing tin and zirconium contained little if any cracked compound or porosity in areas adjacent to the compound after extrusion. On the other hand, the compound was cracked in both the binary and the silicon-containing alloy.

Hollow extrusion billets (26 in. long) of exceptional quality were prepared by centrifugally casting the alloy in air.[20] The outside diameter of these billets needed no further machining, and the inside surface needed a total cleanup of only about 0.075 in. on the diameter. The castings contained no porosity. The metal was poured at 2400°F into a movable pouring spout preheated to 1400°F which moved along the length of the mold, depositing the metal evenly. The molten metal was bottom poured so that dross carry-over was held to a minimum. Enough castings were produced to establish feasibility, and it is believed that billets up to 5 ft long could be prepared by this technique.

In preparation for the irradiation of aluminum-plutonium alloys in Zircaloy sheathings, Chalk River[21] has studied aluminum alloys containing 5, 10, 15, and 20 wt.% uranium. Metallurgical and mechanical bonds between the fuel alloy and the sheathing were evaluated. The metallurgical bonds cracked during cooling and were deemed unsatisfactory. The mechanical bond was adopted as standard and has proven to be satisfactory during various tests. Compatibility tests showed that rapid sheath dissolution occurs in 1 hr at temperatures of 640 to 650°C. The alloys containing 5 and 10 wt.% uranium, when tested for 1 hr in 340°C water, exhibited a penetration of only about 4 mils, whereas the alloys containing 15 and 20 wt.% uranium exfoliated to a depth of about 40 to 80 mils when tested under the same conditions.

Zirconium-Uranium Alloys

Since temperature transients may occur in any reactor, a strong effort is being made to determine the effect of such transients on the swelling characteristics of the zirconium-uranium alloys. Bettis[13] has subjected a number of Zircaloy-3-base binary alloys containing 5.5 wt.% uranium to a series of transient anneals (three cycles to the particular test temperature with a hold of only a few seconds at the temperature). These alloys contained boron additions ranging from 0.02 to 0.113 wt.%. Their U^{235} burn-up ranged from 0.07 to 1.5 at.%.

Alloys with boron contents of 0.06 wt.% and burn-ups of less than 1 at.% U^{235} were given transient treatments to 1300°F. For this test series, no alloy underwent a volume change of greater than 0.5 per cent.

Another series of alloys containing 0.02 wt.% boron which had been irradiated to a burn-up of 1.2 at.% U^{235} was given transient tests to 1300 and 1400°F. After the 1400°F test, the volume change was 3.21 per cent. A third series of alloys containing 0.113 wt.% boron with burn-ups of 1.5 at.% U^{235} exhibited a volume change of 16.1 per cent after three cycles to 1100°F and blistered severely after three cycles to 1200°F.

Alloys containing 9.0 wt.% uranium and 0.04 wt.% boron were irradiated to a burn-up of 1.8 at.% U^{235}. After three transients to 1100°F, these alloys exhibited a volume change of 10.65 per cent and failed by severe blistering after one transient to 1200°F.

These data indicate strongly that for a given transient temperature the amount of swelling is principally dependent on burn-up and also that the boron content has a noticeable effect on swelling. For each burn-up there is definitely a temperature above which severe swelling will occur even after very short times at temperature.

It is interesting to note that, in another experiment, Bettis has annealed a specimen by postirradiation heating for one week at 940°F in argon at a pressure of 2000 psi. This Zircaloy-3–9.0 wt.% uranium–0.04 wt.% boron alloy had a burn-up of 2.1 at.% U^{235}. The fuel volume remained relatively unchanged, whereas the control specimen, annealed under only 1 atm pressure, failed by severe bulging after only a little over 10 hr at 900°F.

As a result of a number of similar tests, Knolls[22] reached the same general conclusions discussed in the previous paragraphs. Annealing at 950°F for 150 hr after the transient treatments caused no further effect. In addition, transients appeared to increase electrical resistivity, whereas subsequent anneals at 950°F seemed to reduce the resistance. (In some cases this treatment reduces resistivity below that of the as-irradiated material.)

Electron-microscope examination of the specimens after the transient anneals showed the presence of bubbles attributed to fission gas. No bubbles were observed in the as-irradiated material. These observations tend to support the theory that the gas is in solution until the temperature is high enough for vacancies to diffuse into a particular region and thus result in bubble formation. If diffusion is the mechanism of bubble formation, few if any bubbles of xenon or krypton could form in zirconium at less than 400°C. On the other hand, theoretical analyses indicate that the gas could be in bubbles in the as-irradiated material but that these bubbles would be too small to resolve. If this is the case, then, surface tension plays an important role in growth restraint, and the specimen would not swell until the temperature reached that point where the pressure in the bubbles overcame the effect of surface tension. It appears that the exact mechanism of swelling has yet to be resolved.

Irradiation data from over 40 zirconium-uranium alloy test specimens have been obtained by Knolls.[23] These specimens have uranium contents of 7 to 22 wt.% and represent burn-ups of 0.15 to 3.2 total at.%. The calculated fuel centerline temperatures were 600 to 1500°F. By using these data, the effects of time, burn-up, and temperature were studied. It was concluded that burn-up produces a volume increase of 3 to 5 per cent per at.% burn-up in the 600 to 900°F temperature range. Doubling the absolute temperature of irradiation can increase swelling tenfold. The increase in swelling is, of course, due to gas, since calculations show that the new atoms resulting from fission will cause a volume increase of about 2.5 per cent per at.% burn-up. All of these atoms, except the gas atoms, are insensitive to temperature. Unfortunately, about 25 per cent of the atoms produced are gas atoms, and the two factors which control volume increase by gas, namely, diffusion of the gas atoms and the strength of the core, are sensitive to temperature.

Tests on binary alloys containing 6 to 12 wt.% uranium irradiated to a burn-up of about 0.7 at.% U^{235} indicate strongly that corrosion rates increase as burn-up increases. This does not mean that irradiation temperatures and times do not play a part. However, the effect of burn-up appears to be the largest contributor to breakdown in corrosion resistance.

The corrosion behavior of an artificial alloy, produced to represent a zirconium–12 wt.% uranium–0.15 wt.% boron alloy that had been irradiated to 3 total at.% burn-up, is being determined by Battelle. The nongaseous fission-product elements or reasonable substitutes were added to a base alloy of zirconium–4.9 wt.% uranium–0.12 wt.% boron in the amounts that would be produced as a result of the irradiation. Although some of the more volatile additions were lost during the melting procedures and others were reduced in content, an alloy of reasonable composition was finally produced. Specimens of the alloy in a number of heat-treated conditions were corrosion-tested in 680°F water. All specimens except those that were furnace-cooled from 900°C suffered severe attack after only 168 hr on test. The 900°C heat-treated alloy exhibited a corrosion rate of −0.62 mg/(cm²)(hr) after 504 hr, whereas a normal sponge zirconium–12 wt.% uranium alloy exhibited a rate of between −0.03 and −0.06 mg/(cm²)(hr). These data show a breakdown in corrosion resistance when fission products build up.

Other data[24] show that a Zircaloy-2–8.2 wt.% uranium–0.042 wt.% boron alloy, irradiated at a calculated centerline temperature between 800 and 875°F to a burn-up of 1 total at.%, is not greatly affected. The greatest change occurred in the plate thickness, which increased about 1.7 per cent.

Niobium-Uranium Alloys

No difficulty was experienced by Battelle[24] in fabricating the binary alloys containing 90 and 80 wt.% niobium. The alloys are forged at 2550°F, which breaks down the cast structure, and are then rolled at 1300°F or below. Although the 70 wt.% niobium alloy has been fabricated at these temperatures, a higher initial temperature is needed for best results. The 60, 50, and 40 wt.% niobium alloys have not as yet been satisfactorily fabricated by forging and rolling, even at temperatures as high as 3000°F. Since the phase diagram indicates no reason for this difficulty, an investigation is in progress to determine the cause of the lack of fabricability. As would be expected, the oxidation resistance of the binary alloys in air[19] is not good. For example, after 48 hr at 300°C the 90 wt.% niobium alloy lost about 15.8 mg/dm^2. After 24 hr at 500°C the loss was on the order of 9600 mg/dm^2. The other binaries exhibited similar amounts of oxidation.

Miscellaneous Alloys

The National Bureau of Standards[14] is studying the phase diagrams for the systems rhodium-uranium, ruthenium-uranium, and palladium-uranium. Melting-point determinations indicate the existence of a congruently melting compound containing about 75 at.% rhodium. From the eutectic location at 872°C and 24.2 at.% rhodium, the liquidus curve rises gradually to a point near 1200°C at a nominal composition of 49.6 at.% rhodium. However, the liquidus then rises sharply to a peak, as indicated by an alloy of nominal 60.7 at.% rhodium being unmelted at 1660°C, an alloy of nominal 74.5 at.% being unmelted at 1960°C, and an alloy of nominal 79.7 at.% rhodium having a melting point of 2160°C. From this peak, the liquidus is lowered to near 1500°C at nominal 89 at.% rhodium.

A study of the ruthenium-uranium system has shown that the solubility of uranium in ruthenium is less than 0.7 wt.% (0.3 at.%) in the region of 1500°C. The phase in equilibrium with the ruthenium solid-solution field is the compound found at 75 at.% ruthenium (URu_3). In the palladium-uranium system, the palladium solid-solution field extends between 70 and 80 wt.% (84 to 90 at.%) palladium. Tentative results indicate room-temperature solubility of uranium in palladium is about 23 wt.% (12 at.%).

(R. F. Dickerson)

Plutonium and Its Alloys

Plutonium

The beta-plutonium phase has been determined[25] to be monoclinic body centered with 34 atoms per unit cell. Possible space groups are I2, Im, and I2/m. At 190°C, a = 9.284 A, b = 10.463 A, c = 7.859 A, $\beta = 92.13°$, and the density is 17.70 g/cm^3. Crystallographic expansion coefficients for the temperature range 133 to 202°C are $\alpha_a = 55 \times 10^{-6}$, $\alpha_b = 21 \times 10^{-6}$, $\alpha_c = 33 \times 10^{-6}$, and $\Delta\beta = -73 \times 10^{-6}$.

Plutonium Alloys

The thermal conductivity of the plutonium-iron eutectic mixture (9.5 at.% iron) was measured[26] in both the solid and liquid states. Thermal conductivity values obtained varied from 0.034 cal/(cm)(sec)(°C) at 220°C to 0.042 cal/(cm)(sec)(°C) at 400°C and from 0.043 cal/(cm)(sec)(°C) to 0.046 cal/(cm)(sec)(°C) at 520°C in the liquid state.

Preliminary data[25] indicate the crystal structure of PuNi to be orthorhombic with a = 3.59 A, b = 10.21 A, and c = 4.22 A. The PuNi is probably isostructural with ThI and CrB, which have four molecules per unit cell and fall into space group Cmcm.

Thermal-expansion curves for a 70 wt.% fission alloy indicate a phase transformation[10] starting at 525°C and ending at 600°C. This was verified through metallography of heat-treated specimens. The coefficient of expansion of the cast alloy from 20 to 500°C is about 16×10^{-6} in./(in.)(°C). (V. W. Storhok)

Thorium and Its Alloys

A publication entitled *Thorium Data Manual* has been prepared by Francis[27] of the United Kingdom. This manual is similar in coverage to its American counterpart, the AEC's *Reactor Handbook*,* and contains somewhat more data in

*A thoroughly revised enlarged second edition of the Reactor Handbook is scheduled for publication during 1960. Details of this four-volume revision are given in a recent book catalogue published by the Commission, Technical Books sponsored by the U. S. Atomic Energy Commission, available without charge from the Technical Information Service Extension, U. S. Atomic Energy Commission, P. O. Box 62, Oak Ridge, Tenn.

the areas of physical, mechanical, chemical, and irradiation properties of thorium.

The crystal structures of the intermetallic compounds, $ThIn_3$, $ThTl_3$, $ThSn_3$, and $ThPb_3$, have been found by Ferro[28] to be of the simple cubic (L12) type like the corresponding uranium compounds.

Measurements of linear-thermal-expansion were made[20] on one unirradiated and two irradiated specimens of thorium–11 wt.% uranium alloy. Heating the unirradiated sample showed mean linear-thermal-expansion coefficients as follows:

Temp., °C	Expansion coefficient, 10^{-6} per °C
20–100	6.9
20–300	8.9
20–500	10.8
20–700	12.8
20–900	13.0

Thermal-expansion coefficients of over 25 × 10^{-6} in./(in.)(°C) were observed for the irradiated samples. This effect presumably was caused by the swelling of internal pockets of fission gas.

The British[29] have measured the dynamic modulus of thorium containing 0.55 wt.% oxygen. The values given below are somewhat higher than those usually obtained by static testing methods:

Temp., °C	Young's modulus (E) 10^{11} dynes/cm^2
20	8
100	7.60
200	7.08
300	6.56

Dynamic modulus measurements have been obtained at Ames[30] on single crystals of thorium metal containing less than 0.1 wt.% total impurities. The values obtained by the pulse-echo technique are summarized as follows:

Temp., °K	Elastic constants, 10^{11} dynes/cm^2 C_{11}	C_{12}	C_{44}
80	7.770	4.820	5.110
180	7.675	4.840	4.990
280	7.560	4.880	4.820
380	7.430	4.940	4.625

An anisotropy factor of between 3 and 4 was calculated from the pulse-echo data. This result suggests that single crystals of thorium possess a small degree of anisotropy in spite of their cubic crystal structure.

Data have been obtained[31] showing the amount of reaction between thorium–7.6 wt.% uranium alloy and stainless steel when the two alloys are separated (or bonded) by a very thin layer of NaK. No information is given as to the actual degree of contact between the thorium alloy and the stainless steel. The rate of reaction is very slow under these conditions at temperatures below the iron-thorium eutectic temperature of 860°C. At 980°C, however, the thorium alloy attacked and penetrated a 0.010-in.-thick cladding layer of stainless steel in about 10 min.

For exposures up to 5 hr in duration in 500°F water, thorium alloys showed the following rates of weight loss:[32]

Alloy, wt.%	Weight loss, mg/(cm^2)(hr)
Th	311
Th–2.2 Zr	88
Th–6.1 Zr	69
Th–6.8 Zr	33
Th–4 Si	59

Complex thorium-uranium-zirconium alloys[24] had the following total weight losses for exposures up to 504 hr in 392°F water:

Alloy nominal composition, wt.%	Total weight loss, mg/cm^2
Th–25 U–25 Zr	399
Th–25 U–25 Zr	591
Th–20 U–20 Zr	400
Th–20 U–20 Zr–4 Nb	508

All four of these alloys were homogenized for 24 hr at 1000°C; the first one was furnace-cooled from 1000°C; the others were water-quenched.

The quantities of fission gas released to the capsules during irradiation of a series of thorium–11 wt.% uranium alloys have been measured.[33] Three of the specimens, prepared by Atomics International, were irradiated at approximately 650°C to burn-ups ranging from 0.57 to 1.5 total at.%. Gas collected from the capsules indicated that the specimens released 0.18, 0.24, and 1.9 per cent of the fission gases

produced in them. The specimen releasing 1.9 per cent of its fission gas was bulged and cracked at the upper end, presumably because it was incompletely covered with NaK during irradiation. The other two specimens were in good condition after irradiation at 650°C.

(W. Chubb)

Dispersion Fuel Materials

The reaction of dispersed uranium dioxide in an aluminum matrix in pressed compacts and fuel plates has been studied at Oak Ridge[35] at temperatures of 500 to 600°C. Correlation of reaction with the accompanying volume increase was made and a growth mechanism was proposed.

Uranium dioxide reacts slowly with aluminum in 50 wt.% UO_2 pressed compacts at 600°C to form UAl_3 and Al_2O_3. A 75 per cent reaction is attained in 80 hr and is accompanied by swelling.

Uranium dioxide reacts with aluminum in 52.3 wt.% UO_2 fuel plates to form UAl_4 and Al_2O_3. Intermediate reaction products are UAl_2 and UAl_3. Reaction is rapid at 600°C, attaining 90 to 100 per cent completion in 10 hr, and moderate at 500°C, attaining 50 to 70 per cent completion in one week. Three reaction-product zones, tentatively identified as containing UAl_2, UAl_3, and UAl_4, are visible by electron microscopy. No evidence of diffusional porosity is noted. Volume increases of 20 to 30 per cent accompany reaction. The rate of volume increase decreases with heat-treatment temperature.

The observed volume increase cannot be explained on the basis of specific volume changes associated with the solid-state reaction, a Kirkendall mechanism, or the presence of hydrogen chemisorbed on the UO_2 surface. A growth mechanism is proposed and supported which is based upon gas generation within the fuel-plate core during reaction, thus causing growth by creep due to internal pressure.

The Martin Nuclear Division[36] has developed a unique process for fabricating tubular dispersion fuel elements. The process has been described previously but perhaps in lesser detail than in this most recent publication. The report covers the fabrication of more than 2000 stainless-steel–UO_2 (enriched) fuel tubes for a zero-power test. All phases of the fabrication are described. The necessary testing of as-received materials; the weighing, blending, and forming of the fuel compacts; the subsequent densification, machining, and forming of the fuel cores; the surface preparation of the assembly parts; and the wall reduction and heat-treatments necessary to obtain a recrystallization bond of the component parts are all discussed. Scrap processing and quality control are also described.

A "powder-rolling" technique is being adapted to the fabrication of tungsten-, molybdenum-, tantalum-, and niobium-UO_2 foils containing between 15 to 25 vol.% UO_2. In the case of niobium- and tantalum-UO_2, the vacuum-sintered strip can be reduced to very thin foil by room-temperature rolling. The molybdenum- and tungsten-UO_2 strip requires special hot-rolling procedures (not yet optimized) to reduce to strip.

Other methods of preparing the refractory metal-UO_2 dispersions include electrophoretically codepositing tungsten and 40 to 65 vol.% UO_2 on a tungsten foil. Some success has been achieved in roll bonding the deposited material between tungsten foil at 1800°C.

Cermet fuel materials containing 60 to 90 vol.% UO_2, UN, or UC dispersed in a continuous metal matrix are being developed at Battelle.[19,20,24] It is reported that these materials are superior to pure ceramics from the standpoint of improved mechanical properties and thermal conductivity. Cermets of UO_2–stainless steel have been prepared by hot press forging, hot swaging, and gas pressure bonding of cold-pressed as well as densified bodies. Electrical-resistivity measurements are being made on these bodies to determine their directional characteristics and to indicate the degree of continuity of the metallic matrix. Thermal-conductivity measurements, presently being made, will be used to test the validity of a mathematical theory developed to relate elec-

trical resistivity to thermal conductivity of cermet materials. The preparation of UO_2, UN, and UC cermets enveloped in matrices of niobium, chromium, and molybdenum is also being investigated. The use of niobium-coated UO_2 powders prepared by the vapor deposition of niobium onto spherical UO_2 is showing particular promise in the fabrication of dense UO_2-niobium cermets. This technique is reported to ensure a continuous nature of the metallic matrix even at very high loadings of the ceramic phase.

The high-temperature irradiation behavior of dispersion fuel elements consisting of 25 wt.% fully enriched UN and UC dispersed in stainless steel is being evaluated at Battelle.[19,20] The initial postirradiation results of eight specimens contained in two capsules are tabulated in Table I-7. Although some specimens blistered (no ruptures reported) at the high temperatures, the authors report that the results are encouraging when compared to the performance of UO_2–stainless-steel specimens tested under similar conditions.

Methods of fabricating stainless-steel–UO_2 dispersion fuel elements for the SM-2 (formerly APPR-1B) reactor are being evaluated.[19,20,24] The reference fuel element contains approximately 28 wt.% spherical UO_2 dispersed in a prealloyed type 347 stainless matrix clad with type 347 stainless steel. Boron is incorporated into the fuel elements as a burnable poison. Work on this program during the past quarter has been concentrated on developing the most satisfactory method for incorporating the burnable poison. These studies are covered in the section on Control and Burnable-poison Dispersions, p. 25.

A recent report[37] described the fabrication development and irradiation of a unique dispersion material, 27 wt.% UO_2 in a uranium-molybdenum alloy matrix. The uranium-molybdenum alloy powder was prepared by first hydriding the wrought alloy. In the case of a uranium–10 wt.% molybdenum alloy, it was necessary to subject the alloy to 70 per cent cold reduction before it was sufficiently reactive with hydrogen at 1 atm pressure. The alloy hydride also could be prepared by reacting the hot-worked alloy at 600°C under 800 psi of hydrogen for 4 hr. Uranium–3.5 wt.% molybdenum alloy could be readily hydrided at low temperatures under 1 atm of hydrogen. Before dehydriding, the powder was mixed with UO_2 to prevent caking. The preferred fabrication technique consisted of tap-packing the mixed powders into a metal sheath, hot press forging, and finally hot rolling to a density of approximately 95 per cent of theoretical. Limited mechanical and physical properties are reported for the dispersion materials.

Duplicate sets of unclad specimens were irradiated to approximately 1 and 2 total at.% burn-ups at calculated centerline temperatures of 650 to 800°F. Neither the UO_2 nor the uranium–10 wt.% molybdenum matrix showed any gross damage attributed to irradiation. Density values decreased an average of 1.5 per cent per at.% burn-up.

Atomics International reports[10] that an ORME fuel element was examined after about 5 per cent burn-up of the uranium (2.4×10^{20} fissions/cm^3) at 775°F maximum fuel temperature. The element is made of 16 plates each containing 25 wt.% UO_2 in a stainless-steel matrix with 0.005-in. stainless-steel cladding. No measurable changes in dimensions or corrosion were noted on the plates. The element operated at 250,000 to 300,000 Btu/(hr)(sq ft).

Dispersions of UO_2 in niobium and niobium-zirconium alloy have been fabricated at Bettis[13] by cold press and sinter (1750 to 1800°C), cold press and extrude, and cold press and hot forge press (1600 to 1900°F) techniques. The latter process gave the best results from the standpoint of an ideal dispersion structure, minimum UO_2 breakup, and absence of reaction between the niobium and UO_2 and, therefore, is being used for the preparation of irradiation specimens. Some of these materials are being clad at Battelle[19] by a gas pressure-bonding technique.

The effect of fabrication variables on the structure and properties of UO_2–stainless-steel dispersion fuel plates was investigated by Battelle.[38] A detailed analysis was made of the stainless steel and UO_2 powders. Results of

Table I-7 PRE- AND POSTIRRADIATION MEASUREMENTS ON 24 WT.% UN- AND UC-STAINLESS STEEL SPECIMENS*

Fuel compound	Average dimensions, in.			Density, g/cm³	Thickness increase, in.	Density decrease, %	Blister height, in.	Est. max.‡ core temp. during last reactor cycle, °F	Est. burn-up, at.% of U^{235} (dosimeter data)
	Length	Width	Thickness†						
				Preirradiation Measurements					
UN	1.4666	0.6906	0.0456	8.165					
UC	1.4698	0.6895	0.0468	8.085					
UN	1.4655	0.6801	0.0471	8.172					
UC	1.4654	0.6873	0.0473	8.093					
UN	1.4704	0.6884	0.0465	8.157					
UC	1.4707	0.6861	0.0466	8.116					
UN	1.47702	0.6835	0.0461	8.172					
UC	1.4707	0.6896	0.0473	8.144					
				Postirradiation Measurements					
UN	1.4703	0.6912	0.0462	8.135	0.0006	0.37	0	1600	5.4
UC	1.4707	0.6914	0.0476	7.852	0.0008	2.88	0.017	1710	5.6
UN	1.4641	0.6822	0.0482	7.995	0.0011	2.16	0.030	1800	7.7
UC	1.4782	0.6892	0.0480	7.599	0.0007	6.12	0.024	1800	7.8
UN	1.4774	0.6878	0.0469	8.134	0.0004	0.28	0	1490	2.2
UC	1.4781	0.6863	0.0468	8.110	0.0002	0.08	0	1600	2.1
UN	1.4752	0.6838	0.0460	8.173	0.0001	Nil	0	1720	
UC	1.4739	0.6889	0.0474	8.121	0.0001	0.28	0	1490	3.4

* Data taken from reference 20.
† Postirradiation thicknesses are averaged over core area but do not include blister.
‡ Core temperatures are estimated from thermocouple temperatures adjacent to each specimen.

petrographic examination of Hi-Fired, spherical, and hydrothermal UO_2 are given. Radiographs and photomicrographs illustrate how various powder blending methods affect the final structure. The problems associated with the sintering of both elemental and prealloyed stainless-UO_2 mixtures are treated in detail. With elemental powders, the major problem appears to be preventing the gettering of oxygen from iron by chromium. The interrelation among compacting density, dew point of hydrogen sintering atmosphere, weight of furnace charge, and purity level of powders is discussed in the light of preventing the formation of Cr_2O_3. With

high silicon prealloyed stainless powders, the formation of ferrite with subsequent transformation to sigma plus new austenite presents a problem, whereas low silicon prealloyed powders contain a large amount of chromite.

Many variables were investigated during the hot- and cold-rolling studies. It was shown that rolling temperature, reduction rate, core compact density, and extent of cold work each have a significant effect on the core structure.

The final heat-treatment required to place the chromium completely in solution in elemental stainless matrices is evaluated with reference to grain size and the formation of extraneous phases including carbides, ferrite, and sigma.

Mechanical-property data are used to demonstrate that elements prepared with elemental stainless-steel powders have better room-temperature bend ductility, lower high-temperature creep properties, and higher transverse tensile properties than elements prepared with prealloyed powders. It is also noted that the use of spherical UO_2 powders improves, significantly, all mechanical properties tested.

(D. L. Keller)

Refractory Fuel and Fertile Materials

Properties and Behavior of Uranium Oxides

The thermodynamic properties of U_3O_8 have been investigated[39] at low temperatures. In a review of the theory of thermal conductivity,[40] this property of UO_2 was discussed. When the oxide is considered as an insulator, there is no theoretical basis for expecting small or moderate chemical additions to increase its thermal conductivity. It is suggested that the thermal conductivity of UO_2 might be increased by treating it as a potential semiconductor and doping it with the proper elements. Size and valence requirements suggest the replacement of some of the U^{+4} atoms with rare-earth atoms. Radiation damage, fissioning, oxygen content, enrichment, and oxide history are recognized factors which qualify doping as a possible method of improving the thermal conductivity.

During this review period, two subjects dealing with UO_2 were found to be of general interest. Canadian work on UO_2 fuel is presented by Lewis.[41] Separately reported[42] are phase studies of the UO_2-Y_2O_3 and UO_2-ZrO_2 systems.

Hanford[43] has irradiated UO_2 – 1 wt.% PuO_2 powder in a Zircaloy-2 can for one MTR cycle. The density of the powder was 5.0 g/cm^3. During irradiation the heat flux and core temperature were 380,000 Btu/(hr)(sq ft) and 5000°F, respectively. The powder sintered and cored during irradiation but was easily removed from the can. A thin unsintered layer of the powder remained next to the can.

If suitable fuel elements consisting of loose UO_2 powder enclosed in a can could be developed, significant reductions in fuel fabrication cost would be achieved. Several such cans have been irradiated by Hanford[44] under conditions designed to promote UO_2 melting. Zircaloy-3 tubes, 1 in. in outside diameter and 6 in. in length, were filled with 3.2 per cent U^{235}-enriched UO_2 powder and sealed with welded end caps. Powder density was 4 g/ml.

No dimensional changes were observed after thermal-neutron exposures of 1.6 to 2×10^{20} nvt at surface heat fluxes as high as 700,000 Btu/(hr)(sq ft). The UO_2 sintered and relocated permanently to one end of the tube. Average density of the UO_2 in the can was 85 per cent of theoretical. Some evidence supports the belief that UO_2 relocation occurred shortly after the start of the irradiation. Mass transfer of UO_2 by a vaporization-deposition cycle is suspected. A central core, which was molten, extended the entire length of the can. Outside the core, radially oriented, columnar grains extended to a cylindrical crack near the can wall. Between this crack and the wall was a region of smaller grains and a layer of loose UO_2 powder. Proof that columnar grain formation does not necessarily require solidification from the melt is given.

(W. S. Diethorn)

Fabrication of UO_2-containing Ceramics

An investigation of the effects of some process variables on the integrity and diametral uniformity of cold-pressed and sintered UO_2 pellets has been made.[45] The amount of "hour-glassing" was found to increase as the L/D ratio of the pressed pellets was increased from 1 to 2. The amount of lubricant used and the forming pressure also affected hour-glassing. Under the conditions studied, variations in the diameter of individual pellets pressed at 80,000

psi were found to be less than when pellets were formed at higher or lower pressures. Steam sintering was found to give erratic results. Likewise, the use of TiO_2 or CaO additives was shown to give inconsistent results. Pellets containing the additives frequently cracked or hour-glassed badly during sintering.

A study of the effect of CeO_2, Y_2O_3, and Nb_2O_3 additives on the thermal conductivity of UO_2 was conducted by Sylvania.[34] All of the additives reduced the conductivity at temperatures below 600°C. Pure MCW ceramic-grade light UO_2 sintered to as high a density (96 per cent of theoretical) in 4 hr at 1300°C in argon, followed by 1½ hr of reduction in hydrogen at the same temperature, as it did in 15 hr at 1620°C in hydrogen. The argon-sintered specimens contained 5 to 10 μ grains, with most of the pores at grain boundaries. The specimens sintered in hydrogen contained 15 to 25 μ grains, with intergranular pores. The differences in microstructure probably can be ascribed to the difference in sintering temperature.

A tumbling technique was reported by Battelle[46] for coating UO_2 particles with a dense Al_2O_3 coating 300 to 500 μ thick. The coating protected the UO_2 from oxidation when the coated particles were heated in air for 100 hr at 1200 or 1800°F. There was no measurable release of fission products from irradiated, clad particles heat-treated at 1700°F in vacuum for seven days after exposure to 6×10^{12} nv for 1 hr at room temperature. (H. D. Sheets)

Properties of Refractory Fuels Other Than Uranium Oxides

The trend toward ceramic fuels for high-temperature reactors has initiated considerable interest in the oxides and carbides of plutonium. The physical and chemical stabilities of plutonium oxides and carbides diluted with 90 wt.% of other materials were reviewed by Harwell.[47] The other materials evaluated include oxides or carbides of beryllium, magnesium, zirconium, aluminum, silicon, thorium, and uranium. Although the oxides of uranium and thorium offer the best prospect as compatible diluents for plutonium oxide, Al_2O_3 offers the advantages of good thermal-shock resistance and high-temperature mechanical properties. X-ray diffraction studies of the ThO_2-PuO_2 and CeO_2-PuO_2 systems were made by Mulford and Ellinger.[48] Both systems show complete solid solubility as does the UO_2-PuO_2 system. A linear change in the lattice parameter is observed between the end members of these systems. Of the carbides studied at Harwell,[47] SiC appears to be the most suitable diluent for plutonium carbide because of its oxidation resistance. However, further evaluation is needed on TiC and ZrC.

Battelle[19,49] developed casting methods for uranium monocarbide, determined some of the physical properties of the cast material, and has in progress a study of the irradiation behavior of cast UC. Also in progress is a program on the preparation of sintered bodies of UC and UN for a study of irradiation effects. The physical properties[49] of cast UC were essentially the same as those reported in the preceding Review for sintered bodies. However, an increase in hardness was observed in the present work on heating UC for 1 hr at 1500°C. Metallographic study revealed the formation of U_2C_3, indicating that uranium volatilized at this temperature. Specimens of UC irradiated to a burn-up of 5000 Mwd/ton have been examined[19] for density and dimensional changes and fission-gas release. The density decreased by approximately 2.5 per cent, which is in good agreement with the observed increase in diameter of 0.9 per cent. The amount of Kr^{85} released to one capsule during the above irradiation was equal to that expected due to recoil. However, another capsule contained approximately 2.5 times the amount of Kr^{85} that would be expected due to recoil. Macroscopic cracks which were observed after irradiation may have caused the greater release of Kr^{85}. The grain structure, however, was unaffected by this amount of burn-up. (D. A. Vaughan)

Fabrication of Ceramic Fuels Other Than Uranium Oxides

Studies of the sintering of ThO_2 at the Indian Atomic Energy Establishment[50] showed that a density of about 96 per cent of theoretical could be achieved at a sintering temperature of only 1500°C by proper selection of the starting material and initial calcining temperature. The highest density at the 1500°C sintering temperature was obtained with ThO_2 prepared by calcining thorium oxalate at 900°C. Work at Oak Ridge[51a] confirmed reports by previous investigators that the addition of as little as ½ wt.% CaO, as the carbonate or fluoride,

promoted sintering of ThO_2 and that the addition of this amount to a specific ThO_2 powder increased the fired density from about 95 per cent to 99 to 100 per cent of theoretical at a sintering temperature of 1750°C. Attempts by Argonne[51b] to improve the thermal-shock resistance of ThO_2 bodies by the addition of metal powders were not successful. The addition of refractory-metal fibers, however, did produce a pronounced improvement in thermal-shock resistance; additions of as little as 5 wt.% of relatively short and thin fibers of molybdenum or niobium gave the greatest improvement.

The methods employed at Battelle in the preparation of dense compacts of UC, UC_2, UN, UB_2, and UBe_{13} were summarized in a recent report.[52] The carbide bodies were prepared by hydrostatic pressing and vacuum sintering of fine powders made by crushing and grinding of the arc-melted compounds. Uranium carbide bodies (94 per cent of theoretical density) were obtained by sintering at 1850°C compacts that were pressed from 5 μ powder. Sintered densities of about 90 per cent of theoretical were obtained by pressing 5 μ UC_2 powder and sintering at 1820°C. The UBe_{13} was prepared by the solid-solid reaction of hydrostatically compacted powders of UH_3 and beryllium in an argon atmosphere at about 1550°C. The relatively porous compact from this reaction was crushed and ground to a fine powder, then repressed and resintered. The two-step sintering procedure resulted in densities of about 97 per cent of theoretical. Preparation of UN was accomplished by denitriding U_2N_3 at 1300°C in a partial vacuum. The resulting powder was ground to an average particle size of 7 μ, hydrostatically compacted, and sintered in vacuum at 1820 to 1850°C. Bulk densities of about 90 per cent of theoretical were obtained. The highest density achieved in attempts to produce a dense UB_2 compact by vacuum sintering was about 60 per cent of theoretical. Arc melting of the porous sintered compact resulted in densification of the compact, but a uranium-rich phase developed at the grain boundaries. Arc melting a mixture containing 2 wt.% excess boron over the stoichiometric amount resulted in dense specimens showing considerably less of the uranium-rich, grain-boundary phase.

(M. J. Snyder)

Diffusion Studies

Castleman[53] discusses the interdiffusional aspects of the diffusion-bonding problem. Certain idealized cases of core-cladding interdiffusion occurring in single-phase, two-phase, and three-phase systems are examined analytically. In the two-phase and three-phase systems, the importance of the roles played by the boundary and interface concentrations and the diffusion coefficients in controlling interface movement and interdiffusion is evaluated in detail.

Diffusion is being studied at Hanford in the uranium/niobium/X-8001 system and in AlSi bonded, X-8001 clad uranium slugs to determine the growth of the UAl_3 layer when the slugs are autoclaved at 300°C for long periods of time.[54] In addition, penetration of uranium into the X-8001 cladding in AlSi bonded, depleted uranium slugs is also being studied.[55]

Sylvania[56] has been investigating the interdiffusion in the aluminum-uranium system and the effects thereon of applied pressure. In confirmation of the results of other investigations, it has been found that UAl_3 layer growth is accelerated by increasing the applied pressure. The growth kinetics are characterized by a transient period, during which growth occurs nonparabolically, followed by a steady-state period of parabolic growth. Interesting correlations are shown to exist between annealing time, annealing temperature, and applied pressure on the one hand, and the nature and distribution of structural defects in the UAl_3 diffusion zone on the other.

The French[57] have studied the interdiffusion in the zirconium-uranium system to determine with precision the coefficients of diffusion in the gamma phase (body-centered cubic) and to contribute important information concerning the mechanism of diffusion. The techniques employed were micrography, Castaing's electronic microprobe, microhardness, and autoradiography. A very marked Kirkendall effect is demonstrated when diffusion is effected in the body-centered cubic phase. Values for the diffusion coefficients, activation energies, and the frequency factors as a function of the concentration are given, and variations in the three quantities are noted.

An investigation of the constitution of the uranium-niobium alloys is being conducted at

Battelle.[20] Diffusion couples are being employed to establish the composition limits of the gamma-phase immiscibility gap in the system. Diffusion coefficients are being determined at several temperatures. The diffusion data for a couple heated at 1000°C for 50 hr have been analyzed graphically by the Matano method, and the initial results are presented in Table I-8.

Table I-8 DIFFUSION COEFFICIENTS FOR THE URANIUM-NIOBIUM SYSTEM AT 1000°C*

Uranium content (balance niobium), at.%	Diffusion coefficient (D), 10^{-12} cm^2/sec
5	1.7
10	1.9
20	2.6
30	2.7
40	1.4
50	1.4
60	1.4
70	2.1
80	3.5
90	11.1
95	12.1

* Data taken from reference 20.

A literature survey on diffusion in reactor materials is being performed by Nuclear Metals,[32,58,59] and progress has been made in the first and second phases of the diffusion program, solid-liquid and solid-solid interactions. The third phase of the program will study solid-liquid-solid interactions. Dip type experiments are to be performed for the solid-liquid-interaction studies. The materials to be studied are Grade I crystal-bar and annealed zirconium, type 304 stainless steel, uranium with high carbon content, and fissium. Dipping temperatures will range from 1150 to 1450°C. For the solid-solid-interaction studies, disks of materials are to be bonded together in the form of diffusion-couple sandwiches. An attempt was made to bond a complete sandwich of vanadium, uranium, iron, uranium, zirconium, uranium, titanium, uranium, and niobium by heating to 750°C and slow cooling; this resulted in bonding some of the pieces into the following sandwiches: iron, uranium, zirconium, and uranium, titanium, uranium. An iron-uranium sandwich was also bonded at 650°C. Metallographic examination showed interaction between the bonded components of the samples. The bonded samples were heat-treated at 700°C for two days and examined metallographically. Several attempts were made to bond vanadium, uranium, niobium sandwiches by heating the samples to temperatures between 750 and 900°C; although some interaction took place, the sandwiches broke during disassembly of the bonding jig. Other methods of surface preparation will be tried to overcome this difficulty.

Diffusion-zone studies have been performed at Bettis[13] with roll-bonded samples composed of Zircaloy-2 and various niobium and zirconium-base alloys. The diffusion anneal was carried out at 788 and 850°C for times up to 16 hr. The over-all growth of the diffusion zones obtained in these couples was measured as a function of time at temperature. Tentative values for the parabolic rate constant for each couple investigated are presented.

(M. A. Gedwill, Jr.)

Mechanism of Corrosion of Fuel Alloys

Theoretical considerations and experimental data for interpreting the corrosion behavior of uranium in several media at temperatures up to 250°C have been reviewed in a recent report issued by Los Alamos.[60] The theory proposes that lattice defects and electrical conduction in the UO_2 corrosion film are responsible for the diffusion of oxygen ions. The reaction rate is believed to be diffusion controlled and is determined by the gradient of lattice defects across the film. On the basis of several assumptions, it is shown that a gradient exists which is dependent upon the sixth root of oxygen pressure.

The detailed quantitative corrosion behavior of uranium is variable and is believed to depend upon various conditions prevailing at the surface. It is felt that neither the condition of fabrication nor impurities in the metal influence the corrosion rate but that the oxygen and moisture content of the environment appear to have a significant effect.

The observed variability in corrosion rates is qualitatively explained if it is assumed that a number of competing, as well as successive, reactions occur simultaneously on the uranium surface and that the rate of several of these reactions is strongly influenced by impurities in the gas corrodent. (W. E. Berry)

Basic Studies of Radiation Effects in Fuel Materials

Distortion of Uranium

A Russian report[61] describes the effects of irradiation upon growth of textured uranium and upon the surface distortion of nontextured uranium. The effects of metallurgical variables, such as grain size and heat-treatment for material rolled at 500°C, are reported for a large number of radiation tests. The effects of small amounts of iron, silicon, and aluminum in combination upon the heat-treating characteristics of uranium are also described.

The "area weight" method for compensating for the nonuniform spatial distribution of the poles of diffraction planes in preferred orientation studies is described in a report from the National Lead Co.[62] The technique described gave better than a twofold improvement in precision compared with a previous method.

The status of experiments to evaluate the role of anisotropic diffusion in the dimensional instability of uranium is reported by Sylvania.[63] Self-diffusion coefficients in different crystallographic directions are being rechecked, and various irradiation tests to clarify further the effect of grain size on growth have been initiated.

A report from the United Kingdom[64] describes the electropolishing and metallographic examination of single crystals of uranium irradiated to about 0.025 per cent burn-up at 200 and 500°C. Severe twinning, which is a common feature of irradiated polycrystalline uranium, did not occur in the single crystals, although they had grown extensively. It is concluded that the pronounced twinning of polycrystalline uranium bars during irradiation arises from the mutual restraint to growth of adjacent grains. These results are not viewed as conflicting with postulated plastic-deformation mechanisms which assume twinning occurs due to fission spikes, since such twins would be too small to be seen optically and would quickly anneal back onto the matrix.

Swelling and Fission-gas Release in Uranium

Alloying of uranium fuel is being studied at Argonne[10] as a means of controlling swelling. The approach taken is based upon research indicating that vacancies tend to be associated with krypton or xenon atoms in a metal lattice. By introducing 0.01 to 0.1 at.% of elements such as cerium or yttrium into the lattice in solid solution, it is believed that the solute atoms will tend to act as gas-atom traps by sharing a vacancy with gas atoms. Such a combination of atoms and vacancies would be less mobile, of course, than single atoms or atom-vacancy pairs.

A study of the escape of fission krypton from uranium by heating and analyzing the evolved gas has been conducted in the United Kingdom.[65] Diffusion coefficients were determined from 300 to 900°C, but the release rates did not follow those predicted by diffusion theory. Grain-boundary diffusion is believed to be responsible for this lack of agreement and for large variations in release rate observed for different specimens at the same temperature. Above 900°C, swelling and cracking occurred, releasing gas rapidly. No evidence was found to indicate that release rates were reduced by trapping of gas internally in bubbles.

At Hanford, various studies related to the problems of swelling in uranium are in progress. High-purity uranium is being prepared for in-reactor swelling studies, and study of fission-product mobility in samples impregnated with rare gases by glow-discharge techniques is in progress.[66] Extensive use of electron microscopy is being made to observe fission-gas voids in irradiated uranium. In this research, pores of 200 to 400 A diameter have been observed at burn-ups as low as 0.01 total at.%. These bubbles become numerous at higher burn-ups. At temperatures of irradiation less than 300°C, the holes or pores are randomly distributed,[66] although a later report of samples irradiated to 0.2 total at.% burn-up indicates clustering occurs in local areas.[67] Larger pores have also been observed. For example, a slug irradiated to 0.2 per cent burn-up at a center temperature of about 420°C had pores ranging in size from 2000 to 20,000 A.[66] In another sample having 0.2 per cent burn-up, and which operated near the melting point of uranium, pores up to 40 μ in diameter were observed.[53] Indications of correlation between microstructural features and pore location were observed in another sample where the center temperature was such as to produce a structure similar to the beta-treated structure of unirradiated uranium. In this case, many pores fell upon grain boundaries and tended to be aligned with crystallographic or twin boundaries.[43]

A report from the United Kingdom describes the release of fission gas from a zirconium–5 wt.% uranium alloy during neutron irradiation.[68] The release is reported to be independent of temperature up to 600°C and is accounted for by recoils from the surfaces. Above 600°C the release increases sharply and diffusion coefficients have been calculated for the range 700 to 900°C. The activation energy for this range is about 23 kcal/mole.

Properties of Uranium

A Russian paper[61] describes and compares creep tests of irradiated and unirradiated uranium. In-pile creep rates are reported to be as much as 50 to 100 times those out of pile. Other effects are also reported. In interpreting such data, it is important to know the thermal history precisely since small temperature cycles can have a great effect upon creep rates of uranium. Short-time tensile tests have also been conducted in a flux of 6×10^{12} nv. Even though the specimens were in the flux for only 30 to 60 min, the elongation was decreased and the ultimate strength was increased markedly.

A series of low-temperature, short-exposure irradiations is being conducted by Hanford[67] to determine the amount of damage induced in uranium by irradiation and the ease of removal of the damage. Exposures range from 10^{15} to 10^{18} nvt, or from 5×10^{-7} to 5×10^{-4} total at.% burn-up. Postirradiation tensile, hardness, and annealing tests are being performed. The data to date suggest that the occurrence of twinning, which is the primary mode of deformation of uranium at room temperature, is highly dependent upon the dispersion and size of point-defect clusters. (F. A. Rough)

References

1. C. L. Angerman, R. T. Huntson, and W. R. McDonell, Grain Refinement of Uranium by a Beta-quench, Alpha-anneal Process, DP-328, February 1959. (Confidential AEC report.)
2. W. H. Hodgson and R. E. Olson, Alpha Extended Solid Uranium Fuel Elements, Production Test, HW-48918(Del.), Oct. 29, 1958. (Secret AEC report.)
3.* G. Y. Sergeyev et al., The Influence of Fabrication Methods on Structure and Properties of Uranium, A/CONF. 15/P/2307.
4. J. S. Llewelyn Leach, Surface Oxide Films and the Breakaway Corrosion of Uranium, *Nature*, 182: 1085-1086, Oct. 18, 1958.
5.* A. A. Bochvar, V. G. Kuznetsova, and V. S. Sergeev, Self-Diffusion of Uranium in the Gamma Phase, A/CONF. 15/P/2306.
6. D. Rhodes and V. W. Eldred, The Swelling of 0.17% Burn-up Uranium on Postirradiation Annealing, IGR-TN/W-933, August 1958. (Unclassified British report.)
7. A. G. Harding and M. B. Waldron, Transformations in Uranium Alloys with High Solute Solubility in the Body-centered-cubic Gamma Phase. Part I, Preliminary Observations on the "Banded Structures" Produced by Nonequilibrium Transformation in Uranium Alloys, AERE-M/R-2673, September 1958. (Unclassified British report.)
8. A. G. Harding, M. B. Waldron, and C. Knight, Transformation in Uranium Alloys with High Solute Solubility in the Body-centered-cubic Gamma Phase. Part II, Transformation in Uranium Alloys of 5, 10, 15, and 20 At.% Titanium on Quenching from the Gamma Phase, AERE-M/R-2673A, December 1958. (Unclassified British report.)
9. I. Sheinhartz and J. L. Zambrow, Dimensionally Stable Uranium Alloys. III. Uranium-Carbon Alloys, SCNC-269, February 1959. (Confidential AEC report.)
10. R. R. Nash, editor, Nuclear Fuels Newsletter, WASH-705, February 1959. (Confidential AEC report.)
11.* B. W. Howlett and A. G. Knapton, The Alloy Systems Uranium-Titanium, Uranium-Zirconium, and Uranium-Titanium-Zirconium, A/CONF. 15/P/1469.
12. Technical Progress Report — Pressurized Water Reactor (PWR) Project for the Period Oct. 24, 1958, to Dec. 23, 1958, WAPD-MRP-77. (Unclassified AEC report.)
13. Westinghouse Electric Corp., March 1959. (Unpublished.)
14. Enrico Fermi Power Plant, APDA-124, January 1959. (Unclassified AEC report.)
15. P. E. Madsen, A Note on the Metallography of the Hydride Phase in Gamma-stabilized Uranium-Molybdenum Alloys, AERE-M/M-208, November 1958. (Unclassified British report.)
16. V. V. Kahashnikov et al., Uranium-Molybdenum Alloys in Reactor Design, *Atomnaya Energiya*, 5: 421-431 (October 1958).
17.* G. Cesoni and G. Shileo, Burn-up Poisons in Aluminum-Uranium Alloys, A/CONF. 15/P/1402.
18. W. C. Thurber and R. J. Beaver, Development of Silicon Modified 48 Wt.% U-Al Alloys for Aluminum Plate Type Fuel Elements, ORNL-2602, Mar. 23, 1959. (Unclassified AEC report.)
19. R. W. Dayton and C. R. Tipton, Jr., Progress Relating to Civilian Applications During March 1959, BMI-1330, Apr. 1, 1959. (Confidential AEC report.)
20. R. W. Dayton and C. R. Tipton, Jr., Progress Relating to Civilian Applications During February

1959, BMI-1324, Mar. 1, 1959. (Confidential AEC report.)
21. T. I. Jones, The Irradiation of Al-Pu Alloys in Zircaloy Sheathing. Part I, Preliminary Experiments with Al-U Alloys, CRFD-810, December 1958. (Unclassified Canadian report.)
22. William V. Johnston, The Swelling of Irradiated U–22 Wt.% Alloys During Temperature Transients, Nuclear Engineering & Science Conference, Preprint V-106, April 6–9, 1959.
23. C. E. Lacy and E. A. Leary, Irradiation Performance of Highly Enriched Fuel, KAPL-1952, June 20, 1958. (Unclassified AEC report.)
24. R. W. Dayton and C. R. Tipton, Jr., Progress Relating to Civilian Applications During January 1959, BMI-1315, Feb. 1, 1959. (Confidential AEC report.)
25. U. S. Atomic Energy Commission, January 1959. (Unpublished.)
26. John E. Deverell, The Thermal Conductivity of a Molten Pu-Fe Eutectic (9.5 At.% Fe), LA-2269, July 1958. (Unclassified AEC report.)
27. E. L. Francis, comp., Thorium Data Manual, IGR-R/R-303, 1958. (Unclassified British report.)
28. Riccardo Ferro, The Crystal Structures of $ThHg_3$, $ThIn_3$, $ThTl_3$, $ThSn_3$, and $ThPb_3$, *Acta Crystallographica*, 11: 737-738 (October 1958).
29. D. J. Livesey, Variation with Temperature of Young's Modulus for Some Uranium Alloys and for Thorium, Vanadium, and Niobium, IGR-TN/W-953, June 1958. (Unclassified British report.)
30. P. E. Armstrong and O. N. Carlson, Elastic Constants of Thorium Single Crystals, ISC-993, June 1957. (Unclassified AEC report.)
31. R. S. Neymark, Rate of Alloying of Metal Fuels with Stainless Steel Above 1500°F, Nuclear Engineering & Science Conference, Cleveland, Ohio, Preprint V-89, Apr. 6, 1959.
32. Fundamental and Applied Research and Development in Metallurgy, NMI-2072, Jan. 13, 1959. (Secret AEC report.)
33. R. W. Dayton and C. R. Tipton, Jr., Progress Relating to Civilian Applications During December 1958, BMI-1307, Jan. 1959. (Confidential AEC report.)
34. L. W. Kates, Quarterly Technical Progress Report for Period Ending Dec. 31, 1958, SCNC-283, February 1959. (Confidential AEC report.)
35. Roger Conant Waugh, The Reaction and Growth of Uranium Dioxide–Aluminum Fuel Plates and Compacts, ORNL-2701, Mar. 23, 1959. (Unclassified AEC report.)
36. Robert J. Akin, Zero Power Test Manufacturing Report, MND-MPR-1580, December 1958. (Unclassified AEC report.)
37. D. L. Keller et al., Fabrication Development and Irradiation of Uranium-Molybdenum Alloy–UO_2 Dispersions, BMI-APDA-647, Mar. 12, 1959. (Unclassified AEC report.)
38. Stan J. Paprocki et al., Battelle Memorial Institute, Feb. 18, 1959. (Unpublished.)
39. E. F. Westrum, Jr., and F. Gronvold, Low-temperature Heat Capacity and Thermodynamic Functions of U_3O_8, AECU-3924, 1958. (Unclassified AEC report.)
40. V. J. Tennery, Review of Thermal Conductivity and Heat Transfer in Uranium Dioxide, ORNL-2656, Apr. 23, 1959. (Unclassified AEC report.)
41. W. B. Lewis, Uranium Dioxide, DL-34, Dec. 8, 1959. (Unclassified Canadian report.)
42.* N. M. Voronov, E. A. Voitekhova, and A. S. Danilin, Phase Equilibrium Diagrams of Systems UO_2-ZrO_2 and ThO_2-ZrO_2, A/CONF. 15/P/2490.
43. F. W. Albaugh, Hanford Atomic Products Operation, Feb. 15, 1959. (Unpublished.)
44. J. L. Bates and W. E. Roake, Irradiation of Fuel Elements Containing UO_2 Powder, Nuclear Engineering & Science Conference, April 6–9, 1959, Cleveland, Ohio, Preprint V-90, Apr. 6, 1959.
45. R. W. Garbe and H. E. Walchli, Quarterly Progress Report for the Period July 1 to Sept. 30, 1958, YAEC-97, Nov. 14, 1958. (Unclassified AEC report.)
46. A. K. Smalley, W. C. Riley, and W. H. Duckworth, Alumina-clad UO_2 for Fuel Applications, BMI-1321, Feb. 18, 1959. (Unclassified AEC report.)
47. L. E. Russell and J. Williams, Atomic Energy Research Establishment, March 1958. (Unpublished.)
48. R. N. R. Mulford and F. H. Ellinger, ThO_2-PuO_2 and CeO_2-PuO_2 Solid Solutions, *The Journal of Physical Chemistry*, 62(11): 1466-1467 (November 1958).
49. A. C. Secrest, Jr., E. L. Foster, and R. F. Dickerson, Preparation and Properties of Uranium Monocarbide Castings, BMI-1309, Jan. 2, 1959. (Unclassified AEC report.)
50.* S. K. Kantan, R. V. Raghavan, and G. S. Tendolkar, Sintering of Thorium and Thoria, A/CONF. 15/P/1705.
51. Thorium-U^{233} Symposium, BNL-483, Jan. 9–10, 1958. (Unclassified AEC report.)
    a. C. E. Curtis, Calcination of Thorium Oxide for Slurries and Suspensions, p.119, Oak Ridge National Laboratory, Oak Ridge, Tenn.
    b. J. H. Handwerk, The Fabrication of Thoria and Thoria-Urania, p.113, Argonne National Laboratory, Lemont, Ill.
52. Arch B. Tripler, Jr., M. Jack Snyder, and Winston H. Duckworth, Further Studies of Sintered Refractory Uranium Compounds, BMI-1313, Jan. 27, 1959. (Unclassified AEC report.)
53. Louis S. Castleman, An Analytical Approach to the Diffusion Bonding Problem, *Nuclear Science and Engineering*, 4: 209-226 (October 1958).
54. F. W. Albaugh, Hanford Atomic Products Operation, Mar. 15, 1959. (Unpublished.)
55. Hanford Atomic Products Operation, Oct. 15, 1958. (Unpublished.)

56. Fundamentals of Diffusional Bonding — III. Third Annual Progress Report for June 30, 1957, to June 30, 1958, SEP-251, June 30, 1958. (Unclassified AEC report.)
57. Y. Adda, C. Mairy, and P. Bouchet, Study of Uranium-Zirconium Diffusion, AEC-tr-3503, February 1957. (Unclassified AEC translation.)
58. Fundamental and Applied Research and Development in Metallurgy, Progress Report for July 1 Through Oct. 31, 1958, NMI-2071, Nov. 28, 1958. (Secret AEC report.)
59. Fundamental and Applied Research and Development in Metallurgy, Progress Report for December 1958, NMI-2073, Feb. 10, 1959. (Secret AEC report.)
60. James T. Waber, A Review of the Corrosion Behavior of Uranium, LA-2035, April 1956. (Unclassified AEC report.)
61.* V. V. Titora, B. M. Levitsky, and Y. N. Sokursky, Influence of Uranium Structure and Properties Upon Its Behavior Under Irradiation, A/CONF. 15/P/2191.
62. P. R. Morris, Summary Technical Report for the Period Oct. 1 to Dec. 31, 1958, NLCO-775. Jan. 22, 1959. (Confidential AEC report.)
63. R. Resnick, L. S. Castleman, and L. Seigle, Dimensional Instability of Uranium — III. Third Annual Progress Report for June 30, 1957, to June 30, 1958, SEP-249, June 30, 1959. (Unclassified AEC report.)
64. V. J. Haddrell and E. C. Sykes, The Metallographic Examination of Some Single Crystals of Uranium Irradiated at 200 and 500°C, AERE-M/R-1518A, November 1958. (Unclassified British report.)
65. J. F. Walker, The Escape of Krypton from Irradiated Uranium on Heating, IGR-TN/W-1046, 1959. (Unclassified British report.)
66. J. C. Tobin, Basic Swelling Studies, in "Quarterly Progress Report Fuels Development Operation, July, August, and September, 1958," HW-58205, Oct. 15, 1958. (Secret AEC report.)
67. F. W. Albaugh, Hanford Atomic Products Operation, Jan. 15, 1959. (Unpublished.)
68. F. J. Stubbs and C. B. Webster, The Release of Fission Product Rare Gas from A Uranium-Zirconium Alloy During Irradiation in the BEPO Reactor, AERE-C/M-372, February 1959. (Unclassified British report.)

*Second United Nations International Conference on the Peaceful Uses of Atomic Energy, Geneva, September 1958. (Individual papers available from the Office of Technical Services, Dept. of Commerce, Washington 25, D. C. Bound volumes of papers are available from United Nations, Office of Public Information, New York.)

Graphite

Results of thermal-conductivity measurements at the University of Buffalo on various types of graphites[1] indicate that, at temperatures between 200 and 3000°C, conductivity depends mainly on the type of filler used rather than on the binder type. For the samples tested, no effect of particle size on thermal conductivity was observed.

A preliminary reactor evaluation of three types of graphite-UO_2 fuel elements in the form of 1.5-in.-diameter spheres containing about 5.3 g of 93.2 per cent enriched UO_2 was carried out at Battelle.[2] The three types differed considerably in fuel particle size and degree of graphitization of the graphite. The elements were irradiated in the Battelle Research Reactor to about 1.8 at.% burn-up of the U^{235}, with surface temperatures of 1200 to 1300°F. Postexposure hot-cell examination revealed no radiation-induced changes in dimensions or mechanical properties that would prove detrimental to the operation of a pebble-bed reactor. The observed changes in mechanical properties indicated a tendency for the graphite to revert to a carbon structure. Dimensional shrinkage in elements containing fuel particles 1 μ in diameter exceeded shrinkage in elements containing fuel particles 150 μ in diameter by a factor of 4. (W. C. Riley)

Beryllium Metal and Alloys

Martin Company data[3] comparing ductility in the thickness direction of QMV beryllium sheet fabricated by upsetting, hot pressing, and extruding and rolling are presented in Fig. 1. The superiority of upset material (presumably due to random grain orientation) is especially marked at high values of the width-thickness ratio. The results are encouraging; however, it is not known whether randomly oriented upset material can be satisfactorily produced on a scaled-up basis.

Beryllium-alloy development studies are being carried out by Brush Beryllium.[4] Binary alloys with 3 wt.% of tin, nickel, copper, and silver have been prepared and tested for mechanical properties. Unfortunately, the tensile properties were not improved significantly by these additions.

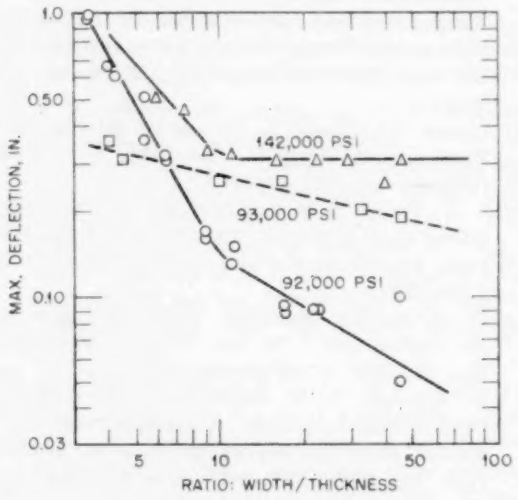

Figure 1 — Ductility in thickness direction (as measured by maximum deflection in bending) of beryllium sheet fabricated by different methods. ○, extruded 12:1, rolled perpendicular to the extruded direction 5:1. □, hot-pressed. △, upset 6:1. Numbers near curves represent average fracture strength in bending. Note that all strips were 0.088 ± 0.002 in. thick by 3.00 ± 0.010 in. long; fracture strength in bending calculated from strips over 1 in. wide. Data taken from reference 3.

To fabricate fuel-capsule end closures from presently available QMV beryllium,[5] Oak Ridge workers machined tubing from QMV bar stock and welded end plugs of various designs to the tubing. No mechanical-property data were reported for welded material; the amount of weld-metal cracking was found to be influenced strongly by the plug design.

Work continues on the Alloyd Research Corporation program to study techniques for producing a small quantity of high-purity beryllium metal.[6] Because of the high vapor pressure of beryllium, zone refining in moderate vacuum has been found impractical. A small amount of beryllium has

been produced by the reduction of purified $BeCl_2$ with high-purity sodium. Purity and properties of the beryllium so produced have not yet been reported. Further experiments will use $BeCl_2$ purified by zone refining.

A revision of an earlier procedure for the determination of oxygen in beryllium has been published by Harwell.[7] The method enables oxygen concentrations down to 0.02 wt.% to be determined by strictly chemical procedures. The revised reagents permit easier dissolution of sintered beryllium.

Several review publications dealing with beryllium have appeared recently. The Library of Congress has summarized the thermal properties of beryllium, as well as those of other metals.[8] Data are presented on heat capacity, thermal conductivity, emissivity, thermal diffusivity, and thermal expansion. A comprehensive bibliography is included. The Health and Safety Laboratory has recently published a summary of 10 years of experience on health protection in beryllium facilities.[9] (A. J. Griest)

Beryllium Compounds

Atomics International[10] analyzed the tensile creep of hot-pressed BeO with reference to the vacancy-diffusion mechanism proposed by Nabarro and Herring. Comparison of the observed and calculated creep rates, summarized in Table II-1, confirmed the vacancy-diffusion

Table II-1 COMPARISON OF OBSERVED AND CALCULATED CREEP RATES OF HOT-PRESSED BeO UNDER TENSILE STRESS OF 108 PSI*

	Steady-state creep rate, %/hr	
Temp., °C	Observed	Calculated
1650	0.33	0.26
1700	0.72	0.54
1745	1.49	1.02

*Data taken from reference 10.

mechanism. Analysis of the BeO creep data by this concept gave an experimental activation energy for tensile creep of 114,000 cal/mole. Research at Battelle on hot-pressed BeO ceramics indicated that at 1510°C a compressive stress of about 350 psi produced 2 per cent deformation in 100 hr.

An exploratory study of fusion behavior and grain growth in the BeO-UO_2-ThO_2 system was reported by Harwell.[11] It was concluded that the maximum permissible operating temperature for a ceramic fuel element in this system would be the solidus temperature, about 2100°C.

Denton and Murray[12] concluded that locally accelerated or "cannibal" grain growth observed in BeO ceramics was related to a wide particle-size distribution in the starting powder. A similar tendency toward exaggerated local crystal growth was observed by Battelle investigators in BeO ceramics containing 1 wt.% Al_2O_3 added as a grain-growth inhibitor. The effect was attributed to nonuniform distribution of the Al_2O_3 in the BeO ceramic. Theories of crystal growth indicate that the observed duplex microstructure stems from both chemical and physical asperities in the starting powder. (John Quirk)

Solid Hydrides

The hydrides of zirconium and its alloys have received the greatest emphasis in recent research. The phase diagrams of these systems are being determined with increasingly greater precision.

Zirconium Hydride

In thesis research done at Westinghouse, it was found[13] that hydrogen can be added to zirconium by gaseous equilibration with zirconium of an initially higher hydrogen concentration. A low level of contamination by oxygen and nitrogen with a minimum of effort seems to be the chief advantage of this technique. It was observed also that dissolved oxygen reduces the absorption of hydrogen by zirconium in amounts proportional to both the oxygen and the hydrogen content.

Hydriding studies with Zircaloy-2 samples at Knolls[14] have shown that geometrically similar specimens may be batch-hydrided to the same hydrogen level, by a technique using a degassing vacuum anneal, regardless of variations in elapsed time up to 25 days between the pickling treatment and the hydrogenation treatment. The samples were pickled for 30 sec in a 50-47-3 vol.% solution of HNO_3-H_2O-HF and exposed to air for periods up to 25 days before hydriding.

Zirconium-Uranium Alloy Hydrides

Hydrogen-absorption isotherms have been determined at Battelle[2,15] to establish the phase diagram of the zirconium – 25 wt.% uranium alloy

hydride system. The latest data are presented in Table II-2. The phases present at different temperatures are being verified by high-temperature X-ray diffraction studies.

Table II-2 PHASE BOUNDARIES IN THE ZIRCONIUM–25 WT.% URANIUM ALLOY HYDRIDE SYSTEM*

Phase boundary	572°C		835°C	
	Hydrogen absorption, cm^3/g	Pressure, cm of Hg	Hydrogen absorption, cm^3/g	Pressure, cm of Hg
1	23.2	0.024	40.6	5.0
2	†	†	48.8	5.0
3	†	†	93.8	26.8
4	116.5	0.024	136.0	28.3

*Data taken from references 2 and 15.

†Only two phase boundaries were found at this temperature.

Table II-3 THE SOLUBILITY OF HYDROGEN IN NIOBIUM AT VARIOUS PRESSURES*

(Temperature, 673°C)

Pressure, atm	Solubility, gram-atom H per gram-atom Nb
1	0.126
5	0.534
10	0.558
20	0.593
30	0.595
50	0.620
100	0.643
300	0.690
500	0.715
800	0.728
1000	0.732

*Data taken from reference 16.

Niobium Hydride

The effect of pressure on the solubility of hydrogen in niobium has been reported by Perminov.[16] A large increase in solubility was noted between 1 and 5 atm pressure, with a gradual increase as the pressure was raised to 1000 atm. The data are given in Table II-3.

(H. H. Krause)

References

1. S. Mrozowski et al., Investigation of Elastic and Thermal Properties of Carbon-base Bodies, WADC-TR-58-360, December 1958. (Unclassified USAF report.)
2. R. W. Dayton and C. R. Tipton, Jr., Progress Relating to Civilian Applications During January 1959, BMI-1315, Feb. 1, 1959. (Confidential AEC report.)
3. C. J. Giemza, Beryllium Structural Development, Phase II, Contract No. AF 33(616)-5780, The Martin Company Progress Report No. 15, Period Ending Jan. 31, 1959. (Unclassified.)
4. J. G. Klein, L. M. Perelman, and W. W. Beaver, Development of Wrought Beryllium Alloys of Improved Properties. Progress Report No. 5, Oct. 1, 1958, to Dec. 31, 1958, Brush Beryllium Co., Dec. 31, 1958.
5. Gas-cooled Reactor Project Semiannual Progress Report for Period Ending December 31, 1958, ORNL-2676, Mar. 16, 1959. (Unclassified AEC report.)
6. M. Basche, Research on the Problems of Ductility in Beryllium, Progress Report No. 5, Alloyd Research Corporation, Jan. 31, 1959.
7. C. G. Wallace, An Improved Procedure for the Volumetric Determination of Oxide in Beryllium Metal, AERE-C/R-2509, November 1959. (Unclassified British report.)
8. T. C. Goodwin, Jr., and Mauree W. Ayton, Thermal Properties of Certain Metals, Part II, WADC-TR-56-423(Pt.II), September 1958. (Unclassified USAF report.)
9. A. J. Breslin and W. B. Harris, Health Protection in Beryllium Facilities. Summary of Ten Years of Experience, HASL-36, May 1, 1958. (Unclassified AEC report.)
10. Roger Chang, Creep of Polycrystalline BeO at High Temperatures and Low Stresses, NAA-SR-2458, May 1, 1958. (Unclassified AEC report.)
11. K. D. Reeve, An Exploratory Study of the BeO-UO_2-ThO_2 System, AERE-M/R-2727, December 1958. (Unclassified British report.)
12. I. Denton and P. Murray, A Note on Grain Growth in Fabricated Beryllia, *Transactions of the British Ceramic Society*, 38(1): 35-39 (January 1959).
13. John J. Kearns, Laboratory Method for Adjusting the Hydrogen Content of Zirconium, WAPD-TM-147, May 26, 1958. (Unclassified AEC report.)
14. A. E. Bibb and A. H. Alberts, Effect of Surface Condition on the Rate of Hydrogen Pickup in Zircaloy-2, KAPL-M-AEB-4, August 1958. (Unclassified AEC report.)
15. R. W. Dayton and C. R. Tipton, Jr., Progress Relating to Civilian Applications During February 1959, BMI-1324, Mar. 1, 1959. (Confidential AEC report.)
16. P. S. Perminov, The Effect of Pressure on the Solubility of Molecular Hydrogen in Niobium and Tantalum, *Doklady Akademii Nauk S.S.S.R.*, 121: 1041-1042 (August 1958).

The results of an extensive literature search dealing with the chemistry of boron and boron compounds have been compiled by W. E. Bost. The publications cover AEC classified[1] and recent unclassified[2] report literature.

Metals and Alloys for Control Rods and Burnable Poisons

Hafnium

Preliminary data at Bettis indicate that hafnium strip produced by electron-melting sponge hafnium is equivalent to crystal-bar hafnium with respect to tensile and corrosion properties and fabricability.

Silver-Indium-Cadmium Alloys

The effect of boric acid on the corrosion behavior of unplated silver–15 wt.% indium–5 wt.% cadmium in 600°F, semidynamic (0.1 fps) water has been investigated.[3] In water containing LiOH, Bettis found that 9145 ppm H_3BO_3 (1600 ppm boron) decreased the weight gain from 107 mg/(dm^2)(month) (without H_3PO_3) to 34 mg/(dm^2)(month). In a KOH solution, 9145 ppm H_3BO_3 decreased the corrosion rate from 76 to 21 mg/(dm^2)(month).

Knolls[4] has issued a report which contains a résumé of work done at Knolls on silver–15 wt.% indium–5 wt.% cadmium alloys since July 1957.

(V. W. Storhok)

Control and Burnable-poison Dispersions

In a Los Alamos study of Boral reactor-control material, 5 wt.% B^{10} of particle size less than 0.8 μ in diameter was incorporated in an aluminum matrix. Small additions of manganese, copper, nickel, and magnesium were tested as a possible means of improving fabricability. Copper (4 to 5 wt.%) was thought to improve rollability, but no conclusive data were obtained. Additions of 1.2 wt.% manganese seemed to make the pressing temperature less critical and did not alter the rolling characteristics of the compacts. Metal powders used in the study were minus 325 mesh. The reactor-control material was prepared by hot pressing a mixture of 93.8 wt.% aluminum, 1.2 wt.% manganese, and 5 wt.% B^{10} powders at 1000 psi and 550°C in graphite dies. The compacts were rough machined, annealed at 440°C for several hours, reduced 10 per cent in thickness, annealed several hours at 440°C, and reduced to the final size of 0.040 in.

In work at Knolls on B_4C-Zircaloy dispersions,[4,5] the use of spherical B_4C particles has been shown to result in extrusions with far less breakup and stringering of B_4C; unfortunately, all B_4C produced at Knolls or by outside vendors contains 20 to 30 wt.% of free graphite. During extrusion the graphite forms stringers, which are believed to be the cause of low transverse mechanical properties, poor corrosion resistance, and high leak rate of the B_4C-Zircaloy dispersions. A major effort is now being directed toward the production of B_4C with little or no excess carbon or free boron. Spherical B_4C is prepared by sintering boron carbide fines in a graphite crucible or by heating angular particles in a graphite tube furnace just below the melting point of B_4C. Other than a high-temperature plasma jet process, no commercial methods are reported. The plasma jet process resulted in approximately 40 wt.% free boron.

Homogeneity of the dispersion is reported to be a function of the ratio of the number of Zircaloy-2 particles to the number of B_4C particles, i.e., with a ratio greater than 3:1 the homogeneity is good, but ratios of less than 2:1 result in poor distribution of the B_4C. As a method of testing soundness of the core and the effect of "waterlogged" cores under reactor conditions, clad specimens are defected by drilling 0.0135- and 0.030-in. holes halfway through the core and the elements waterlogged by heating 3 days in 680°F water. They are then immersed in an 850°F salt bath. The cladding of 5 out of 16

strips tested in this way bulged in height ranging from 3 to 22 mils. Only those specimens showing high leak rate ($>1 \times 10^{-5}$ cm^3/sec helium STP) bulged. Resistance-welding methods continue to be investigated as a method of cladding, and, although the method is reported as promising, completely satisfactory results still have not been obtained.

Postirradiation examination of a large number of B_4C-Zircaloy dispersions, B_4C-Al_2O_3 dispersions, B_4C-ZrB_2 dispersions, and boron–stainless-steel alloys is in progress. Results reported to date are given in Tables III-1 to III-4. Apparently, the data cannot be correlated to give a relation between burn-up and swelling. Postirradiation annealing of B_4C-Zircaloy specimens at 450 to 600°C have also been carried out. No dimensional changes and only 0.5 per cent change in density were observed after annealing at 550°C. Only traces of helium and other gases were released at 550°C, but measurable amounts of helium were collected during the 600°C anneal.

Attempts at Oak Ridge to incorporate 60 ppm of boron as ZrB_2 in UO_2 fuel particles as a burnable poison have been unsuccessful.[6] The boride and UO_2 were ball-milled in a rubber-lined ball mill with alumina balls, and compacts of these powders were sintered at 1700 to 1750°C in atmospheres of helium, hydrogen, or a $7N_2$-$3H_2$ mixture. With initial compositions of 600 ppm boron, losses on sintering ranged from 595 ppm in hydrogen to 400 ppm in the N_2-H_2 mixture. The most consistent losses were obtained in helium (350 to 420 ppm). When the boron was added by adding orthoboric acid to the uranyl nitrate solution used to produce UO_2, subsequent sintering of the UO_2 powder resulted in losses to below detectable amounts. These studies have been discontinued since a burnable poison will not be required for N. S. *Savannah*.

At Bettis, dispersions of Fe_2B^{10} in iron and compartmented B_4C sintered pellets clad with Zircaloy are being prepared for irradiation tests.[7]

Methods of incorporating borides in UO_2–stainless-steel fuel elements as a discrete burnable poison are also being investigated.[8] The two most promising compounds are ZrB_2

Table III-1 BURN-UP ANALYSES OF KAPL 42-1 CAPSULE ASSEMBLY

Material	Per cent of theoretical density	B^{10} burn-up, %	Helium released, %
B_4C	55	66	20
30 wt.% $B_4C-Al_2O_3$	60	72	14
23 wt.% $B_4C-Al_2O_3$	60	78	11
5 wt.% B_4C–Zircaloy-2	90	72	1
5 wt.% B_4C–Zircaloy-2	90	72	0.9

Table III-2 GAS-RELEASE DATA OF KAPL 42-2 CAPSULE ASSEMBLY*

Material	Per cent of theoretical density	Helium released, %
B_4C (7 at.% B^{10} in B)	72.9	5
25 vol.% $B_4C-Al_2O_3$	71.4	3
0.5 wt.% B^{10} austenitic S.S.	100	0.006
5 wt.% B^{10} ferritic S.S.		0.01
5 wt.% B_4C–Zircaloy-2	As extruded	2
5 wt.% B_4C–Zircaloy-2	As roll bonded	0.7

*Estimated 90 per cent depletion of B^{10}.

Table III-3 HELIUM RELEASE AND DIMENSIONAL CHANGES IN 5 WT.% B_4C–ZIRCALOY-2 DISPERSIONS IN KAPL CAPSULE ASSEMBLY 42-3

Fabrication	Preirradiation heat-treatment	Helium* released, %	Average change in dimensions, %		
			Length	Width	Thickness
Cold sized	As extruded	1.0	0.2	0.6	1.2
Cold sized	Vacuum annealed†	3.2	0.1	0.8	1.7
Roll bonded	Vacuum annealed†	1.2	−0.2	−0.3	2.0
Roll bonded	Vacuum annealed	0.95			
Roll bonded	As roll bonded	1.3	−0.4	0.2	3.2
Roll bonded	As roll bonded	1.0	0.05	0.5	2.9

*Assuming 90 per cent depletion of B^{10}.
†22 hr at 1500°F, 5×10^{-4} mm Hg vacuum.

Table III-4 POSTIRRADIATION CORROSION DATA ON B_4C-ZIRCALOY DISPERSIONS*

Burn-up, %	Test duration, hr	B_4C-Zircaloy swelling, mils		
		End	Middle	End
90	750	1.2	0.7	2.1
90	350	0.5	0	0.9
70	350	1.2	1.0	1.3
70	98	2.3	1.5	1.9
65	750	0.4	0	0
95	98	0.8	1.0	1.1
95	750	2.6	3.3	3.7
85	98	0.3	0	0
85	750	0	0	0
70	750	2.6	4.0	0
0	750	1.5	1.6	1.5
0	350	2.5	2.4	2.2
0	98	0	0	0

*Specimens were run in 650°F deoxygenated, deionized water.

and NbB_2. When vacuum sintering rather than hydrogen sintering is used, both of these compounds can be placed in the stainless matrix without evidence of reaction. The ZrB_2 is the more stable compound; but purity, composition, and physical characteristics of the ZrB_2 are important in determining whether a reaction will take place during sintering. Increases in temperature also affect the boron loss during sintering, but little or no loss occurs when ZrB_2 dispersions are sintered at 2200°F and NbB_2 dispersions are sintered at 2000°F *in vacuo*. Irradiation specimens are currently being fabricated. (G. W. Cunningham)

References

1. W. E. Bost, U. S. Atomic Energy Commission, January 1959. (Unpublished.)
2. W. E. Bost, Chemistry of Boron and Boron Compounds. A Literature Search, TID-3523, January 1959. (Unclassified AEC report.)
3. R. W. Garbe and H. E. Walchli, Quarterly Progress Report for the Period July 1 to Sept. 30, 1958, YAEC-97, Nov. 14, 1958. (Unclassified AEC report.)
4. Reactor Technology Report No. 8. Metallurgy, KAPL-2000-5, March 1959. (Unclassified AEC report.)
5. L. D. Kirkbride et al., Knolls Atomic Power Laboratory, Nov. 28, 1958. (Unpublished.)
6. Maritime Reactor Project Annual Progress Report for Period Ending Nov. 30, 1958, ORNL-2657. (Unclassified AEC report.)
7. Pressurized Water Reactor (PWR) Project Technical Progress Report for the Period Oct. 24, 1958, to Dec. 23, 1958, WAPD-MRP-77. (Unclassified AEC report.)
8. R. W. Dayton and C. R. Tipton, Jr., Progress Relating to Civilian Applications During March 1959, BMI-1330, Apr. 1, 1959. (Confidential AEC report.)

Corrosion

Zirconium

In the field of zirconium corrosion, studies at various laboratories continue to be concentrated on hydrogen pickup during exposure to high-temperature water and steam. At Bettis,[1] for example, nickel-free Zircaloy-2 alloys containing 0.13 and 0.24 wt.% iron were found to pick up less hydrogen than plain Zircaloy-2 during exposure to 600 and 680°F water and 750°F steam. Of the three alloys, the 0.13 wt.% iron material showed the lowest hydrogen absorption.

Hydrogen pickup by Zircaloy-2 during loop irradiation was found by Knolls to be only slightly greater than that normally obtained for Zircaloy-2 samples exposed to high-temperature water in the absence of radiation. Similarly, oxide weight gains in irradiated samples were comparable to those expected for the same water temperature and exposure times in static autoclave tests.

Results of hydriding studies at Hanford[2] confirm an earlier hypothesis that the ZrO_2 film is protective against hydrogen, so long as the film is defect free. Sections of specimens hydrided at 350°C in a hydrogen atmosphere at 25 psi showed evidence of hydrogen diffusion into the metal at an edge where the oxide film was not continuous. Also, it would appear that the ZrO_2 film will admit hydrogen only when the oxygen or water content is below some critical level, the value of which is currently under study.

Fretting-corrosion studies of Zircaloy-2 have been conducted at Hanford[2] in water (pH adjusted to 10) at 290°C, using wire samples. No acceleration of corrosion or indication of fretting has been observed to date. On the other hand, Bettis found that Zircaloy-2 versus Zircaloy-2 sheet specimens showed indications of fretting corrosion in 600°F water at 2000 psi pressure. Specimens involving type 304 stainless steel versus Zircaloy-2 did not show fretting attack. However, general corrosion rates were considerably higher than those observed for the Zircaloy-2 versus Zircaloy-2 couples.

The spontaneous ignition of zirconium and titanium in oxygen has been investigated at Stanford Research Institute.[3] The oxygen partial pressure for spontaneous ignition upon rupture of a titanium sample drops from 350 psi at room temperature to 210 psi at 300°C, 150 psi at 500°C, and to only 75 psi at 1000°C. Zirconium exhibits spontaneous ignition under similar conditions. However, considerable variation in susceptibility was observed from test to test; thus, at the present time, it is not possible to establish critical oxygen partial pressures. Reactions were observed at room temperature at oxygen partial pressures as low as 75 psi. In other cases, no ignition occurred at oxygen pressures of 500 psi or higher. (W. K. Boyd)

Aluminum

Previous experience has indicated that, under dynamic conditions, the corrosion rate of aluminium in high-temperature water is substantially higher than that indicated by static autoclave studies. It has been postulated that increased oxide dissolution is the principal cause of increased corrosion rates at high flow rates. Recent studies at Hanford[4] appear to confirm this belief. It was found that an autoclave pretreatment of either one day at 300°C or one week at 250°C in water saturated with aluminum corrosion products reduced the dynamic corrosion rates to values comparable with those obtained under static conditions. This is attributed to aging of the soluble component of the oxide film, which renders it less soluble under dynamic conditions.

Considerable improvement in the corrosion resistance of aluminum-nickel-iron alloys has been obtained by small additions of titanium and zirconium. At Hanford[4] an alloy containing 1.0 wt.% nickel plus 0.1 wt.% titanium exhibited 0.8 mil of attack after 10 months of exposure to water at 360°C. The structure of this alloy is

characterized by the extreme fineness of the second-phase dispersion. A similar effect with small additions of titanium, zirconium, and beryllium has been observed at Chalk River.[5] An aluminum alloy containing 2.0 wt.% nickel, 0.5 wt.% iron, 0.2 wt.% silicon, 0.2 wt.% titanium, 0.05 wt.% zirconium, and 0.05 wt.% beryllium evinced a corrosion rate of 0.005 in./year under static conditions in water at 300°C.

Extruded power-product aluminum alloys are of interest because of their high tensile strength at elevated temperatures. Extrusions have been made which exhibit double the strength of the wrought X-8001 alloy. However, the high-temperature corrosion resistance of these alloys leaves much to be desired. In studies at Argonne,[6] experimental extrusions prepared from an atomized aluminum alloy and several powdered additives, including SiO_2, $AlPO_4$, and Al_2O_3, exhibit early failures during corrosion testing in water at 290 and 350°C. On the other hand, some compacts have shown short-time corrosion resistance approaching that of the wrought X-8001 alloy. (W. K. Boyd)

Stainless Steels

Some pressurized-water reactors utilize fuel elements clad with an austenitic stainless steel. Stainless steels find their greatest use, however, in the steam-boiler sections of nuclear power plants where they are exposed both to high-purity primary water and to secondary water contaminated with chlorides. In general, the martensitic, ferritic, and austenitic grades exhibit good resistance to the high-purity primary water. However, the straight chromium martensitic and ferritic grades are prone to pitting attack, especially in crevice areas. Work at Knolls[7] has indicated that the martensitic type 410 alloy also is susceptible to stress-corrosion cracking in high-purity water at 300°F. In air-saturated water, failure occurred at applied stress levels of the order of 40,000 psi. On the other hand, the material exhibited a low susceptibility to cracking in water containing 30 to 40 ppm of dissolved oxygen. The data also indicate that cracking can be minimized by shot peening of the surface. In other studies,[8] stressed samples of type 347 stainless steel were exposed to 500°F, pH 10-11, lithium hydroxide–containing water. No cracks were observed after a two-month exposure period.

It is well known that austenitic stainless steel will exhibit stress-corrosion cracking in secondary water containing chlorides or free caustic. This fact has stimulated considerable interest in the ferritic steels, which are known to be more resistant to cracking than the austenitic grades. In tilting-autoclave studies at Bettis,[9] the ferritic, Croloy 16-1 alloy was found to be immune to stress cracking in chloride-contaminated water. Similar results have been observed at Martin Nuclear Division[10] for type 430 stainless steel. However, both the Croloy 16-1 and type 430 stainless are prone to pitting attack in crevice areas.

(W. K. Boyd)

Niobium

The reaction of unalloyed niobium with water vapor at 5 cm of mercury pressure was also investigated by Bettis.[11] This reaction follows the cubic rate law at temperatures up to 600°C (1110°F) for times up to 2 hr. Above this temperature, linear behavior is observed. Comparison of these data with previously published data[12] on the reaction of niobium with 7.6 cm of oxygen pressure indicates that the niobium-water vapor reaction is slower by a factor of 2 up to 375°C (710°F), above which temperature the niobium-oxygen reaction becomes linear. The low-pressure water-vapor reaction rates are similar to the high-pressure hot-water and steam reaction rates, indicating the pressure has little influence on the niobium-water reaction.

A British study[13] has been conducted on the transformations in Nb_2O_5. Whereas Nb_2O_5 was considered previously to exist in three allotropic forms, this study indicates that the oxide exists in only two major forms: an unstable low-temperature form and a stable high-temperature form. The alpha-Nb_2O_5 (low temperature) transforms irreversibly to beta-Nb_2O_5 (high temperature), the reaction being temperature and time dependent. The transformation occurs at about 900°C for normal heating rates and is apparently the cause of observed anomalies[14] in the oxidation behavior of unalloyed niobium in this temperature range.

(W. D. Klopp)

Molybdenum

Various coating methods for the protection of molybdenum from oxidation are reviewed in a

recent DMIC report.[15] To date, the most satisfactory coatings developed by General Electric for turbine-bucket applications are the chromium-nickel-chromium electroplate (described in the February 1959 Review, *Reactor Core Materials*[16]) and a complex chromium-nickel-NiSiB-Nichrome coating, hard-faced with CoCrWB. Buckets are clad with the latter coating by electroplating with chromium and nickel, flame spraying with NiSiB, fusion-cladding with a preshaped Nichrome boot, and final flame spraying with a CoCrWB hard-facing alloy. Molybdenum buckets clad with these materials are under evaluation in engine tests at 1800 to 2000°F. (W. D. Klopp)

Nickel-base Alloys

Studies on the corrosion resistance of Inconel in high-temperature (500 to 600°F) pressurized water have continued. Yankee Atomic[17] workers found Inconel to be mildly inferior to type 304 stainless steel in boric acid–buffered water (pH 5 to 6) and mildly superior in lithium-containing water (pH 8). Inconel was superior to type 304 stainless in resisting corrosion in simulated start-up, shut-down tests. In hydrogenated, ammoniated and aerated, pressurized, high-temperature, high-velocity water, Inconel was found by Knolls[7] to exhibit some scaling loss. The significance of the activity of the high-nickel-content scale in pressurized-water-reactor environments is now under study. While investigating the corrosion of Inconel in 200°F hydrogenated water containing 6 to 7 ppm hydrazine (for deoxidation), Bettis workers[18] observed only very slight weight loss. None of the investigators detected any galvanic effects as a result of coupling Inconel with the 300-series stainless steels in high-temperature, pressurized-water environments.

The general conclusions from these various studies are:

1. Inconel is acceptable as the construction material for primary systems of pressurized-water reactors.

2. Inconel has an advantage over the 300-series stainless steels in that it exhibits no susceptibility to stress-corrosion cracking in the presence of chloride ions. (E. S. Bartlett)

Chromium-base Alloys

The oxidation behavior of chromium–5 wt.% molybdenum and chromium–10 wt.% tungsten alloys under stress at 1750°F in air was found by Australian investigators[19] to be essentially the same as that of unalloyed chromium. Oxidation penetration was from ½ to 1 mil, with a nitride layer to a depth of about 1½ mils beneath the oxide layer after about 300-hr exposure. (E. S. Bartlett)

Iron-Chromium-Aluminum Alloys

Iron–7.5 wt.% aluminum–5 wt.% chromium formed the base alloy for development studies toward an oxidation-resistant cladding material at Martin Nuclear Division.[20] The effects on oxidation resistance of ternary, quaternary, and quintary additions of molybdenum, zirconium, and niobium were studied in a statistically balanced program. It was concluded that zirconium additions are detrimental to oxidation resistance of the base at 1650 and 1800°F, whereas niobium is beneficial at 1800°F. Molybdenum has no significant effect upon the oxidation resistance of the base alloy.

(E. S. Bartlett)

Magnesium

At the Second Geneva Conference, Russian scientists presented the results of a fundamental study of the effect of beryllium additions on the oxidation resistance of magnesium alloys,[21] wherein the effects of beryllium were divorced from those of other additives through the use of high-purity materials. Additions in excess of 0.1 wt.% beryllium are required to achieve parabolic oxidation in air at temperatures of 970 to 1080°F. The parabolic oxidation rates decrease with increasing beryllium contents up to at least 1.25 per cent. In flowing CO_2 atmospheres, alloys containing in excess of 0.1 per cent beryllium are unaffected in 150 hr at 1080°F; unalloyed magnesium is destroyed in less than 50 hr, and the magnesium–0.01 per cent beryllium alloy is destroyed in about 200 hr. Protective mechanisms were studied, and it was found that when the protective scale developed the amount of beryllium in the oxide film approached 50 per

cent. Fuel elements were plated with magnesium alloys containing from 0.2 to 15 wt.% beryllium (prepared by special techniques) and exposed for 10,000 hr at 930 to 1000°F in air, helium, argon, and CO_2 atmospheres under reactor conditions. Performance under all conditions was reported to be excellent.

(E. S. Bartlett)

Vanadium

Because of its low density and refractoriness, vanadium may be of interest as a structural material in certain reactor applications. A recent publication by the United Kingdom Atomic Energy Authority briefly summarizes some of the chemical behavior of the metal.[23] As is true of its sister elements, molybdenum and tungsten, vanadium oxidizes catastrophically in air at temperatures above 1300°F. In CO_2 at 930°F and 8-atm pressure, vanadium is oxidized at the slow rate of about 0.25 mil/year. It is resistant to salt-water attack and to dilute solutions of nonoxidizing acids. (E. S. Bartlett)

Corrosion by Liquid Metals and Fused Salts

As mentioned in previous Reviews, a number of experimental programs are being conducted at Oak Ridge to investigate corrosion attack by molten fluoride salts. Recently acquired data[24] from inspections of Inconel forced-circulation loop systems indicate light attack (1½ to 4 mils average intergranular penetration) after 3000 to 9000 hr of operation. The test salts, NaF-ZrF_4-UF_4 (57-42-1 mole %) and LiF-BiF_2-UF_4 (53-46-1 mole %), were circulated between 1300 and 1100°F. In another study, Inconel pipe is being subjected to thermal-stress cycling in an environment of NaF-ZrF_4-UF_4 (56-39-5 mole %) salt, nominally at 1400°F; temperature amplitudes of about 1 ± 100°F are achieved by flowing hot and cold salt through the test piece with temperature oscillation as rapid as 1 cycle/sec. It was found that the material is prone to crack and that the severity of the cracking is probably a direct function of the stress level at the fluid-contacting wall. This level is estimated from temperature amplitude, wall thickness, and cycle frequency. For example, with a calculated stress of 12,000 psi, there was no evidence of cracking after 360,000 cycles (at 1.0 cycle/sec); with 21,700 psi stress, severe cracks (to 0.2 in. across a 0.445-in. wall) occurred after 72,000 cycles (at 0.1 cycle/sec).

A recently declassified report[25] presents details of an investigation of the behavior of slurries of UO_2 powders (25 wt.%) in eutectic NaK at a maximum temperature of 700°C. This work, conducted at Knolls, had the objective of determining the engineering feasibility of using such a slurry as a fuel system for high-power-density reactors. Although the research was discontinued before accomplishing its final objective, namely, that of studying slurry behavior in a dynamic in-pile loop system, its net results were encouraging. The most promising system studied was based on a mixture of 85 per cent ball-milled UO_2 and 15 per cent UH_3; the UH_3 decomposed to uranium, which acted as an oxygen getter. In isothermal loop tests, this slurry remained in suspension well, although in ΔT loops, settling was observed in regions where the fluid velocity was less than 3 fps. Some particle agglomeration occurred during the runs but, in general, did not appear serious; corrosion and erosion (of types 304 and 316 stainless-steel containers) were quite low.

Corrosion experiments in conjunction with the Liquid Metal Fuel Reactor Experiment (LMFRE-1) are directed toward investigating containment problems presented by the molten bismuth-uranium fuel. Croloy-2¼ and Croloy-1¼ are receiving detailed study. In a recent progress report,[26] status information for capsule and loop tests is given. It is reported, for example, that a pumping loop constructed of Croloy-2¼ and operating with conditions listed in Table IV-1 displayed intergranular attack in the hottest part of the loop and some intergranular corrosion at the outside surface of the tubing at the heat-exchanger entrance; the cold-leg section displayed transported metal but no corrosion. The corrosion rate measured on a machined tube section in the hot leg was 16 to 20 mils/year; attack of specimens inserted in the hot-leg stream was about 0.7 mil/year. A loop constructed of Croloy-1¼, operating with conditions also listed in Table IV-1, exhibited a hot-leg-specimen corrosion rate of 0.8 mil/year. (J. H. Stang)

Table IV-1 OPERATING CONDITIONS FOR URANIUM-BISMUTH PUMPING LOOPS*

Croloy-2¼ system, 500 hr preconditioning (1000–920°F), 2780 hr, 885–750°F	Croloy-1¼ system, 145 hr preconditioning (1000–920°F), 4537 hr, 885–750°F
Zirconium, ppm	Zirconium, ppm
Average 157	Average ~155
Minimum 110	Minimum ~75
Magnesium, ppm	Magnesium, ppm
Average 325	Average ~360
Minimum 276	Uranium, ppm
Uranium, ppm	Average ~775
Average 830	
Minimum 370	

* Data taken from reference 5.

Radiation Effects in Nonfuel Materials

Basic Studies

The British[27] have studied vacancies in copper and aluminum by means of low-angle X-ray scattering and electron microscopy. They found that clusters of vacancies form during aging of the quenched metals. The low-angle X-ray scattering increased with aging temperature up to 500°C for copper and 350°C for aluminum and was interpreted either as clusters 130 A in diameter or as 100 to 500 A dislocation loops. Transmission electron microscopy on etched thin sections showed dislocation loops. Similar experiments were made with specimens irradiated to 10^{19} to 10^{21} neutrons/cm^2. Slight low-angle scattering was found at the greatest irradiation for copper with no change observed by electron microscopy. However, dislocation loops were seen in sections of irradiated aluminum.

The physical expansion of synthetic sapphire is found[28] to change with extent of neutron irradiation. Up to 2×10^{18} nvt, the expansion is 100 ppm/10^{18} nvt parallel to the c-axis and 61 ppm/10^{18} nvt perpendicular to the c-axis. From 4 to 14×10^{18} nvt, the parallel and perpendicular expansion rates decrease to 23 and 19 ppm/10^{18} nvt, respectively. There are two annealing stages at 350 and 550°C.

Hanford,[4] in studying the annealing of molybdenum irradiated to 1.2×10^{20} nvt, has found a small amount occurring at 100°C and no further effect until 600°C, according to the breadth of the X-ray diffraction lines. (A. E. Austin)

Effects of Irradiation on Mechanical Properties

Hanford,[29] in studies of the effect of an irradiation of 7×10^{19} thermal nvt on the room-

Table IV-2 TENSILE PROPERTIES OF UNIRRADIATED AND IRRADIATED ZIRCALOY-2 AND ZIRCALOY-3*

(Integrated exposure = 7×10^{19} thermal nvt)

Specimen	Condition	Strain rate, in./min	Strength, 1000 psi		Elongation, %		Elastic modulus, 10^6 psi
			0.2% offset yield	Ultimate	Uniform	Total	
Zircaloy-2							
3	Unirrad.	0.005/0.05	$41.4^{+3.1}_{-2.4}$	$56.5_{-2.1}$	$16.8^{+2.0}_{-2.9}$	$29.8^{+3.2}_{-2.5}$	$13.3^{+0.7}_{-0.5}$
4	Irrad.	0.005/0.05	$60.1^{+1.4}_{-1.2}$	$65.2^{+1.6}_{-1.4}$	$7.4^{+1.3}_{-1.1}$	$24.0^{+1.2}_{-2.3}$	$13.8^{+0.7}_{-0.3}$
	% Change		+45.2	−15.4	−56.0	−19.5	+ 3.8
1	Unirrad.	0.05	46.0	58.6	12.6	26	13.4
1	Irrad.	0.05	64.7	66.4	7.9	24	14.6
	% Change		+40.6	+13.3	−37.3	−37.3	+ 8.9
Zircaloy-3							
3	Unirrad.	0 005/0.05	$35.2^{+2.8}_{-2.2}$	$57.0^{+2.9}_{-4.9}$	$14.4^{+1.1}_{-1.3}$	$27.3^{+1.7}_{-1.3}$	$13.4^{+1.1}_{-0.6}$
4	Irrad.	0.005/0.05	$51.8^{+2.0}_{-3.3}$	$66.3^{+1.3}_{-2.1}$	$8.0^{+0.7}_{-0.9}$	$21.7^{+3.3}_{-3.4}$	$14.5^{+0.4}_{-0.2}$
	% Change		+47.2	+16.3	−44.4	−20.5	+8.2
1	Unirrad.	0.05	36.5	55.3	16.6	26	13.9
1	Irrad.	0.05	56.5	67.7	8.9	35	14.2
	% Change		+54.8	+22.4	−46.4	+34.6	+2.2

* Data taken from reference 29.

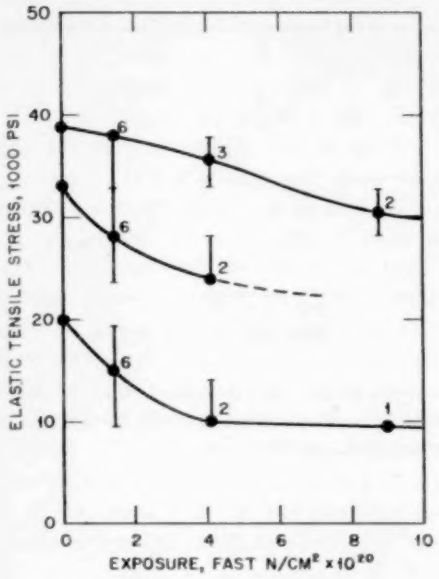

Figure 2—Effect of irradiation on stress relaxation in type 304 stainless steel. Fast neutrons include all those with energies greater then 0.1 Mev; numbers above each data point are total points averaged to obtain indicated value; specimens were loaded in simple tension. Data taken from reference 30.

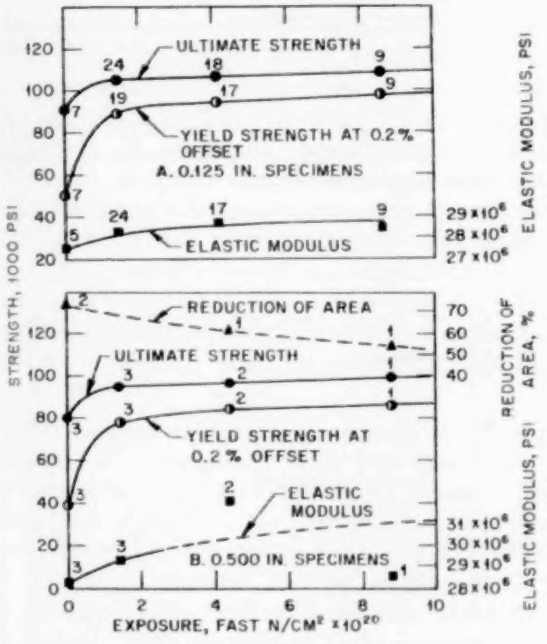

Figure 3—Effect of irradiation on tensile properties of type 304 stainless steel. Fast neutrons include all those with energies greater then 0.1 Mev; numbers above each data point are total points averaged to obtain indicated value. Data taken from reference 30.

temperature tensile properties of Zircaloy-2 and Zircaloy-3, found a significant increase in the yield and tensile strengths, as indicated in Table IV-2. A drop-in-load yield point in the stress-strain curves for Zircaloy-2 amounting to 360 psi was consistently observed. This behavior was not found in Zircaloy-3. The most marked effect of the irradiation was the decrease in the uniform elongation.

Work by Du Pont[30] shows that exposure to fast neutrons causes significant room-temperature relaxation in type 304 stainless steel. For example, an original tensile stress of 20,000 psi decreased by 50 per cent at an exposure of about 5×10^{20} fast neutrons/cm^2. A summary of the results is given in Fig. 2. However, the room-temperature tensile properties of type 304 stainless steel changed continuously as a result of neutron exposures up to 9×10^{20} fast neutrons/cm^2 as indicated in Fig. 3. The Rockwell A hardness increased from 47.4 to 56.7 as a result of the irradiation. Similar effects of neutrons on stress relaxation and hardness of 1100 aluminum and tensile properties of 1100 and 6063 aluminum were measured.

The results of a survey of the effect of neutron irradiation on the mechanical properties of iron, ferritic steels, and austenitic steels, including comparisons of reported data with recent theory, have been published by Harwell.[31] A graphical compilation of the mechanical properties of 46 metals and 55 plastics as functions of integrated radiation is presented in a Wright Field report.[32] (B. C. Allen)

Selected Metallurgical Aspects of Cladding and Structural Materials

Metallurgy of Zirconium Alloys

In their study of the zirconium-iron-tin system,[33] Armour found very little solubility for tin in the compound $ZrFe_2$. The single-phase field in this system is believed to exist in the vicinity of 55 wt.% iron. The compound theta appears to be a continuous phase origirating at the binary compound (Zr_4Sn) and dissolving up to about 7.5 wt.% iron while maintaining a constant tin composition of the order of 24.5 wt.%. A four-phase ternary eutectic ($L \rightleftharpoons \beta + \theta + ZrFe_2$) occurs between 930 and 935°C. A four-phase ternary peritectoid ($\beta + \theta \rightleftharpoons \alpha + ZrFe_2$) probably occurs at a temperature just above

the binary zirconium-iron eutectoid which occurs between 790 and 800°C. An alternative possibility is the existence of a four-phase ternary eutectoid ($\beta \rightleftharpoons \alpha + \theta + ZrFe_2$) which would occur just above the zirconium-iron eutectoid. The solubility limit of alpha zirconium was found to be extremely low in the presence of iron.

Hanford[29] has investigated the recovery of 50 per cent cold-worked zirconium, heat-treated in helium at six temperatures from 300 to 800°C for 10 and 100 min, by measuring X-ray line broadening. Two quantities, $B_{1/2}$ and $H/I_{max.}$, were used as an index of cold-work recovery. $B_{1/2}$ is the half width of the α_1 peak at half of the maximum intensity, and $H/I_{max.}$ is a measure of α_1-α_2 resolutions (see Fig. 4).

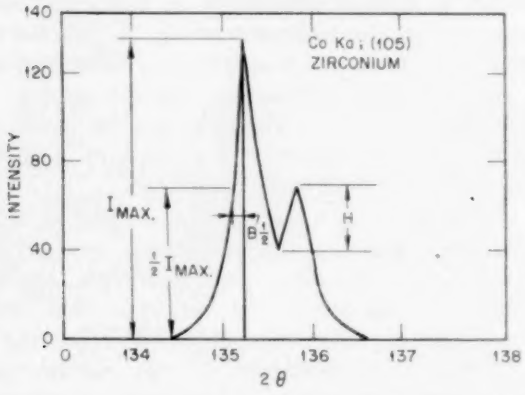

Figure 4—Distribution of intensity as a function of diffraction angle for completely recrystallized zirconium. Data taken from reference 29.

Cobalt Kα radiation was used, and the measured peak was (105). The two sets of recovery data are shown in Figs. 5 and 6. These figures clearly show the recrystallization temperature for cold-worked zirconium to be 600 and 640 to 650°C, respectively, for the 100- and 10-min heat-treatments. Line-width measurements indicate a gradual recovery below 400°C. This reflects a change in the structure which does not affect the hardness noticeably. Hardness data are summarized in Fig. 7. A small increase in hardness occurring at 600 and 700°C for the 100- and 10-min heat-treatments is probably due to gas pickup. This increase was not observed in X-ray work.

Knolls[34] describes a method for producing single crystals of alpha zirconium. Rapidly cooling small arc-melted charges in a button

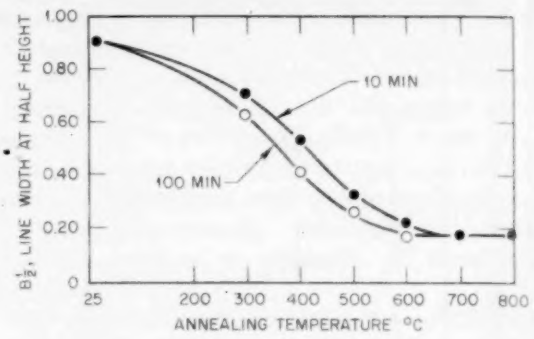

Figure 5—Recovery of line width for 50 per cent cold-worked zirconium heat-treated in helium. Data taken from reference 28.

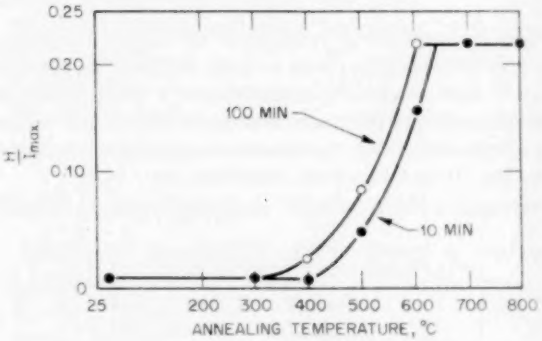

Figure 6—Recovery of $\alpha_1 - \alpha_2$ resolution for 50 per cent cold-worked zirconium heat-treated in helium. Data taken from reference 29.

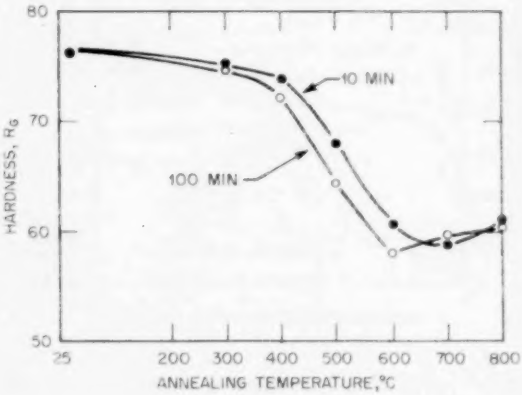

Figure 7—Recovery of hardness for 50 per cent cold-worked zirconium heat-treated in helium. Data taken from reference 29.

furnace produced large crystals which showed considerable substructure and lattice distortion. These were eliminated by an 18-day anneal in an argon atmosphere at 840°C, followed by furnace cooling; this anneal also resulted in grain growth. Crystals were also grown in 3-in.-long, 0.120-in.-diameter rods which were tapered to a fine point on each end. These rods were sealed in an evacuated Vycor tube and heat-treated as follows: 5 hr at 1000°C in a gradient furnace, slow cooling to 800°C, annealing at 800°C for 60 hr, and furnace cooling.

Westinghouse[35] states that excessive grain growth which can occur during vacuum annealing of cold-worked Zircaloy-2 material can be prevented. They suggest that either the material be cold-worked 10 per cent or more before it is annealed or the vacuum annealing temperature be reduced to about 670°C.

(J. A. DeMastry)

Yttrium Systems

Workers at the Denver Research Laboratories[36] state that in the yttrium-hafnium system there is a single eutectic at approximately 23 wt.% hafnium. The solid solubility of yttrium in hafnium is about 2 wt.% and the solubility of hafnium in yttrium is about 4 wt.%. In the yttrium-vanadium system, on the basis of work with cast structures, there appears to be a eutectic reaction at approximately 7 wt.% vanadium and at 1435°C (2615°F). The solid solubility of vanadium in yttrium is about 0.5 wt.%. A liquid immiscibility gap has been established in the system extending from about 9 to 99 wt.% vanadium. A monotectic reaction $L_2 \rightleftharpoons V_{ss} + L_1$ occurs at a composition which is greater than 99 wt.% vanadium and at a temperature which is not very different from that of the melting point of vanadium, 1900°C (3452°F).

The maximum solubility of iron in yttrium was found by Armour[37] to be less than 1 wt.%. The melting point of yttrium drops sharply with the addition of iron, terminating in a eutectic reaction at 25 wt.% iron and 915 ± 10°C (1680 ± 18°F). This reaction can be written as $L \rightarrow Y_{ss} + YFe_2$. The first intermediate phase encountered with increasing iron content is a $MgCu_2$ type Laves phase, YFe_2; this compound forms by a peritectic reaction $L + YFe_3$ (?) $\rightarrow YFe_2$ at 1175 ± 25°C (2150 ± 45°F). The YFe_2 appears at 56 wt.% iron. The next intermediate phase is tentatively placed at 65.5 wt.% iron, corresponding to a stoichiometric YFe_3. A third intermediate phase, YFe_4, has been positioned at 71.6 wt.% iron. A maximum-melting intermediate phase is next encountered at 85 wt.% iron, corresponding to stoichiometric YFe_9. No additional intermediate phases exist between YFe_9 and iron; at 87.5 wt.% iron a eutectic ($L \rightarrow Fe_{ss} + YFe_9$) is present.

In the yttrium-nickel system, the addition of nickel lowers the melting point of yttrium rather severely until the first eutectic in the system is reached at 25 wt.% nickel, involving the compounds Y_4Ni and Y_3Ni_2. A second eutectic reaction occurs at approximately 47.5 wt.% nickel and involves the compound YNi and YNi_2.

(J. A. DeMastry)

Microstructure of Nickel Alloys

The University of Michigan[38] reports on the influence of heat-treatments on the microstructure and high-temperature properties of a precipitation-hardening alloy (55 nickel–20 chromium–15 cobalt–4 molybdenum–5 titanium–5 aluminum). They studied the stress-rupture properties at 1600°F and 25,000 psi. The study indicates that the effects of heat-treatments on high-temperature properties are related to size and distribution of a gamma-prime phase, provided the rolling effects have been removed by solution treatment. A solution temperature of 1975 to 2000°F for 4 hr resulted in complete solution of the gamma phase and of grain-boundary carbides. General precipitation of gamma-prime particles proceeded at 1200, 1400, and 1600°F. No evidence of overaging at 1200 and 1400°F for 100 hr was found. Overaging did occur after 4 hr at 1600°F.

A study was made[39] of the relation between microstructure and creep-rupture properties of "A" nickel (cold-rolled 20 per cent and annealed at 1600°F for 1 hr) and A-286 (as received, heat-treated). For "A" nickel, the properties at 1100°F appeared to be a function of degree of reduction, independent of the initial or final temperature of working. No direct relation of creep-rupture properties to grain size was noted. With the A-286 alloy, the properties seemed to be governed more by the temperature of heating for working than by the degree of reduction or finishing temperature. This is not conclusive since the effects may have been due mainly to the prior history of

the stock. No correlations between creep and grain size or other microstructural characteristics were developed. (J. A. DeMastry)

Selected Mechanical Properties of Cladding and Structural Materials

Zirconium Alloys

An annealing study has been carried out with Zircaloy-2 in an attempt to restore the ductility of beta heat-treated Zircaloy-2 to that of alpha by subsequent anneals in the alpha temperature range. Tensile properties measured after annealing showed no improvements in ductility, the 0.2 per cent offset yield strength did not change, and the ultimate tensile strength was decreased by approximately 15 per cent, after 8 hr at 1450°F. The effect of high oxygen content at the surface of Zircaloy-2 on its mechanical properties has been investigated at Knolls. An oxide layer was formed by exposure to 650°F water for one day and 750°F steam for two days, followed by a diffusion anneal in vacuum for 1 hr at 1200°F. There was no significant difference in the mechanical properties at room temperature between those specimens containing high and low oxygen. Tests on Zircaloy-2 0.55-in.-ID tubes given similar heat-treatment showed a marked reduction in ductility; effective strain was reduced from 38.2 to 14.3 per cent. The tensile properties of Zircaloy-2 strip prepared from 80 ingots were determined at 600°F and showed that the 0.2 per cent offset yield strengths in the longitudinal and the transverse to rolling directions were 15,000 and 19,800 psi, respectively.

Relaxation data from Zircaloy-2 bend specimens at 750°F were also obtained. Two materials, carborundum and sodium-reduced material, were used. The specimens were beta quenched after being held at 1010°C for 1 hr in vacuum. Both had identical relaxation characteristics. Typical values after 1, 10, and 100 hr were 26,000, 15,000, and 13,000 psi, respectively. Fully annealed Zircaloy-2, 750°C for 20 hr, relaxed to lower stresses at 750°F for equivalent times. Typical values for 1, 10, and 100 hr were 15,000, 8,000, and 6,000 psi, respectively. Fully annealed material, subsequently cold-worked 15 per cent, yielded higher values for the same relative times, i.e., 22,500, 15,000, and 7,500 psi, respectively.

Relaxation data obtained from tensile test specimens on beta-quenched Zircaloy-2 at 1,050, 950, 850, 750, and 650°F after 24 hr at test were 7,000, 13,000, 19,000, 27,000, and 33,000 psi, respectively.

The effects of small additions of beryllium to Zircaloy-2 and Zircaloy-3 on the tensile properties at 600°F were also investigated. The results obtained are shown in Table IV-3.

Stress-rupture properties of the beryllium-modified Zircaloys at 600°F were determined. A comparison made at a creep rate of 5×10^{-4} in./(in.)(hr) between the Zircaloys with and without the beryllium addition indicated that a stress increase of 17 per cent is needed for Zircaloy-3 plus 0.2 wt.% beryllium to yield a creep rate the same as that for the unmodified alloy.

The effect of strain rate on the mechanical properties of vacuum-melted and atmosphere-melted Zircaloy-2 is being continued at Bettis.[18] The variation of the 0.2 per cent offset yield strength with strain rate is shown in Figs. 8 and 9. Preliminary strain fatigue data have been obtained on base-annealed flat specimens from Zircaloy-2. Typical data from unnotched

Table IV-3 TENSILE PROPERTIES AT 600°F OF ZIRCALOY-2 AND ZIRCALOY-3 WITH BERYLLIUM ADDITIONS

Alloy	Yield strength (0.2% offset), psi	Ultimate tensile strength, psi	Total elongation, %	Reduction of area, %
Zircaloy-2 + 0.1 wt.% Be	19,400	33,100	9	60
Zircaloy-2 + 0.2 wt.% Be	24,400	37,000	10	11
Zircaloy-2 + 0.3 wt.% Be	25,700	39,800	13	21
Zircaloy-2 + 0.3 wt.% Be	25,700	39,300	17	32
Zircaloy-2 + 0.4 wt.% Be	31,600	47,700	8	21
Zircaloy-3 + 0.2 wt.% Be	18,800	30,000	29	56
Zircaloy-3 + 0.4 wt.% Be	21,400	36,200	20	51
Zircaloy-3 + 0.4 wt.% Be	21,400	36,600	20	49

Zircaloy-2 at room temperature and 600°F are shown in Fig. 10. Figure 11 gives the same data replotted, showing nominal stress versus cycles to failure. Figure 12 shows the comparison of data for notched and unnotched specimens.

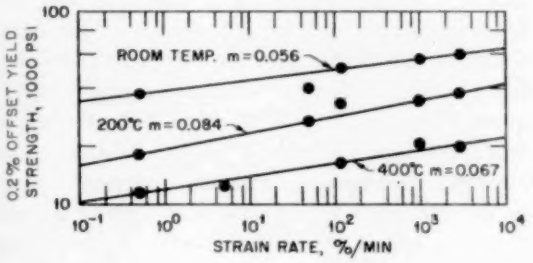

Figure 8—Effect of strain rate on 0.2 per cent yield strength of atmosphere-melted Zircaloy-2. Data taken from reference 18.

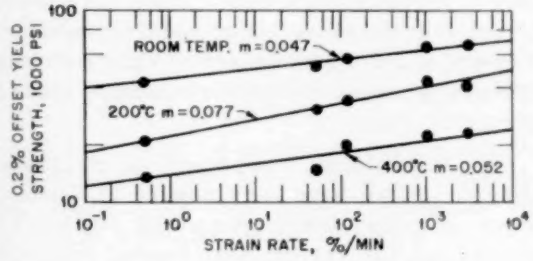

Figure 9—Effect of strain rate on 0.2 per cent offset yield strength of vacuum-melted Zircaloy-2. Data taken from reference 18.

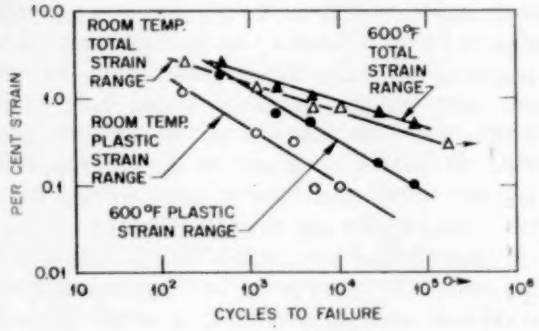
ROOM TEMP. TOTAL STRAIN RANGE
600°F TOTAL STRAIN RANGE
ROOM TEMP. PLASTIC STRAIN RANGE
600°F PLASTIC STRAIN RANGE
PER CENT STRAIN
CYCLES TO FAILURE

Figure 10—Unnotched strain-fatigue properties of Zircaloy-2. Vacuum-melted Zircaloy-2 base-annealed rolled plate; specimens tested transverse to the rolling direction. △○, room-temperature tests. ▲●, 600°F temperature tests. Data taken from reference 18.

The results of physical-metallurgy studies of reactor-grade Zircaloy-2 have been reported by Knolls.[7,40] Experimental values of the dynamic modulus of elasticity of Zircaloy-2 and a comparison of these values with those obtained by static testing are shown in Tables IV-4 and IV-5. These data indicate that static and dynamic modulus testing yields adequately equivalent results. Lowering of the modulus of elasticity with temperature is linear up to 1000°F, and earlier findings[40] that the modulus of elasticity of Zircaloy-2 is insensitive to processing techniques are verified. It is reported that the thermal expansion of 25 per cent

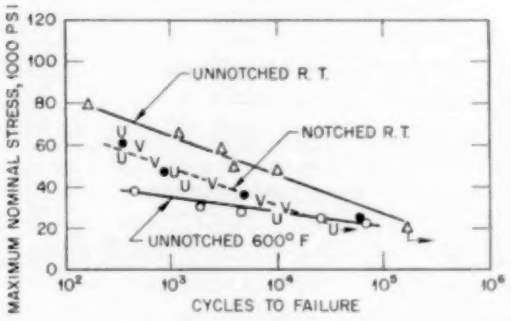

Figure 11—Stress fatigue of Zircaloy-2. Vacuum-melted Zircaloy-2 base annealed; specimens tested transverse to rolling direction. △, unnotched specimens $K_t = 1.0$. ∨, V-notched specimen $K_t = >6$. ∪, U-notched specimen $K_t = 4.0$. ●, center hole specimen $K_t = 2.5$. ○, unnotched, 600°F. Data taken from reference 18.

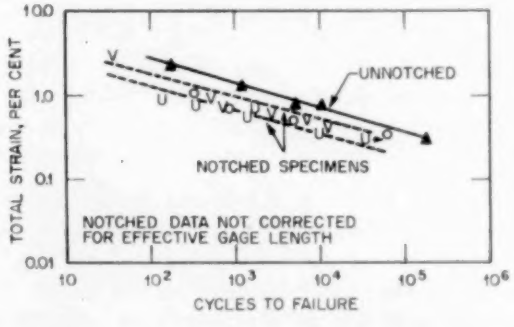

Figure 12—Comparison of strain-fatigue properties of unnotched and notched Zircaloy-2 at room temperature. Vacuum-melted Zircaloy-2. ▲, unnotched specimen $K_t = 1.0$. ∨, V-notched specimen $K_t = >6$. ∪, U-notched specimen $K_t = 4.0$. ○, center hole specimen $K_t = 2.5$. Data taken from reference 18.

Table IV-4 TEST RESULTS FOR DYNAMIC MODULUS OF ELASTICITY DETERMINATIONS*

Specimen	Temp., °F	Vibration frequency, cycles/sec	Length, in.	Diam., in.	Weight, g	Specific weight, lb/in.^{3}	Elasticity, 10^6 psi
1	77	1000	6.2450	0.2929	45.132	0.2365	13.71
	310	957					12.56
	604	893					10.93
	805	860					10.14
	1006	820					9.22
2	76	1001	6.2447	0.2928	44.958	0.2357	13.70
	315	955					12.47
	608	898					11.03
	796	856					10.02
	1005	812					9.02
3	85	1002	6.2425	0.2930	45.048	0.2360	13.70
	300	956					12.47
	610	895					10.93
	813	859					10.07
	1013	815					9.07

* Data taken from reference 7.

Table IV-5 COMPARISON OF STATIC AND DYNAMIC MODULI FOR ZIRCALOY-2 AT ROOM TEMPERATURE*

Static modulus, 10^6 psi	Dynamic modulus, 10^6 psi
13.64	13.71
13.72	13.70
	13.70
Av. 13.68	Av. 13.70

* Data taken from reference 7.

cold-rolled and annealed Zircaloy-2 plate in the three principal directions of rolling can be expressed by the equation

$$L_T = L_0 (0.99983 + 5.63 \times 10^{-6} T + 1.58 \times 10^{-9} T^2)$$

for

$$30°C \leq T \leq 500°C$$

No major effect of structural anisotropy was found, which was attributed to the inadequate development of directional texture existing in the thick slab material used for the tests. The tensile behavior of Zircaloy-2 as affected by grain size, presence of notches, heat-treatment, and rate is summarized in Table IV-6. It was concluded that increasing the strain rate in the range 0.02 to 20 in./(in.)(min) increases strength properties but has little effect on the fracture ductility at room temperature. Of the three heat-treatments studied, the α plus β conditions tend to lower strength and ductility, particularly at large grain sizes and at room temperature. Increasing grain size causes only slight strength changes, whereas the fracture ductility tends to decrease.

The mechanical properties of zirconium-niobium alloys have been studied at Westinghouse at room temperature and 500°C. The results for the various heat-treated conditions are shown in Table IV-7.

Nickel Alloys

A program to determine the creep strength of INOR-8, a nickel alloy containing 16 wt.% molybdenum – 7.5 wt.% chromium – 6.0 wt.% iron – 0.14 wt.% carbon, in molten salt is in progress at Oak Ridge (references 24, 41, and 42). On the basis of 1 per cent creep strain, the data indicate that the environment does not seriously affect the creep properties at 1500, 1700, and 1800°F; however, the times to greater than 1 per cent strain and to rupture are much longer in salt than in air. These data are shown in Table IV-8. A comparison of rod and sheet materials at 1250°F in air is shown in Table IV-9. The effects of notches on the tensile properties at room temperature and at 1500°F are given in Table IV-10. Rotating-beam fatigue studies on INOR-8 at 1500°F under alternating stresses of ±30,000 psi at 100 rpm have given fatigue lives of 730,000 and 930,000

cycles for two specimens. The comparable rupture life for Inconel under similar conditions was produced by a stress of approximately 18,000 psi.

The creep and rupture properties of Inconel have also been investigated with both internal pressure and axial stress. The creep data obtained compare favorably with Soderberg's analysis and the Von Mise flow theory. Fracture could not be predicted by the maximum-principal-stress criterion. Cyclic strain fatigue of Inconel rods and tubes indicated that a single relation in the form $N^a E_p = K$ existed between the number of cycles to fracture and the plastic strain absorbed during each cycle. The constant K varied as a function of the material and temperature. Temperature variation in the range 1300 to 1600°F and small variation in chemical composition did not appear to change the cycle life appreciably.

The creep rate and rupture life of Inconel at 1500°F were investigated. Axially loaded, pressurized tubes were studied to develop a failure criterion based on properties measured in a conventional uniaxial tension test. A comparison of creep rates on the basis of the established theories of stress analysis showed good correlation between uniaxial test results and the results from tests with multiaxial stresses. The rupture-life data tended to support the maximum-principal-stress criterion for time-dependent fractures, although there was significant difference between the criterion and the test results, illustrating that a simple model will not present a realistic analysis of the data.

The effects of carburization on the mechanical properties of Inconel and INOR-8 were studied at Oak Ridge. Exposure time to a sodium-graphite system was varied as was the exposure temperature. The results of the mechanical properties at room temperature and 1250°F after various exposures are shown in Tables IV-11 and IV-12. For the INOR-8 specimens, the yield strength was increased, the tensile strength was decreased slightly, and the ductility was greatly reduced. These changes were dependent on the amount of carburization. The carburized specimens tested at 1250°F showed trends to lower ductility; however, some carburized specimens were more ductile than the control specimens. The effect of carburization on the rupture properties of INOR-8 and Inconel at 1250°F are shown in Table IV-13. Room-temperature and elevated-temperature mechanical-property tests of INOR-8 weld metal, both in the as-welded and in the aged condition, were made. The results, compared with similar data for Hastelloy B and Hastelloy W, are shown in Fig. 13. Aging seriously reduced the room-temperature ductility of Hastelloys B and W weld metal, while the ductility of the INOR-8 weld metal improved with aging.

The effect of prior thermal fatigue on the stress rupture of Inconel 550 was found by National Advisory Committee for Aeronautics[43] to be a lowering of the subsequent time to rupture. However, prior exposure to stress-rupture conditions produced a slight increase in the subsequent thermal-fatigue life, as illustrated in Fig. 14.

Stainless Steel

Cobalt is present as an impurity element in stainless steels in amounts ranging from 0.03 to 0.3 wt.%. When these steels are used in the core of a reactor, the activity build-up from Co^{60} in the primary loop presents potential maintenance difficulties. Oak Ridge,[44] in studying the problem, concluded that the maximum safe cobalt content is 0.006 wt.%. The price to guarantee such specifications was found to be exorbitant; however, by careful selection of charge materials containing small amounts of cobalt and close cooperation of the vendor, Allegheny Ludlum Steel Corporation, a 0.005 wt.% cobalt alloy was prepared. Cost for the finished plate and sheet was $2.60 per pound. The tensile properties of the type 304L stainless steel containing 0.005 wt.% cobalt were comparable with those of standard stock, which had 0.07 wt.% cobalt. The 0.2% offset yield strength was 34,000 psi, the ultimate tensile strength was 83,000 psi, and the reduction in area was 80 per cent at room temperature. This demonstrates that, by careful monitoring of inexpensive materials required in the making of stainless steel, the desired maximum cobalt content of 0.006 wt.% could be obtained at a cost which was not unreasonable.

A fabrication study and testing program was conducted by Nuclear Development Corp.[45] to determine the manufacturing feasibility and strength characteristics of various welded joints in the types 316 and 304 stainless-steel coolant tubes and associated pigtails (expansion piping) of the sodium-deuterium reactor. Tensile tests run on butt-welded tube joints indicate that all

Table IV-6 TENSILE DATA FOR ZIRCALOY-2*

Annealing practice	Strain rate, in./(in.)(min)	Test temp., °F	Notch condition	H_2 content, ppm	Yield strength (0.2% offset), 1000 psi		Ultimate tensile strength, 1000 psi		Reduction of area, %		Elongation in 1.1 in., %		Uniform elongation in 1.1 in., %		Fracture stress, 1000 psi	
					Ind.	Av.	Ind.	Av.	Ind.	Av.	Ind.	Av.	Ind.	Av.	Ind.	Av.
ASTM Grain Size 7-8																
α	0.0182	77	Unnotched	12	44.8 42.8	43.8	68.0 69.9	69.0	50.0 41.8	45.9	24.4 22.9	23.6	13.1 12.9	13.0	109.0 97.4	103.2
α	1.09	77	Unnotched	12	49.3 52.4	50.8	68.6 67.0	67.8	50.2 49.5	49.8	17.7 19.2	18.4	8.7 10.0	9.4	102.9 101.0	102.0
α	18.2	77	Unnotched	12	51.2 50.8	51.0	73.7 76.3	75.0	46.2 47.6	46.9	19.3 17.8	18.6	11.7 11.2	11.4	98.3 102.8	100.6
α	18.2	77	Unnotched	150	55.6 55.6	55.6	73.7 76.1	74.9	44.7 38.3	41.5	15.6 14.0	14.8	8.8 7.9	8.4	97.8 96.4	97.1
α	18.2	77	Notched	12			114.1 121.8	117.9	14.4 12.6	13.5					133.0 139.4	136.2
α	18.2	77	Notched	150			109.0 100.7	104.8	5.2 5.8	5.5					114.9 106.8	110.8
α	0.0182	600	Unnotched	12	16.1 16.4	16.2	30.9 29.9	30.4	74.8 76.1	75.4	34.7 29.2	32.0	17.8 16.9	17.4	77.0 75.0	76.0
α	18.2	600	Unnotched	12	30.1 29.7	29.9	41.4 39.1	40.2	70.8 70.5	70.6	25.2 32.9	29.0	10.1 12.3	11.2	75.0 66.1	70.6
α	18.2	600	Notched	12			64.9 72.9	68.9	26.0 32.9	29.4					66.0 87.7	
α	18.2	600	Notched	150			75.4 65.9	70.6	32.9 25.0	29.0					104.5 66.8	
α + β	0.0182	77	Unnotched	12	39.8 39.2	39.5	62.6 63.8	63.2	36.3 34.7	35.5	20.3 19.9	20.1	12.5 12.6	12.6	84.3 83.0	83.6
α + β	1.09	77	Unnotched	12	46.9 48.2	47.6	68.6 70.8	69.7	34.2 30.8	32.5	15.3 15.5	15.4	8.9 9.2	9.0	87.6 85.9	86.8
α + β	18.2	77	Unnotched	12	48.8 48.9	48.8	73.9 71.8	72.8	32.3 35.6	34.0	14.9 16.0	15.4	11.3 11.0	11.2	89.9 88.8	89.4
α + β	0.0182	600	Unnotched	12	15.4 15.1	15.2	28.5 29.1	28.8	64.5 58.7	61.6	31.2 28.1	29.6	17.3 15.9	16.6	59.1 51.2	55.2
ASTM Grain Size 3-5																
α	0.0182	77	Unnotched	12	39.2 40.7	40.0	65.6 64.8	65.2	37.0 40.7	38.8	21.3 22.9	21.1	12.4 12.0	12.2	89.1 92.9	91.0
α	0.0182	600	Unnotched	12	16.6 16.4	16.5	28.8 27.5	28.2	69.0 58.2	63.6	36.4 34.8	35.6	15.9 15.5	15.7	61.4 41.8	51.6
α + β	0.0182	77	Unnotched	12	40.8 39.4	40.1	66.0 66.3	66.2	28.3 26.6	27.9	17.7 19.2	18.4	11.7 12.2	12.0	83.2 80.0	81.6
α + β	0.0182	77	Notched	12			90.4 92.3	91.4	7.7 6.7	7.2					119.0 120.0	119.5
α + β	1.09	77	Unnotched	12	42.7 43.8	43.2	70.3 68.6	69.4	27.6 34.5	31.0	15.2 15.6	15.4	11.0 11.6	11.3	84.9 91.3	88.1
α + β	1.09	77	Notched	12			94.2 91.3	92.8	7.7 10.6	9.2					119.5 120.3	119.9
α + β	18.2	77	Unnotched	12	51.9 49.2	50.6	72.8 73.9	73.4	27.7 27.6	27.7	13.9 15.9	14.9	7.2 9.4	8.3	86.5 84.7	85.6

$\alpha + \beta$	1.09	77	Notched	12			94.2 91.3	92.8	7.7 10.6	9.2					120.3	119.9
$\alpha + \beta$	18.2	77	Unnotched	12	51.9 49.2	50.6	72.9 73.9	73.4	27.7 27.6	27.7	13.9 15.9	14.9	7.2 9.4	8.3	86.5 84.7	85.6
$\alpha + \beta$	18.2	77	Notched	12			98.3 103.9	101.1	6.7 8.2	7.4					105.3 113.2	109.2
$\alpha + \beta$	0.0182	600	Unnotched	12	17.0 14.5	15.8	29.6 27.6	28.6	55.9 53.6	54.8	27.5 34.2	30.8	15.3 15.5	15.4	53.7 46.7	50.2
$\alpha + \beta$	0.0182	600	Notched	12			47.0 41.5	44.2	25.3 27.9	26.6					53.4 38.0	45.7
$\alpha + \beta$	1.09	600	Unnotched	12	19.9 19.8	19.9	32.8 33.8	33.3	54.2 53.6	53.9	26.2 23.6	24.9	10.7 10.7	10.7	51.7 51.1	51.4
$\alpha + \beta$	1.09	600	Notched	12			50.2 50.5	50.4	19.2 18.3	18.8					61.0 53.2	51.1
$\alpha + \beta$	18.2	600	Unnotched	12	27.1 28.0	27.6	37.9 40.9	39.4	49.5 48.2	48.8	25.5 19.0	22.2	9.4 8.5	9.0	47.4 53.1	50.2
$\alpha + \beta$	18.2	600	Notched	12			56.3 55.7	56.0	13.3 13.5	13.4					66.7 68.7	67.7
β	0.0182	77	Unnotched	12	50.0 48.3	49.2	65.0 64.2	64.6	31.0 25.9	28.4	19.0 20.0	19.5	15.6 15.2	15.4	92.8 81.2	87.0
β	1.09	77	Unnotched	12	51.7 51.0	51.4	64.0 62.5	63.2	32.5 27.9	30.2	17.2 17.2	17.2	10.7 10.9	10.8	85.7 82.3	84.0
β	18.2	77	Unnotched	12	51.8 48.2	50.0	68.2 65.8	67.0	34.3 35.9	35.1	17.1 17.4	17.2	14.3 13.8	14.0	88.0 90.2	89.1
β	0.0182	600	Unnotched	12	18.8 19.2	19.0	28.1 28.2	28.2	57.3 59.7	58.5	20.7 30.1	25.4	16.0 18.8	17.4	50.5 54.3	52.4
ASTM Grain Size 0-2																
α	0.0182	77	Unnotched	12	41.4 40.1	40.8	64.3 64.5	64.4	32.4 28.6	30.5	20.7 19.5	20.1	11.5 10.9	11.2	83.7 74.5	79.1
α	1.09	77	Unnotched	12	45.6 48.5	47.0	67.9 67.8	67.8	36.9 36.2	36.5	15.9 16.2	16.1	9.6		83.3 84.0	83.6
α	18.2	77	Unnotched	12	47.5 45.9	46.7	72.4 73.9	73.2	31.9 34.9	33.4	15.1 16.8	16.0	10.9 10.7	10.8	86.3 88.7	87.5
α	0.0182	600	Unnotched	12	17.3 15.4	16.4	27.1 28.0	27.6	69.1 64.9	67.0	29.8 30.6	30.2	11.9 13.0	12.4	52.5 52.2	52.3
$\alpha + \beta$	0.0182	77	Unnotched	12	37.6 40.7	39.2	63.1 65.1	64.1	24.7 24.1	24.4	17.1 15.7	16.4	10.3 9.8	10.0	80.8 80.8	80.8
$\alpha + \beta$	1.09	77	Unnotched	12	44.9 46.5	45.7	67.6 69.1	68.4	20.9 24.6	22.8	13.2 13.3	13.2	8.7 8.5	8.6	79.0 61.6	70.3
$\alpha + \beta$	18.2	77	Unnotched	12	44.1 45.7	44.9	73.1 74.1	73.6	23.0 24.0	23.5	14.7 14.4	14.6	11.5 11.7	11.6	83.2 83.9	83.6
$\alpha + \beta$	0.0182	600	Unnotched	12	15.8 15.4	15.6	30.2 28.0	29.1	51.5 52.0	51.8	26.1 29.4	27.8	13.5 16.5	15.0	50.5 47.4	49.0
β	0.0182	77	Unnotched	12	48.5 48.3	48.4	62.8 63.3	63.0	26.5 26.9	26.7	19.8 20.0	19.9	15.2 15.1	15.2	80.3 81.6	81.0
β	1.09	77	Unnotched	12	51.5 54.4	53.0	66.6 67.2	66.9	26.1 29.4	27.8	16.9 17.9	17.4	10.3 10.5	10.4	64.6 70.1	67.4
β	18.2	77	Unnotched	12	50.9 48.6	49.8	70.2 70.0	70.1	30.2 28.2	29.2	19.3 17.8	18.6	14.9 12.5	13.7	91.9 86.3	89.1
β	0.0182	600	Unnotched	12	18.8 18.5	18.6	28.2 27.1	27.6	56.4 60.5	58.4	34.1 26.5	30.3	18.8 17.8	18.3	47.7 53.7	50.7

* Data taken from reference 7.

Table IV-7 MECHANICAL PROPERTIES OF NIOBIUM-ZIRCONIUM ALLOYS*

Nominal composition, wt.%		Condition†	Test temp., °C	Yield strength (0.2% offset), 1000 psi	Tensile strength, 1000 psi	Total elongation, %	Reduction of area, %	Elastic modulus, 10^6 psi
Nb	Zr							
5	95	As-fab.	R.T.	93.6	190.2	5	1.4	
		Homog.	R.T.	91.9	145.2	8	9.7	
		Homog.	500	50.0	68.0	22	75.0	
		Reacted	R.T.	71.1	133.1	20	18.7	
		Reacted	500	37.5	40.0	30	91.0	
17.5	82.5	As fab.	R.T.	122.1	125.8	8	26.0	
		Homog.	R.T.	80.6	90.0	20	35.5	
		Reacted	R.T.	61.3	159.7	5	6.5	
25	75	As fab.	R.T.	90.3	94.8	22	35.0	
		As fab.	500		74.8	16	29.0	
50	50	As fab.	R.T.	135.3	137.4	1	4.7	
		As fab.	500	102.0	123.0	20	29.6	
		Reacted	R.T.	147.0	158.0	12	33.5	16.7
		Reacted	500	111.5	133.3	12	23.1	
96	4	As fab.	R.T.	52.5	73.0	20	65.6	
		As fab.	500	44.9	60.6		61.0	
		Homog.	R.T.	41.4	63.7	27	72.4	16.2
		Homog.	500	33.7	50.1	25	74.2	

* Data taken from reference 18.

† As fabricated, no heat-treatment after working; homogenized, 24 hr at 1000°C, air cooled; reacted for 24 hr at 1000°C, air cooled, and for one week at 500°C, air cooled.

Table IV-8 COMPARISON OF CREEP DATA FOR INOR-8 SHEET SPECIMENS TESTED IN FUEL SALT 107 AND IN AIR*

Temp., °F	Stress, psi	Environment	Time, hr, to specified strain				Time to rupture, hr
			0.5%	1.0%	2.0%	5.0%	
1800	3,000	Salt	4.5	17	48	115	130
		Air	8	17	35		75
1700	5,000	Salt	4.5	12.5	31	110	250
		Air	5.4	12.5	25	58	90
1500	8,000	Salt	19	52	125	350	880
		Air	29	49	86	175	260
1250	20,000	Salt†	110	265	680	1600	2400
		Air	180	320	720	1500	2180

* Data taken from reference 41.

† Interpolated data.

Table IV-9 COMPARISON OF CREEP DATA FOR INOR-8 SHEET AND ROD SPECIMENS TESTED IN AIR AT 1250°F*

Stress, psi	Specimen	Time, hr, to specified strain						Time to rupture, hr
		0.1%	0.2%	0.5%	1.0%	2.0%	5.0%	
20,000	Sheet	30	80	190	350	730	1700	1786
	Sheet	30	64	180	320	720	1500	2177
	Rod	20	125	300	510	920	1800	3535
	Rod	15	100	300	510	920	2200	
15,000	Sheet	190	350	750	1400			
	Sheet	120	330	780	1500			
	Rod	130	300	740	1500			
12,000	Sheet	600	931	2275				
	Rod	320	740	2082				
10,000	Sheet	1650	2600	4270				
	Rod	760	1600	3596				

*Data taken from reference 41.

Table IV-10 EFFECT OF NOTCHES ON THE TENSILE STRENGTH AND DUCTILITY OF INOR-8*

Temp.	Geometry	Tensile strength, psi	Reduction of area, %	Notch strength ratio
Room	Unnotched	116,000	48	1.08
	Notched (0.005-in. radius)	125,000	20	
1500°F	Unnotched	48,500	15	1.37
	Notched (0.0045-in. radius)	66,500	8	

*Data taken from reference 41.

the types of welds considered were adequate and of essentially equivalent strengths. The major test effort was made on the fatigue tests of pigtail-headers, T-joints, and pigtail-tube T-joints subject to bending loads. The tests indicated a life of 100,000 cycles before failure at 16,500 psi, the design stress.

The iron-aluminum alloys are suitable for use in reactors because of their excellent oxidation resistance at elevated temperatures and lower thermal-neutron cross sections. Experimental work is being conducted to determine the main effect of zirconium, niobium, and molybdenum on a base alloy of iron-chromium and aluminum.[19] Additions of these elements increased the stress-rupture life of the base alloy at elevated temperatures. Zirconium had a deleterious effect on the oxidation resistance of the base alloy of samples treated at 1650 and 1800°F. Zirconium improved the high-temperature yield strength, but the room-temperature ductility of the base alloy decreased with increasing additions of zirconium and niobium.

Creep buckling and tube burst tests were made on type 304 stainless-steel tubing at Oak Ridge.[46] Different modes of collapse of the tubes under external pressure were determined. Conditions for uniform collapse of tubing around UO_2 pellets were determined at temperatures ranging from 1300 to 1700°F. The results of burst tests are given in Table IV-14.

Niobium

Interest in niobium as a structural and cladding material remains strong. Begley et al.[11] have determined the results of physical- and mechanical-property studies of cage-zone-melted, electron-beam-melted, and production-quality (Fansteel) niobium. Yield strength and tensile elongation data for these materials are shown in Fig. 15. Higher yield strengths of production-quality niobium were attributed to the presence of 0.6 wt.% zirconium in the material. In other studies, the recrystallization temperature of 80 per cent cold-worked, high-purity, cage-zone-melted niobium was determined to be 1080°C (½ hr). The dynamic modulus of elasticity of cage-zone-melted zirconium was determined at 16.89×10^6 psi at 25°C. Niobium specimens subjected to repeated dynamic modulus testing displayed increases of 0.5 to 2.5 per cent of the modulus as an effect of atmospheric contamination of the specimen during test. Atmospheric contamina-

Table IV-11 RESULTS OF MECHANICAL TESTS IN ROOM-TEMPERATURE AIR OF INCONEL AND INOR-8 SPECIMENS CARBURIZED IN SODIUM-GRAPHITE SYSTEMS*

Exposure temp., °F	Exposure period, hr	Specimen treatment	Mechanical properties: Yield strength, 1000 psi	Tensile strength, 1000 psi	Elongation in 2 in., %
			Inconel		
1200	40	Control†	24.1	80.8	40.1
		Carburized	27.2	84.2	38.0
1400	40‡	Control	23.9	81.3	38.8
		Carburized	27.0	83.9	36.8
	400‡	Control	24.3	81.7	37.9
		Carburized	30.9	92.9	27.0
1600	40§	Control	20.9	75.9	47.3
		Carburized	28.5	91.5	25.7
			INOR-8		
1200	40	Control†	53.3	120.3	43.6
		Carburized	53.1	119.6	43.8
1400	40‡	Control	53.7	122.0	42.6
		Carburized	53.9	120.5	36.9
	400‡	Control	53.2	120.7	43.0
		Carburized	57.4	103.2	8.8
1600	40§	Control	50.5	116.3	50.0
		Carburized	52.8	98.5	7.8

* Data taken from reference 24.
† Control specimens exposed to argon at the conditions given.
‡ Test values given for these specimens are averages of two tests.
§ Test values given for these specimens are averages of three tests.

Table IV-12 RESULTS OF MECHANICAL TESTS IN 1250°F AIR OF INCONEL AND INOR-8 SPECIMENS CARBURIZED IN SODIUM-GRAPHITE SYSTEMS*

Exposure temp., °F	Exposure period, hr	Specimen treatment	Mechanical properties: Yield strength, 1000 psi	Tensile strength, 1000 psi	Elongation in 2 in., %
			Inconel		
1200	40	Control†		50.3	38.5
		Carburized		48.6	33.5
1400	40	Control†		46.7	36.5
		Carburized		49.9	23.0
	400	Control†	16.4	45.2	26.5
		Carburized	22.0	50.7	21.0
1600	40	Control†	11.3	42.4	16.5
				41.4	18.5
		Carburized	20.5	53.9	24.8
				51.1	28.5
			INOR-8		
1200	40	Control†		70.2	17.0
		Carburized		74.4	19.0
1400	40	Control†		74.6	18.5
		Carburized		76.8	19.5
	400	Control†	36.8	70.3	16.5
				74.5	20.5
		Carburized	42.4	82.9	18.0
				85.2	22.0
1600	40	Control†	33.8	68.9	18.5
				70.6	6.5
		Carburized	40.5	82.8	13.0

* Data taken from reference 24.
† Control specimens exposed to argon at the conditions indicated.

tion problems were also prevalent in high-temperature vacuum creep-rupture tests of niobium; resulting data were inconclusive. However, short-time rupture strengths of production quality niobium were approximately double those determined for the more pure electron-beam-melted niobium.

Table IV-13 CREEP TEST RESULTS OF INOR-8 AND INCONEL SPECIMENS IN A SODIUM-GRAPHITE SYSTEM FOR 40 HR AT 1600°F

(Test conditions: temp., 1250°F; environment, argon; stress, 18,500 psi)

Specimen	Time to rupture, hr	Elongation in 2 in., %
INOR-8:		
Control	1734	23.8
Carburized	4031†	9.0†
Inconel:		
Control	38	21.2
Carburized	160	47.5

*Data taken from reference 24.
†Still in test.

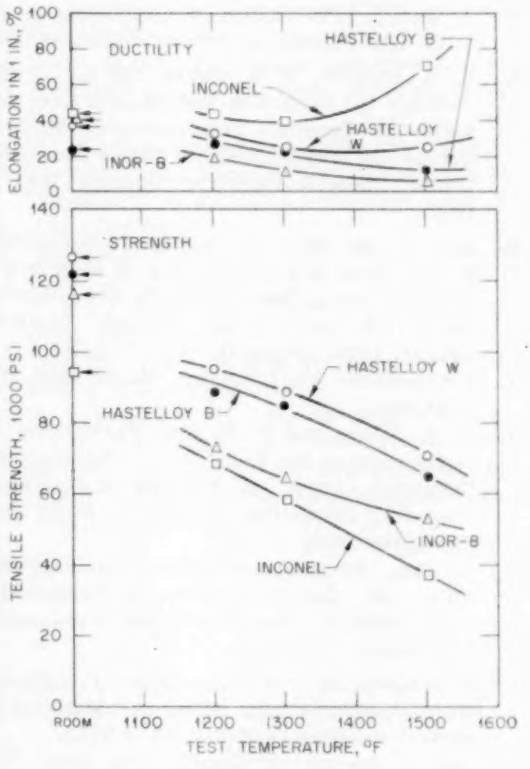

Figure 13—Mechanical properties of weld metal in as-welded condition. Data taken from reference 24.

A brittle-to-ductile transition is reported for niobium at −125°C. It is also reported that niobium can be reduced 99 per cent without intermediate annealing and with little danger of rapid strain hardening. (F. R. Shober)

Recent Literature Surveys

A comprehensive compilation of published data on zirconium and its alloys is presented by Lowenstein and Gilbert.[47] This review gives in detail the physical, chemical, and mechanical properties of both zirconium and zirconium alloys and includes corrosion resistance, alloy preparation, structure, and fabrication data.

A bibliography, compiled by T. F. Davis, deals with refractory metals and their alloys. Classified[48] and unclassified[49] AEC reports and non-AEC references have been included, covering materials with reasonably high melting points.

Sylvania has compiled[50] a "Bibliography on the Effects of Irradiation in Solids" (5th edition,

Table IV-14 RESULTS FROM BURST TESTS ON 0.200-IN.-WALL TYPE 304 STAINLESS-STEEL TUBING*

Temp., °F	Internal pressure, psi	Time to rupture, hr	Tangential stress, psi	Av. tangential strain, %
1500	400	375	7,140	6.36
1500	200	1184	3,750	2.04
1500	700	306	12,495	1.86

*Data taken from reference 46.

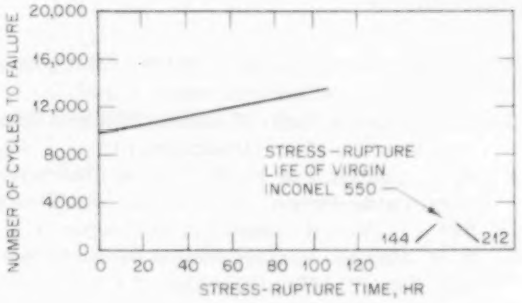

Figure 14—Effect of exposure to stress rupture at 1350°F on subsequent thermal-fatigue life for cycling between 1350 and 200°F on 30-15-30-15-sec cycle. Inconel 550 stressed at 56,500 psi during stress rupture. Data taken from reference 43.

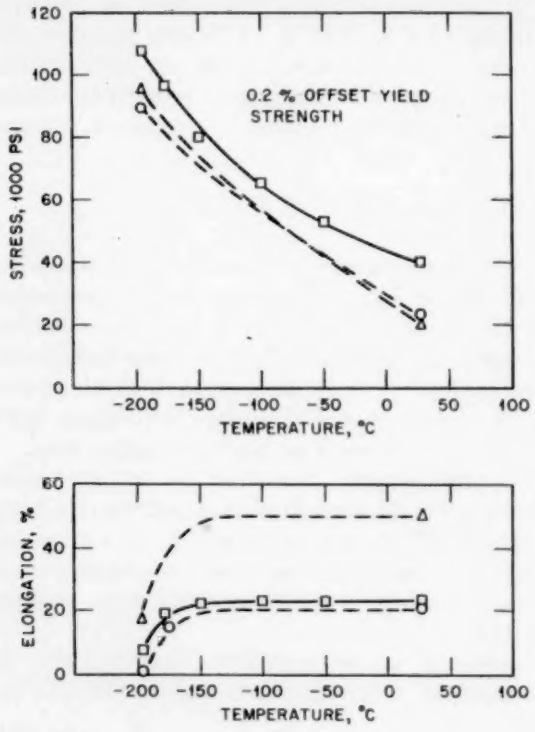

Figure 15—Effect of temperature on the yield strength and elongation of niobium. △, SEG-2 niobium. ○, CZ-2, niobium. □, Fansteel bar 1207. Data taken from reference 11.

1958), which is an extension of the 1955 publication. It contains a complete subject index covering the 958 references under three categories: theoretical aspects, effects on metals, and effects on nonmetals.

References

1. Zirconium Highlights, WAPD-ZH-15, March 1959. (Unclassified AEC report.)
2. F. W. Albaugh, Hanford Atomic Products Operation, Mar. 15, 1959. (Unpublished.)
3. F. E. Littman and F. M. Church, Reactions of Metal with Oxygen and Steam, AECU-4092, Feb. 15, 1959. (Unclassified AEC report.)
4. F. W. Albaugh, Hanford Atomic Products Operation, Feb. 15, 1959. (Unpublished.)
5. G. J. Biefer, Effects of Alloying Additions and Temperature on the Corrosion of Aluminum-Nickel-Iron Alloys in High-temperature Water, CR-MET-796, July 1958. (Unclassified Canadian report.)
6. J. E. Draley and W. E. Ruther, Corrosion Resistance and Mechanical Properties of Aluminum Powder Products, ANL-5927, March 1959. (Unclassified AEC report.)
7. Reactor Technology Report No. 8. Metallurgy, KAPL-2000-5, March 1959. (Unclassified AEC report.)
8. G. H. Borrmann and G. E. Galonian, Results of Thermal Cycling Stress Corrosion Tests of Type 347 Stainless Steel in 500°F pH 10-11 Lithium Hydroxide, KAPL-M-GHB-1, Jan. 8, 1959. (Unclassified AEC report.)
9. Bettis Technical Review, Reactor Chemistry and Plant Materials, WAPD-BT-11, December 1958. (Unclassified AEC report.)
10. J. W. McGrew, Autoclave Testing of Type 430 Stainless Steel, MND-E-1602, Martin Co., Nuclear Div., January 1959.
11. R. T. Begley, ed., Development of Niobium-base Alloys, WADC-TR-57-344(Pt.II), Nov. 30, 1958. (Unclassified USAF report.)
12. E. A. Gulbransen and K. F. Andrew, Kinetics of the Reactions of Columbium and Tantalum with O_2, N_2, and H_2, *Transactions of the American Institute of Mining Engineers*, 188: 586 (March 1950).
13. H. J. Goldschmidt, A High-temperature X-Ray Investigation of Niobium Pentoxide and Some Problems Concerning the Oxidation of Niobium, *Journal of the Institute of Metals*, 87: 235 (April 1959).
14. H. Inouye, The Scaling of Columbium in Air, AIME-IMD Special Report No. 5, Jan. 31, 1957.
15. E. S. Bartlett, H. R. Ogden, and R. I. Jaffee, Coatings for Protecting Molybdenum from Oxidation at Elevated Temperatures, DMIC-109 (ASTIA AD-210978), Defense Metals Information Center, Battelle Memorial Institute, Mar. 6, 1959.
16. *Reactor Core Materials*, 2(1): 29 (February 1959).
17. D. D. Whyte et al., Corrosion of Materials of Construction, in "Quarterly Progress Report for the Period July 1 to Sept. 30, 1958," YAEC-97, Nov. 14, 1958. (Unclassified AEC report.)
18. Westinghouse Electric Corp., March 1959. (Unpublished.)
19. G. R. Wilms and T. W. Rea, Preliminary Investigations on the Properties of Chromium and Chromium Alloys at Elevated Temperature, *Journal of the Institute of Metals*, 87(3): 77-78 (November 1958).
20. F. Tate, Development of Iron-Aluminum Base Alloys for Gas-cooled Reactor Components, MND-DB-2523, September 1958. (Unclassified AEC report.)
21. * K. D. Smelnikov, V. E. Ivanov, and V. F. Zelensky, Magnesium-Beryllium Alloys As Material for Nuclear Reactors, A/CONF. 15/P/2153.
22. Atomic Energy of Canada, Ltd., June 1958. (Unpublished.)
23. E. L. Francis, Vanadium Data Manual, IGR-R/R-306, 1958. (Unclassified British report.)

24. Molten Salt Reactor Program Quarterly Progress Report for Period Ending Oct. 31, 1958, ORNL-2626, Jan. 23, 1959. (Unclassified AEC report.)
25. J. H. Consiglio et al., Knolls Atomic Power Laboratory, June 15, 1957. (Unpublished.)
26. Babcock and Wilcox Co., January 1959. (Unpublished.)
27. R. E. Smallman and K. H. Westmacott, The Structure of Quenched and Irradiated Metals, AERE-M/R-2699, December 1958. (Unclassified British report.)
28. D. G. Martin, Dimensional Changes in Single Crystals of Synthetic Sapphire After Irradiation, AERE-M/M-212, November 1958. (Unclassified British report.)
29. Quarterly Progress Report Fuels Development Operation, July, August, and September, 1958, HW-58205, Oct. 15, 1958. (Secret AEC report.)
30. M. G. Buck, comp., Semiannual Confidential Technical Progress Report for July–December 1958, DP-366, February 1959. (Confidential AEC report.)
31. D. R. Harries, A Survey of the Effects of Neutron Irradiation on the Properties of Iron and Steels, AERE-M/TN-54, November 1958. (Unclassified British report.)
32. R. M. Hale, Graphical Compilation of Radiation Effects on Mechanical Properties of Solids, WADC-TN-58-335, November 1958. (Unclassified USAF report.)
33. L. E. Tanner, The System Zirconium-Iron-Tin, ARF-2068-5, July 29, 1958. (Unclassified AEC report.)
34. F. W. Kunz and A. E. Bibb, Habit Plane for Hydride Precipitation in Zirconium and Uranium-Zirconium, KAPL-2002, Jan. 22, 1959. (Unclassified AEC report.)
35. Zirconium Highlights, WAPD-ZH-12, November 1958. (Unclassified AEC report.)
36. C. E. Lundin, Denver Research Institute, May 20, 1958. (Unpublished.)
37. R. F. Domagala, Illinois Institute of Technology, Oct. 6, 1958. (Unpublished.)
38. R. F. Decker et al., Influence of Heat Treatment on Microstructure and High-temperature Properties of a Nickel-base Precipitation-hardening Alloy, NACA-TN-4329, National Advisory Committee for Aeronautics, 1958.
39. A. P. Coldren and J. W. Freeman, An Investigation of the Relationship Between Microstructure and Creep-rupture Properties of Heat-resistant Alloys, WADC-TR-58-204, July 1958. (Unclassi- USAF report.)
40. B. Lustman and F. Kerze, Jr., "The Metallurgy of Zirconium," p. 633, McGraw-Hill Book Company, Inc., New York, 1955.
41. Molten Salt Reactor Project Quarterly Progress Report for Period Ending Jan. 31, 1959, ORNL-2684, Mar. 17, 1959. (Unclassified AEC report.)
42. C. R. Kennedy, W. O. Harms, and D. A. Douglas, Multiaxial Creep Studies on Inconel at 1500°F, ORNL-2622, Feb. 5, 1959. (Unclassified AEC report.)
43. F. J. Clauss and J. W. Freeman, Thermal Fatigue of Ductile Metals, Part II, NACA-TN-4165, National Advisory Committee for Aeronautics, 1958.
44. Oak Ridge National Laboratory, Apr. 6, 1959. (Unpublished.)
45. D. Burgreen and J. Cummins, Experimental Evaluation of Austenitic Stainless-steel Piping for Sodium-Deuterium Reactor, NDA-84-11, Aug. 26, 1958. (Unclassified AEC report.)
46. Gas-cooled Reactor Project Semiannual Progress Report for Period Ending Dec. 31, 1958, ORNL-2676, Mar. 26, 1959. (Unclassified AEC report.)
47. H. Lowenstein and H. L. Gilbert, Zirconium: A Review and Summary of Published Data, AECU-3818, October 1958. (Unclassified AEC report.)
48. T. F. Davis, U. S. Atomic Energy Commission, January 1959. (Unpublished.)
49. T. F. Davis, comp., Refractory Metals and Their Alloys, A Literature Search, TID-3524, January 1959. (Unclassified AEC report.)
50. Bibliography on the Effects of Irradiation in Solids (5th Edition–1958), Sylvania-Corning Nuclear Corp.

---

*Second United Nations International Conference on the Peaceful Uses of Atomic Energy, Geneva, September 1958. (Individual papers available from the Office of Technical Services, Dept. of Commerce, Washington 25, D. C. Bound volumes of papers are available from United Nations, Office of Public Information, New York.)

Melting, Casting, Heat-treatment, and Hot Working

The occurrence of hydrogen in as-reduced uranium in quantities greater than 2 ppm has been responsible for considerable effort to establish its source and eliminate it from fuel material. Despite this effort, no procedure other than vacuum outgassing at high temperatures has been successful. In this regard, 7-in.-diameter bars were vacuum outgassed by Mallinckrodt[1] at 1700°F for 27½ hr at 2.5×10^{-1} mm Hg abs and the hydrogen content dropped from 6.6 and 6.4 ppm to 1.5 and 1.7 ppm. A broader program is being planned in which liner additives, isolation of metal from reaction slag, agitation of regulus by bomb tilting, outgassing of molten stream, and the behavior of multiple charges in a single bomb will all be investigated.

Impurities that uranium picks up during vacuum melting were investigated by National Lead.[2] Specifically, mold coatings applied to graphite crucibles were evaluated in reference to the type of coating and the method by which it was applied. The materials tested were BeO, MgO, $MgZrO_3$, UO_2, Al_2O_3, $CaO \cdot ZrO_2$, $MgO \cdot Al_2O_3$, $MgO \cdot ZrO_2$, TiC, and ZrC. Flame-sprayed magnesium zirconate ($MgZrO_3$) was determined to be best in that the carbon pickup averaged only 73 ppm for as-reduced uranium charges. However, if temperatures above 2500°F were encountered, the graphite reacted with the coating and CO was produced.

The favorable irradiation properties exhibited by cast uranium with fine-grain, randomly oriented structures were responsible for a review of methods of refining the as-cast structure of uranium by Culcheth Laboratories.[3] They concluded that:

1. Grain refinement by such methods as fast cooling and turbulence are not promising in that, although they refine grains, they produce a preferred orientation.

2. The mechanisms by which grain-refining additives act are not completely understood and the proposed theories, in the case of uranium, can only be tested experimentally.

3. Nucleation at the mold wall would be best if the grain refinement persisted to the ingot center since no impurity would be introduced.

4. Nucleation methods found to be effective with unalloyed uranium on a small scale proably would have to be modified for large-scale use in the production of unalloyed or alloyed fuel-element material.

The economics involved in fabricating tubular shapes from uranium to obtain hollow fuel elements is of continuing interest. Bridgeport Brass[4] now considers that the economics of extruding tubing is borderline for processes involving a tipped mandrel. Future investigations are being confined to processes employing a projectile type mandrel. Longer mandrel life and improved tube concentricities are anticipated. Polson et al. of National Lead recently reported[5] on scoping studies to demonstrate that conventional industrial equipment could be used for making uranium tubes. Static and centrifugal casting, elongations by an Assel Mill, Rotoroll or Rockrite tube forming, and Hamiroll swaging are covered. No economics were discussed since the qualities of the products were undefined.

Development work on the forge rolling of Zircaloy fuel-element components was reported[6] by Clevite. In this study, recesses in Zircaloy-2 cover plates were formed to reproducible dimensions by a two-pass system. Sensitivity of the qualities of the cover plates to such operating conditions as reductions, roll lubrication, and strip temperature made roll design difficult.

Westinghouse research workers have been concerned with the investigation of niobium as a high-temperature, high-strength material. In attempting to establish the qualities of unalloyed niobium, they have been hampered to some extent by the lack of high-purity niobium. Therefore a portion of their efforts has been devoted to preparing materials of low and known impurity content. In this regard, Begley[7] reports on a variety of processes to which niobium was subjected in order to effect purification. "Cage

zone" melting, in which a square bar of niobium is induction melted while in a vertical position, is described. The configuration of the bar is such that the corners support the molten core and volumes greater than normal can be zone melted. In niobium the impurities in the corner supports obscured the zone-refining effects and the "floating zone" techniques were tried. Analyses before and after zone refining demonstrated that decreases in oxygen from 0.014 to 0.0037 wt.% and nitrogen from 0.030 to 0.008 wt.% were effected.

Subsequently, larger quantities of relatively pure niobium melted by the electron-beam technique (Temescal Corporation, Richmond, Calif.) became available. The ingots so obtained were easily cold forged and rolled. Niobium ingots were also prepared by vacuum arc melting. However, impurity levels were not consistent or as low as those obtained in electron-beam melted material, and hot working of the cast structure was necessary. The most satisfactory breakdown procedure described was that of closed-die forging. The major problem of hot working (from argon-atmosphere furnace) was contamination and embrittlement of the surface. After successful hot working, it was necessary to remove 25 to 40 mils from the hot-worked surface before it was possible to cold work without cracking.

A technique borrowed from the ceramist, slip casting, has been used to form metallic shapes from metal powders. New York Operations[6] reports on the slip casting, sintering, and physical testing of type 316 stainless-steel powders. The use of slip casting as an economic process where production quantities are limited and the extension of its application to cermets is forecast.

(E. L. Foster)

Cladding

Pressure Bonding

The technique of bonding reactor components by use of gas pressure at elevated temperatures is being investigated by several laboratories. The process is extremely versatile and can be applied to the cladding and bonding of brittle materials and complex shapes that cannot be fabricated readily by conventional processes. A description of this process and discussion of its application to the bonding of various reactor components is summarized in a Geneva Conference report prepared by Battelle[11] and in a preprint of a paper presented by Sylvania[12] at the latest Nuclear Engineering and Science Conference.

Investigations[10,13–15] are also being made of the use of the gas-pressure bonding process for the preparation of Zircaloy-clad flat-plate uranium dioxide fuel elements. The uranium dioxide cores, in the form of rectangular plates, are compartmented by use of Zircaloy ribs designed to reinforce the element and form gas-pressure chambers capable of containing released fission gas. The compartments also serve to minimize fission-gas release and to localize damage in the event of a cladding failure. The uranium dioxide

ANNOUNCING

An AEC-sponsored symposium on

CHEMICAL REPROCESSING OF POWER FUELS

to be held

OCTOBER 20-21, 1959

RICHLAND, WASHINGTON

Additional information may be obtained from J. T. Christy, Chief, Separations Branch, Hanford Operations Office, AEC, Richland, Washington

cores are coated with a spray coat of graphite to prevent reaction with the Zircaloy cladding during the bonding operation. The components are assembled and contained in an envelope which is evacuated and sealed, or they are assembled, edge welded, and evacuated prior to bonding. These assemblies are bonded at 1550°F for 4 hr utilizing an inert-gas pressure of 10,000 psi. Bond integrity has been evaluated by both gas-pressure testing for intercompartment leakage and by determining maximum burst strength. Occasionally, intercompartment leakage has been detected.

Integral Zircaloy-clad zirconium-uranium subassemblies were prepared by Battelle[16] in a one-step gas-pressure bonding operation. The assembly was formed with a series of simple rectangular components. Flat Ti-Namel sheet was employed as spacer material. After bonding, the Ti-Namel sheet was dissolved with acid to form the coolant channels of the assembly. Assemblies containing 16 fuel plates and measuring 2 by 2 by 20 in. were prepared by bonding at 1550°F for 4 hr with 10,000 psi of helium gas.

A study[13,14,17] is being conducted to determine the mechanism and kinetics associated with the formation of a bond interface during the gas-pressure bonding process. Copper and zirconium specimens prepared with different surface roughness are being bonded under controlled but variable conditions of pressure and temperature.

(Stan J. Paprocki)

Diffusion Bonding

Two general methods of fabricating Zircaloy-2, compartmented receptacle plates for Core 2 fuel-element loadings by assembly of pieced components are of continuing interest at Bettis.[10] One method involves the assembly and joining of pieced rib, edge strip, and end-piece components. Compartments are formed by mechanically positioning longitudinal ribs with slotted transverse ribs. The second receptacle plate, pieced, fabrication method involves the use of preformed compartments. In this method, receptacle plates are assembled by mechanically placing the integral compartments within the confines of a picture frame which is formed by welding edge strips and end pieces. The compartment units are made by (1) forming rectangular Zircaloy-2 wire into ¼-in.-wide by 6-in.-long square-ended compartments and resistance welding a lap joint along the ¼-in. compartment end, and (2) by stretch forming 0.102-in.-wide rings obtained by cutting segments from a 4-in.-diameter Zircaloy-2 tube.

Intercompartment communication tests at 700 psi test pressure on copper-eutectic, diffusion-bonded, PWR-2 blanket fuel elements indicate that the use of UO_2 fuel wafers having a thickness greater than the receptacle rib thickness was the major cause of the lack of complete bonding in these elements.[15] These tests showed 100 per cent bonding in one element of those tested. Intercompartment integrity test results, metallographic examination, and rupture-test results for 11 bonded elements are to be reported later.

(M. A. Gedwill, Jr.)

Coextrusion

To reduce the cost of producing uranium tubing, an investigation of the applicability of the coextrusion process was conducted by the Bridgeport Brass Company.[4] The conventional mandrel method in which a tipped mandrel is used to size the inside diameter of the tubing was considered too costly due to the initial cost and short life of the mandrel. It appeared that, if the tooling could be minimized by use of a coextrusion method incorporating some core material that could be removed later, the cost of the extruded piece would be greatly reduced. In this investigation the uranium billet was pierced, a brass core was assembled into the billet, and the assembly was extruded to specified tubing dimensions. The brass core was then pulled from the center of the uranium tube. The results of the investigation indicated that coextrusion of uranium with a brass core to form a tube is possible; however, it is too early to evaluate the method in terms of either process control or cost. It was felt that dimensional control could be greatly improved by using billets of fine-grain material to prevent a rough interface.

Investigations have been made by Nuclear Metals[18] of coextrusion methods for providing clad metals for special service conditions. The coextrusion of various metals to form a variety of shapes has been developed. Some typical applications have included the coextrusion of stainless-steel-clad molybdenum, stainless-steel-clad niobium, zirconium-clad copper, and titanium-clad copper tubing.

A method of hot coextruding complex shapes through a round die has been developed by Knolls[19,20] to fabricate clad powder-metallurgy

parts. Multiblade rods of X and Y shapes consisting of a rare-earth oxide dispersed in a stainless-steel core and encased in stainless-steel cladding have been successfully coextruded with good dimensional control and reproducibility. The procedure involves the assembling and extruding of steel billets of a round cross section which contain an axially located assembly of powder-metallurgy and sheet-metal parts. The mild-steel parts are removed by machining and pickling after extrusion, leaving a fully clad, dense rod having the desired shape and composition. Rods with thin stainless-steel cladding over stainless-Sm_2O_3 dispersions, ranging in composition from 15 to 40 vol.% of the oxide, have been fabricated with entirely satisfactory results.

Nuclear Metals[21,22] has experimentally coextruded several rods of uranium–2 wt.% zirconium alloy clad with beryllium so that the dimensions are fairly uniform and the cladding uncracked. The multitemperature method was used with many temperature combinations. Rods approximately 2 ft long by 0.350-in. in diameter with a 0.015-in.-thick beryllium cladding were extruded. Some conditions were standardized as follows: reduction, 7.1X; ram speed, 20 in./min; lubricant, Oil Dag; liner temperature, 900°F; canning material, mild steel; wall thickness of outer-jacket components, ½ in.; and cutoff, graphite. The process appears feasible for scaling up in size. However, when this technique was tried with unalloyed uranium as the core, satisfactory cladding with beryllium could not be achieved.

Experiments indicate that acceptable extrusion claddings of beryllium can be made on those uranium alloys in which the beta-uranium-phase field is restricted or eliminated by the alloying element. Uranium–2 wt.% zirconium does not exhibit a beta-phase region, and this is believed to be one reason why this material can be extruded satisfactorily. Other differences between unalloyed uranium and uranium–2 wt.% zirconium alloy which would be reflected in extrudability are: (1) grain size is coarser in unalloyed material, and (2) sharp discontinuities in the extrusion constant and thermal-expansion characteristics exist in unalloyed material at phase boundaries. In order to study further the effect of beta phase on the coextrudability, cladding experiments were done on uranium–0.14 wt.% silicon alloy. This alloy has a restricted beta-phase field and thus should exhibit cladding performance intermediate between that of unalloyed uranium and uranium–2 wt.% zirconium alloy. As expected, the uranium–0.14 wt.% silicon alloy did clad more satisfactorily than did unalloyed uranium but less so than uranium–2 wt.% zirconium alloy. Other multitemperature extrusions are being investigated[22] for certain combinations of otherwise desirable fuel-rod materials which are not coextruded at present because of their difference in stiffness at a given temperature. These include uranium or thorium-uranium alloys clad with stainless steel, uranium or thorium-uranium alloys clad with magnesium, and ceramics and cermets clad with stainless steel.

Two Zircaloy-2-clad solid uranium rods were successfully coextruded by Hanford[23] on a 280-ton extrusion press. The extrusion billets consisted of a solid cylinder of beta heat-treated uranium, 1.685-in. in outside diameter by 4⅜ in. long, placed inside a 0.185-in.-wall Zircaloy-2 can. The can was then evacuated and sealed by electron-beam welding a ⅛-in. flat Zircaloy-2 disk in each end. The evacuated assembly was then placed in a 0.062-in.-wall copper can with a 45 deg beveled nose plug and a ½-in. end plug. The copper can was also evacuated and sealed by electron-beam welding. The extrusion was carried out at a 10 to 1 ratio with the billet preheated at 650°C. Investigations[24] of billet design and component fabrication were conducted to learn the influence of copper cladding thickness and uranium structure on the uranium–Zircaloy-2 interface. There was a pronounced improvement in smoothness of the interface with the fine-grained alpha-rolled core over that of the beta heat-treated core with the same copper thickness. Reduction of the copper thickness produced some improvement of the interface.

The French[25] have obtained promising results in the coextrusion of fuel rods of solid uranium–1 to 2 wt.% zirconium clad with zirconium and fuel tubes of powdered uranium-aluminum alloy with 30 wt.% uranium clad inside and outside with aluminum.

An extensive investigation was conducted by Knolls[26] into the coextrusion and other manufacturing variables in the fabrication of boron carbide–Zircaloy-2 dispersion. The effects of fabrication variables on the fracturing and distribution of the boron carbide particles and on core dimensional uniformity were studied. The results of the investigation indicated that the shear stresses developed during extrusion were

not the primary cause of particle fracturing and, consequently, of the stringering.

Nuclear Metals[21] has been investigating the causes and methods of minimizing or eliminating different defects sometimes contained in coextruded rods and tubes. Two of these defects studied have been named "shift" and "whiskers." The shift has been defined as the asymmetric flow of metal about the extrusion axis and whiskers as thin strands of core material which extend into the end-seal region beyond the main terminus of the core. Methods of minimizing or eliminating shifts and whiskers are being studied. (C. B. Boyer)

Canning

Canning of pellet type fuel elements has been greatly facilitated by the use of a vacuum-loading technique.[27] Pellet chipping tendencies and loading friction of Yankee type fuel tubes have been reduced by this method. The fuel pellets are first drawn into the tube and the tube is then stretched so as to obtain the minimum amount of clearance between the pellets and tube walls.

Air pressure is used in a promising injection-casting technique[23] at Hanford. However, the problem of removing what is apparently deeply embedded lubricant from the interior of Zircaloy tubing must be resolved before good bonding can be achieved. Castings made into 0.008-in.-wall stainless-steel tubing have resulted in good bonds. (Paul H. Bonnell)

Nonelectrolytic Chemical-plating Techniques

As a result of projected high-temperature operation in nuclear reactors, missiles, and space vehicles, interest in the protective coating of materials has shown a steady increase. Jelinek[28] has reviewed various processes available for the protective coating of metal, hot dipping, cementation, cladding, electroplating, metal spraying, and vapor deposition.

In the U.S.S.R.[29] uranium wires 40 mm in diameter were coated with 0.5 mm of a magnesium – 2 to 5 wt.% beryllium alloy by alternate condensation of the metal vapors in vacuum. Bundles of wire were jacketed in magnesium-beryllium alloy tubes as fuel elements. Vacuum evaporation of aluminum, chromium, gold, and nickel was used at National Research Corporation[30] in an attempt to impart oxidation resistance to molybdenum powder. However, the protection was inadequate and the suggestion was made that improved coatings might be obtained by vapor-deposition reactions in a fluidized bed of the powder. Attempts to coat graphite with SiC by a solid-solid-diffusion-controlled vapor-deposition process (references 13 and 31) gave results inferior to those obtained with NbC, TaC, and ZrC.

The heat-treating of electroless nickel coatings was studied at Union Carbide.[32] A peak hardness of 69 Rockwell C was obtained, the time depending upon the temperature of treatment (250 to 750°C). Subsequent heat-treatment softened the coating and increased the ductility to an extent dependent upon the phosphorus content. (J. M. Blocher, Jr.)

Ceramic Coatings

Preliminary bismuth absorption tests on four graphite samples coated with SiC from the American Lava Corporation were performed by Babcock and Wilcox.[33] The test specimens were heated for approximately 14 hr at 770°F and 52 psi. Weight measurements before and after testing indicated a small change, which was ascribed to the presence of small amounts of bismuth and Bi_2O_3 clinging to the rough surface of the specimens. Subsequent microscopic examination revealed no attack or penetration of the SiC coatings.

An investigation[34] is being made of the behavior of ceramic-coated metal composites under mechanically and thermally induced stresses. A theoretical analysis of the behavior of coated metal composites in the form of flat plates was found to be in close agreement with the experimental results for annealing specimens, provided there was no plastic flow. Cobalt-bearing, vitreous ceramic coatings were observed to fracture at a strain of 1000 μ in./in. in tension or 10,000 μ in./in. in compression. The maximum allowable induced strain for these enamels was found to be a function of the initial residual stress. Further study of the physical nature of ceramic-coated metal showed that, when a good bond was obtained, oxides of the metal were present in the coating. When the coating adhered, lower valence oxides of that metal were present at the coating-metal interface.

A procedure for cladding UO_2 pellets with Al_2O_3 has been developed[35] that permits the UO_2 to be heated for 100 hr in air at 1200 to 1800°F without damage. There was no measurable release of fission products from clad particles

heat-treated at 1700°F for seven days after exposure to 6.0×10^{12} nv for 1 hr at room temperature.

Claddings of a special alumina were applied to UO_2 by a tumbling technique. The clad pellets were isostatically pressed at 100,000 psi and sintered at 2800°F in hydrogen. (B. W. King)

Welding and Brazing

A study of methods for producing zirconium-to-stainless-steel joints in heavy-wall tubing is reported by Armour.[36] Flash welding and brazing showed promise of producing satisfactory joints, but reproducibility of performance was poor. Brazing with a zirconium−4 wt.% beryllium was judged to afford the most promise for future development.

Zircaloy-3 spot- and seam-welding conditions are reported by Nippes and coworkers.[37] An HCl-HF pickle was required for cleaning to obtain a suitable surface resistance on the Zircaloy parts before welding. Acceptable tensile shear strengths were readily obtained in weldments made from sheet 0.062 to 0.110 in. thick. However, normal or cross-tension weldment strength was low, indicating poor weldment ductility. At 500°F, a slight lowering of tensile shear strength and an increase in normal tensile strength occurred, resulting in an improved relative ductility.

A survey of the state of the art on welding and brazing molybdenum was published by Battelle.[38] Metallurgical considerations involved in joining molybdenum and testing, cleaning, and joining procedures are discussed.

An extensive metallurgical analysis to select weldable niobium alloys is presented by Platte.[7] An experimental program including good and bad alloys is recommended to verify this theoretical analysis. Platte recommends the following alloying elements: titanium, hafnium, and zirconium as neutralizers and molybdenum, titanium, tantalum, tungsten, vanadium, and zirconium as strengtheners. Elements that should contribute to poor weldability are cobalt, chromium, thorium, and aluminum. Preliminary weldability studies of a niobium−0.6 wt.% zirconium alloy have shown that welds produced in a high-purity atmosphere are ductile at temperatures down to −30°C. No oxygen or nitrogen pickup occurred during the welding of this alloy.

Oak Ridge studies[39,40] of the welding of a nickel-molybdenum alloy, INOR-8, have included mechanical-property determinations, filler-metal modification, and welding to dissimilar metals. INOR-8 weld metal has low as-welded ductility at elevated temperatures but does not age harden like similar commercial alloys such as Hastelloy B and Hastelloy W. In fact, long-time exposure (200 to 500 hr) of INOR-8 at 1200 to 1500°F increases the ductility. Short exposure (4 hr) at 1800°F also improves the ductility. The improvement obtained from these treatments appears to result from spheroidization of carbides. Lowering and elimination of carbon in the alloy did not increase the ductility; however, promising results are being obtained from special additions being made to filler wires to assist deoxidation and purification of the weld metal. The effects of these additions on aging characteristics have not been studied yet, but some tendency of age hardening would be expected.

Studies of Inco Weld "A," a coated electrode, and Inco Weld "A" wire, a wire for gas-shielded processes, indicate that coated-electrode deposits do not age harden but that gas-shielded deposits will age harden. Niobium is present in the coated electrode in place of a titanium addition to the gas-shielded filler wire. Dissimilar-metal welds can be made to INOR-8 with the coated electrode provided the process is suitable.

Beryllium welding is also being studied at Oak Ridge.[41] Edge fusion welds joining 20- and 30-mil-thick parts have been made by inert-gas tungsten-arc welding. The large-grained cast structure of these welds is expected to result in brittle behavior. (R. E. Monroe)

Nondestructive Testing

The development of high-integrity nondestructive testing methods for nuclear materials and components continues to center around the application of the standard ultrasonic, eddy current, radiographic, and X-ray techniques to the individual problems. In general, these separate efforts[26,41–51] have resulted in a significant advance in the accuracy and reliability of testing methods.

Some basic studies in the standard inspection techniques are being made. A study of the attenuation of ultrasound in metals is being made

at Oak Ridge.[52] The objective of their program is to relate ultrasonic inspection to actual conditions inside metals. Unfortunately, large energy losses are found in many nuclear materials, e.g., uranium, niobium, and stainless steel.

The attenuation of X-rays (or gamma rays) from radiochemical sources is being used with success in determining the uranium content of reactor fuel elements.[46,53] Determination of the uranium in the presence of fuel additives and determination of the presence of the additives themselves are readily possible. The method has proved valuable for ascertaining fuel loss because it is rapid, nondestructive, reliable, and sensitive and may be adapted to routine testing of a large number of samples. (C. V. Weaver)

References

1. D. E. Treadway, W. C. Weber, and B. J. Buntz, Progress Development Quarterly Report, Part II, Pilot Plant Work, MCW-1421, Nov. 1, 1958. (Confidential AEC report.)
2. R. Magoteaux, D. L. Elston, and C. F. Hall, Laboratory Evaluation of Graphite Crucible Coatings for Vacuum Melting Uranium, NLCO-759, Oct. 24, 1958. (Unclassified AEC report.)
3. P. G. England, A Review of Possible Methods for Refining the As-cast Structure of Uranium, RDB(C)/TN-112, Feb. 11, 1955. (Unclassified British report.)
4. D. R. Jefferson, Process Development Quarterly Report for April–June 1958, BRB-47, Feb. 15, 1959. (Confidential AEC report.)
5. C. E. Polson et al., The Fabrication of Tubular Fuel Elements, Nuclear Engineering and Science Conference, Preprint V-101, Apr. 6, 1959.
6. R. D. Johnson, R. J. Gridley, and R. L. Clark, Forge Rolling Zircaloy Components, Nuclear Engineering and Science Conference, Preprint V-110, Apr. 6, 1959.
7. R. T. Begley, comp., Development of Niobium-base Alloys, Part II, WADC-TR-57-344(Pt.II), December 1958. (Unclassified USAF report.)
8. H. H. Hausner, Slip Casting of Metal Powders, Part III, NYO-8666, Feb. 12, 1959. (Unclassified AEC report.)
9. Westinghouse Electric Corp., March 1959. (Unpublished.)
10. Pressurized Water Reactor (PWR) Project Technical Progress Report for the Period Oct. 24, 1958, to Dec. 23, 1958, WAPD-MRP-77, Dec. 23, 1958. (Unclassified AEC report.)
11.* S. J. Paprocki, E. S. Hodge, and C. B. Boyer, Preparation of Reactor Components by a Gas-pressure Bonding Technique, A/CONF./15/P/788.
12. J. Fugardi and J. L. Zambrow, Bonding of Various Metals and Alloys by Isostatic Pressing at Elevated Temperatures, Nuclear Engineering and Science Conference, Preprint V-104, December 1958.
13. R. W. Dayton and C. R. Tipton, Jr., Progress Relating to Civilian Applications During January 1959, BMI-1315, Feb. 1, 1959. (Confidential AEC report.)
14. R. W. Dayton and C. R. Tipton, Jr., Progress Relating to Civilian Applications During February 1959, BMI-1324, Mar. 1, 1959. (Confidential AEC report.)
15. Pressurized Water Reactor (PWR) Project Technical Progress Report for the Period Dec. 23, 1958, to Feb. 23, 1959, WAPD-MRP-78. (Unclassified AEC report.)
16. S. J. Paprocki et al., Gas-pressure Bonding of Flat-plate Fuel Assemblies, BMI-1312, Jan. 20, 1959. (Unclassified AEC report.)
17. R. W. Dayton and C. R. Tipton, Jr., Progress Relating to Civilian Applications During March 1959, BMI-1330, Apr. 1, 1959. (Confidential AEC report.)
18. N. R. Gardner, Coextruded Parts Can Simplify Design, *Materials in Design Engineering*, 48(7): 91 (December 1958).
19. W. E. Ray and C. J. Beck, A Method of Hot Coextruding Complex Shapes Through Round Dies, *Nuclear Science and Engineering*, 1: 481-494 (September 1956).
20. W. E. Ray, Extrusion of a Complex Shape Through A Round Die, *Metal Progress*, 72(3): 65-69 (September 1957.)
21. Fundamental and Applied Research and Development in Metallurgy, Progress Report for July 1 Through Oct. 31, 1958, NMI-2071, Nov. 28, 1958. (Secret AEC report.)
22. R. R. Nash, editor, Nuclear Fuels Newsletter, WASH-705, February 1959. (Confidential AEC report.)
23. Hanford Atomic Products Operation, Jan. 15, 1959. (Unpublished.)
24. F. W. Albaugh, Hanford Atomic Products Operation, Mar. 15, 1959. (Unpublished.)
25. R. Montagne and L. Meny, Coextrusion Applied to the Construction of Fuel Elements in Solid or Powder Form, Fuel Element Conference, CEA-784, Nov. 18–23, 1957. (Unclassified French report.)
26. Reactor Technology Report No. 8. Metallurgy, KAPL-2000-5, March 1959. (Unclassified AEC report.)
27. R. W. Garbe and H. E. Walchli, Quarterly Progress Report for the Period July 1 to Sept. 30, 1958, YAEC-97, Nov. 14, 1958. (Unclassified AEC report.)
28. R. V. Jelinek, Protective Coatings Limit Corrosion, *Chemical Engineering*, 65(21): 163-168 (1958).

29.* K. D. Sinelnikov, V. F. Ivanov, and V. F. Zelensky, Magnesium-Beryllium Alloys As Material for Nuclear Reactors, A/CONF./15/P/2153.

30. Paul L. Raymond, Oxidation Resistant Coating for Molybdenum, AD-158412, National Research Corporation, Jan. 8, 1958.

31.* J. M. Blocher, Jr., and I. E. Campbell, Carbide Coatings for Graphite, A/CONF./15/P/1428.

32. K. T. Ziehlke, W. S. Dritt, and C. H. Mahoney, The Heat-Treatment of Electroless Nickel Coatings, K-1308, Feb. 2, 1959. (Unclassified AEC report.)

33. Babcock and Wilcox Co., January 1959. (Unpublished.)

34. J. H. Lauchner and D. G. Bennett, Fatigue and Internal Stress Analysis of Ceramic-coated Metal Composites, AFOSR-TN-58-129, September 1958. (Unclassified USAF report.)

35. A. K. Smalley, W. C. Riley, and W. H. Duckworth, Alumina-clad UO_2 for Fuel Applications, BMI-1321, Feb. 18, 1959. (Unclassified AEC report.)

36. J. B. McAndrew, R. Necheles, and H. Schwartzbart, Joining of Zircaloy to Stainless Steels, *Welding Journal*, 37(12): 529s-534s (December 1958).

37. E. F. Nippes, N. F. Savage, and R. C. Wu, Optimum Spot and Seam Welding Conditions for Zircaloy-3, AECU-3964, February 1958. (Unclassified AEC report.)

38. N. E. Weare and R. E. Monroe, Welding and Brazing of Molybdenum, DMIC-108, Defense Metals Information Center, Battelle Memorial Institute, Mar. 1, 1958.

39. Molten Salt Reactor Quarterly Progress Report for Period Ending Oct. 31, 1958, ORNL-2626, Jan. 23, 1959. (Unclassified AEC report.)

40. Molten Salt Reactor Quarterly Progress Report for Period Ending Jan. 31, 1959, ORNL-2684, Mar. 17, 1959. (Unclassified AEC report.)

41. Gas-cooled Reactor Project Semiannual Progress Report for Period Ending Dec. 31, 1958, ORNL-2676, Mar. 26, 1959. (Unclassified AEC report.)

42. J. Guon, J. R. Foltz, and W. Cockrell, Remote Inspection of Cast Slugs, NAA-SR-2798, Dec. 15, 1958. (Unclassified AEC report.)

43. J. W. Allen, Oak Ridge National Laboratory, Feb. 5, 1959. (Unpublished.)

44. R. W. McClung, Immersed Ultrasonic Inspection of Metal Plates, ORNL-2650, April 1959. (Unclassified AEC report.)

45. R. A. Nance and J. W. Allen, Eddy-current Measurements of Metal Thickness and Cladding Thickness, ORNL-2672, April 1959. (Unclassified AEC report.)

46. Reactor Fuel Measurement Techniques Symposium, TID-7560, January 1958. (Unclassified AEC report.)

47. Westinghouse Electric Corp., March 1959. (Unpublished.)

48. D. E. Elliot and G. H. Lennen, Radiography and Autoradiography of Plutonium, *Journal of the Society for Nondestructive Testing*, 16: 430-437 (September–October 1958).

49. P. T. Barnes, Use of Radioisotopes in Filler Metal for Nondestructive Inspection, *Welding Journal*, 37: 1176-1181 (December 1958).

50. A. K. Gurvich, The Development of Ultrasonic Apparatus for Controlling the Quality of Welding Joints (in Russian), *Zavodskaya Laboratory*, 24: 342-346 (1958).

51. A. Donbrowski, Modern Devices Using Radioisotopes for the Nondestructive Testing of Weld Seams, *Brennstoff-Wärme-Kraft*, 10: 437-439 (1958).

52. J. H. White, R. W. McClung, and J. W. Allen, Implications of Ultrasonic Attenuation to Nondestructive Testing, ORNL-2651, April 1959. (Unclassified AEC report.)

53. John H. Carpenter, University of California Radiation Laboratory, Jan. 7, 1959. (Unpublished.)

---

*Second United Nations International Conference on the Peaceful Uses of Atomic Energy, Geneva, September 1958. (Individual papers available from the Office of Technical Services, Dept. of Commerce, Washington 25, D. C. Bound volumes of papers are available from United Nations, Office of Public Information, New York.)

LEGAL NOTICE

This document was prepared under the sponsorship of the U. S. Atomic Energy Commission. Neither the United States, nor the Commission, nor any person acting on behalf of the Commission:

A. Makes any warranty or representation, expressed or implied, with respect to the accuracy, completeness, or usefulness of the information contained in this report, or that the use of any information, apparatus, method, or process disclosed in this report may not infringe privately owned rights; or

B. Assumes any liabilities with respect to the use of, or for damages resulting from the use of any information, apparatus, method, or process disclosed in this report.

As used in the above, "person acting on behalf of the Commission" includes any employee or contractor of the Commission, or employee of such contractor, to the extent that such employee or contractor of the Commission, or employee of such contractor prepares, disseminates, or provides access to, any information pursuant to his employment or contract with the Commission, or his employment with such contractor.

NUCLEAR SCIENCE ABSTRACTS

The U. S. Atomic Energy Commission, Technical Information Service, publishes *Nuclear Science Abstracts (NSA)*, a semimonthly journal containing abstracts of the literature of nuclear science and engineering.

NSA covers (1) research reports of the U. S. Atomic Energy Commission and its contractors; (2) research reports of government agencies, universities, and industrial research organizations on a world-wide basis; and (3) translations, patents, books, and articles appearing in technical and scientific journals.

Complete indexes covering subject, author, source, and report number are included in each issue. These are cumulated quarterly, semiannually, and annually providing a detailed and convenient key to the literature.

Availability of *NSA*

SALE: *NSA* is available on subscription from the Superintendent of Documents, U. S. Government Printing Office, Washington 25, D. C., at $18.00 per year for the semimonthly abstract issues and $15.00 per year for the four cumulated-index issues. Subscriptions are postpaid within the United States, its Territories, Canada, Mexico, and all Central and South American countries, except Argentina, Brazil, British and French Guiana, Surinam, and British Honduras. Subscribers in these Central and South American countries, and in all other countries throughout the world, should remit $22.50 per year for subscriptions to semimonthly abstract issues and $17.50 per year for the four cumulated-index issues.

EXCHANGE: *NSA* is also available on an exchange basis to universities, research institutions, industrial firms, and publishers of scientific information. Inquiries should be directed to the Technical Information Service Extension, U. S. Atomic Energy Commission, P. O. Box 62, Oak Ridge, Tennessee.